

การศึกษาการดูดซับและส่วนที่เกี่ยวข้องของสีฟลาโวนอยด์จากแก่นแกลแล
(*Maclura cochinchinensis* (Lour.) Corner) ในการย้อมไหม

นางสาวชุติมา เสพย์ธรรม

วิทยานิพนธ์นี้เป็นส่วนหนึ่งของการศึกษาตามหลักสูตรปริญญาวิทยาศาสตรดุษฎีบัณฑิต
สาขาวิชาเคมี
มหาวิทยาลัยเทคโนโลยีสุรนารี
ปีการศึกษา 2549

**ADSORPTION AND RELATED STUDIES ON SOME
FLAVONOID DYES FROM *MACLURA COCHINCHINENSIS*
(LOUR.) CORNER AND SILK DYEING**

Chutima Septhum

**A Thesis Submitted in Partial Fulfillment of the Requirements
for the Degree of Doctor of Philosophy in Chemistry**

Suranaree University of Technology

Academic Year 2006

**ADSORPTION AND RELATED STUDIES ON SOME
FLAVONOID DYES FROM *MACLURA COCHINCHINENSIS*
(LOUR.) CORNER AND SILK DYEING**

Suranaree University of Technology has approved this thesis submitted in partial fulfillment of the requirements for the Degree of Doctor of Philosophy.

Thesis Examining Committee

(Assoc. Prof. Dr. Malee Tangsathitkulchai)
Chairperson

(Assoc. Prof. Dr. Saowanee Rattanaphani)
Member (Thesis Advisor)

(Prof. Dr. John Barnard Bremner)
Member

(Assoc. Prof. Dr. Vichitr Rattanaphani)
Member

(Assoc. Prof. Dr. Ruangsri Watanesk)
Member

(Assoc. Prof. Dr. Anan Tongraar)
Member

(Assoc. Prof. Dr. Saowanee Rattanaphani)
Vice Rector for Academic Affairs

(Assoc. Prof. Dr. Sompong Thammathaworn)
Dean of Institute of Science

ชุติมา เสพย์ธรรม : การศึกษาการดูดซับและส่วนที่เกี่ยวข้องของสีฟลาโวนอยด์จากแก่น
แกลแล (*Maclura cochinchinensis* (Lour.) Corner) ในการย้อมไหม (ADSORPTION AND
RELATED STUDIES ON SOME FLAVONOID DYES FROM *MACLURA*
COCHINCHINENSIS (LOUR.) CORNER AND SILK DYEING) อาจารย์ที่ปรึกษา :
รองศาสตราจารย์ ดร.เสาวณีย์ รัตนพานี, 179 หน้า.

งานวิจัยนี้เป็นการศึกษาอันตรกิริยาระหว่างฟลาโวนอยด์ และอลูมิเนียมไอออน โดยเทคนิค
ยูวี-วิสิเบิล สเปกโทรสโกปี รวมทั้งศึกษาจลนพลศาสตร์และอุณหพลศาสตร์ทางเคมีของการย้อมสี
มอรินและสีสกัดจากแก่นแกลแลบนเส้นไหม ในการทดลองได้ทำการหาปริมาณสัมพันธของการ
เกิดสารประกอบเชิงซ้อนระหว่างอลูมิเนียมไอออนและมอริน (M) และเคอซีติน (Q) ในสภาวะที่
พีเอช 4.5 และไม่มีการควบคุมพีเอช นอกจากนี้ยังได้ศึกษาการเกิดสารประกอบเชิงซ้อนระหว่าง
อลูมิเนียม (Al) และแกลเลียม (Ga) กับมอรินและเคอซีตินด้วยเทคนิคอิเล็กโทรสเปกโทร
เมทรี จากการทดลองพบว่าองค์ประกอบหลักของสารประกอบเชิงซ้อน Al:M และ Al:Q เป็น 1:2
เมื่อทำการเติมอะเซทิลเซอรีนเมทิลเอสเทอร์ (Ser) ซึ่งเป็นองค์ประกอบในเส้นไหมลงไป
ในสารประกอบเชิงซ้อน Al:M, Ga:M, Al:Q และ Ga:Q พบว่าอัตราส่วนของ Ser:Al:M และ Ser:Al:Q
เป็น 1:1:1 และ 1:1:2 นอกจากนี้ยังได้คำนวณค่าความร้อนของการเกิดสารประกอบเชิงซ้อนโดย
เปรียบเทียบระหว่างมีและไม่มีโมเลกุลของน้ำเป็นองค์ประกอบด้วยวิธีเคมีอมพีริกัล PM3

การศึกษาจลนพลศาสตร์และอุณหพลศาสตร์ของการดูดซับในการย้อมมอรินและสีสกัด
จากแก่นแกลแลบนเส้นไหม พบว่าความสามารถในการดูดซับมอรินและสีดังกล่าวบนเส้นไหม
ขึ้นอยู่กับ พีเอช ความเข้มข้นเริ่มต้นของสารละลายสีย้อม อัตราส่วนของเส้นไหมต่อปริมาณของ
สารละลายสีย้อม และอุณหภูมิอย่างมีนัยสำคัญ และยังพบว่าอัตราเริ่มต้นของการดูดซับสีบนเส้นไหม
ก่อนเข้าสู่สมดุลเพิ่มขึ้นตามอุณหภูมิ สมการอัตราของการดูดซับมอรินและสีสกัดจากแก่น
แกลแลบนเส้นไหมที่พีเอช 4.0 จัดเป็นปฏิกิริยาอันดับสองเสมือน โดยมีพลังงานก่อกัมมันต์ (E_a)
เท่ากับ 45.3 และ 18.7 กิโลจูลต่อโมล ตามลำดับ การศึกษาทางอุณหพลศาสตร์พบว่าค่าเอนทัลปี
ของการดูดซับมอรินและสีสกัดจากแก่นแกลแลบนเส้นไหมมีค่าเท่ากับ -31.3 และ -14.2 กิโลจูล
ต่อโมล ตามลำดับ นอกจากนี้ได้หาค่าพลังงานอิสระของกิบส์ (ΔG°) และค่าเอนโทรปี
ที่เปลี่ยนแปลงไป (ΔS°) ของการดูดซับสีมอรินและสีสกัดจากแก่นแกลแลบนเส้นไหมอีกด้วย

นอกจากนี้งานวิจัยนี้ได้ทำการศึกษาจลนพลศาสตร์และไอโซเทอร์มของการดูดซับ
อลูมิเนียมบนไคโทซาน พบว่าความสามารถในการดูดซับขึ้นอยู่กับพีเอช ความเข้มข้นเริ่มต้นของ
สารละลายอลูมิเนียม และอุณหภูมิ และพบว่าอัตราการดูดซับอลูมิเนียมบนไคโทซานจัดเป็น

ปฏิกิริยาอันดับสองเสมือนโดยมีพลังงานก่อกัมมันต์ (E_a) 56.4 กิโลจูลต่อโมล แสดงให้เห็นว่าการดูดซับอลูมิเนียมบนโคโทซานเป็นการดูดซับทางเคมี สำหรับการศึกษาด้านอุณหพลศาสตร์พบว่า การดูดซับอลูมิเนียมบนโคโทซานเป็นการดูดซับแบบแลงเมียร์ ค่าเอนทัลปีของการดูดซับเท่ากับ -51.0 กิโลจูลต่อโมล และได้หาค่าพลังงานอิสระกิบส์ (ΔG°) และค่าเอนโทรปีที่เปลี่ยนแปลงไป (ΔS°) ของการดูดซับอลูมิเนียมบนโคโทซานอีกด้วย

สาขาวิชาเคมี

ปีการศึกษา 2549

ลายมือชื่อนักศึกษา _____

ลายมือชื่ออาจารย์ที่ปรึกษา _____

ลายมือชื่ออาจารย์ที่ปรึกษาร่วม _____

ลายมือชื่ออาจารย์ที่ปรึกษาร่วม _____

CHUTIMA SEPTHUM : ADSORPTION AND RELATED STUDIES ON
SOME FLAVONOID DYES FROM *MACLURA COCHINCHINENSIS*
(LOUR.) CORNER AND SILK DYEING. THESIS ADVISOR : ASSOC.
PROF. SAOWANEE RATTANAPHANI, Ph.D. 179 PP.

ADSORPTION/KINETICS/THERMODYNAMICS/MORIN/QUERCETIN/
ALUMINIUM/GALLIUM/*N*-ACETHYL SERINE METHYL ESTER

The interaction of flavonoids with metal ions and kinetics and thermodynamics of the adsorption of flavonoid and extracted dyes from heartwood *Maclura cochinchinensis* (Lour.) Corner onto silk were carried out in this research project. The formation of complexes between alum with morin (M) and quercetin (Q) in aqueous solution at pH 4.5 and without pH control have been studied by UV-visible spectroscopy. In addition, Al(III) and Ga(III) complexes formed by morin and quercetin in aqueous solution were investigated by means of electrospray mass spectrometry (ES-MS). In the full scan mass spectra, Al:M and Al:Q showed major 1:2 stoichiometric ratios. When (*S*)-*N*-acetylserine methyl ester (Ser), as a partial mimic of the serine residue in silk, was added to Al:M, Ga:M, Al:Q and Ga:Q complexes in aqueous solution, the mass spectra of Ser:Al:M and Ser:Al:Q showed 1:1:1 and 1:1:2 stoichiometric ratios. Calculated heats of formation of potential structures of the complexes, with and without bound water, were obtained using semiempirical PM3 calculations.

The adsorption kinetic and thermodynamic studies of alum-morin and alum-extracted dye from *M. cochinchinensis* dyeing onto silk fibres indicated that the

adsorption capacities are significantly affected by pH, the material to liquor ratio (MLR), the initial dye concentration, and temperature. The initial dye adsorption rates of alum-morin and alum-extracted dye on silk before equilibrium time was reached increased at higher dyeing temperature. The pseudo second-order kinetic model indicated for both alum-morin and alum-extracted dye dyeing of silk pH 4.0 with activation energies (E_a) of 45.26 and 18.73 kJ/mol, respectively. The values of the enthalpy for the alum-morin and alum-extracted dye dyeing on silk at pH 4.0 were -31.29 and -14.16 kJ/mol, respectively. The experimental isotherm data were analyzed using the Langmuir and Freundlich equations. Additionally, adsorption-desorption of morin and alum-morin dyeing onto silk were investigated.

In addition, kinetics and isotherm of the adsorption of Al(III) from aqueous solutions onto chitosan was studied. It was found that the adsorption capacities depend on pH, initial concentration of Al(III) and temperature. The pseudo second-order kinetic model indicated for Al(III) adsorption on chitosan at pH 4.0 with activation energies (E_a) of 56.4 kJ/mol. It is suggested that the overall rate of Al(III) ion adsorption is likely to be controlled by the chemical process. Equilibrium data fitted very well to the Langmuir model in the entire concentration range (5-40 mg/L). The enthalpy (ΔH°) of the adsorption is -51.0 kJ/mol. The free energy (ΔG°) and entropy (ΔS°) of the adsorption of Al(III) onto chitosan were also investigated.

School of Chemistry

Student's Signature _____

Academic Year 2006

Advisor's Signature _____

Co-advisor's Signature _____

Co-advisor's Signature _____

ACKNOWLEDGEMENTS

I would like to express my sincere gratitude to Assoc. Prof. Dr. Saowanee Rattanaphani, my supervisor, and Prof. Dr. John Barnard Bremner and Assoc. Prof. Dr. Vichitr Rattanaphani for their exceptional generous support, academic guidance and advice throughout the course of my graduate study. My appreciation also goes to my committee members, Assoc. Prof. Dr. Malee Tangsathitkulchai, Assoc. Prof. Dr. Ruangsri Watanesk and Assoc. Prof. Dr. Anan Tongraar for their time and useful suggestions. I would also like to thank all lectures at the School of Chemistry, Suranaree University of Technology for their good attitude and advice.

I would like to thank the staff of the scientific equipment center F1 and F2, Suranaree University of Technology for providing all equipments and glassware. I would like to thank the members of the Department of Chemistry in Wollongong, the University of Wollongong, Australia. Special thanks go to all the MS crew, especially Larry Hick for his help with MS analyses. Thanks also to Dr. Jody Morgan for her guidance and help with modeling analyses.

I would also like to thank all of my good friends in the Saowanee group the School of Chemistry, Suranaree University of Technology and the Bremner lab at the University of Wollongong, Australia for their friendship and all the help they have provided.

I wish to thank Suratthani Rajabhat University, Suratthani, Thailand, for supporting my scholarship throughout my study. I also thank Suranaree University of Technology and the University of Wollongong for partial financial support.

Finally, I would like to express my deepest gratitude to my parents, and my brothers for their unconditional love and continual encouragement during my education.

Chutima Septhum

CONTENTS

	Page
ABSTRACT IN THAI.....	I
ABSTRACT IN ENGLISH.....	III
ACKNOWLEDGEMENTS.....	V
CONTENTS.....	VII
LIST OF TABLES.....	XV
LIST OF FIGURES.....	XVIII
LIST OF ABBREVIATIONS.....	XXV
CHAPTER	
I GENERAL INTRODUCTION.....	1
1.1 Natural dyes.....	2
1.1.1 Organic non-nitrogenous molecules.....	3
1.1.2 Organic-nitrogenous molecules.....	7
1.2 Synthetic dyes.....	11
1.3 Textile fibres.....	13
1.3.1 Natural protein fibres.....	13
1.3.1.1 Physical properties.....	14
1.3.1.2 Chemical properties.....	14
1.3.2 Cellulosic fibres.....	16
1.4 Natural dyes for fibres.....	17
1.4.1 Direct dyes.....	17

CONTENTS (Continued)

	Page
1.4.2 Vat dyes.....	17
1.4.3 Mordant dyes.....	17
1.5 Synthetic dyes for protein fibres.....	19
1.5.1 Acid dyes.....	19
1.5.2 Mordant dyes.....	20
1.5.3 Premetallised dyes.....	21
1.6 Natural organic dyes.....	22
1.7 Research objectives.....	24
1.8 Scope and limitations of the study.....	24
1.9 References.....	25
II CHARACTERIZATION OF DYE-METAL COMPLEXES AND DYE-METAL-AMINO ACID COMPLEXES.....	28
2.1 Abstract.....	28
2.2 Introduction.....	29
2.3 Experimental.....	34
2.3.1 Chemicals.....	34
2.3.2 Instruments.....	34
2.3.3 Experimental methods.....	35
2.3.3.1 Determination of the mole ratio for Al(III) ion with morin and quercetin complexes.....	35

CONTENTS (Continued)

	Page
2.3.3.2 Effect of alum concentration on morin in aqueous solution.....	36
2.3.3.3 Extraction of dye	36
2.3.3.4 Determination of the amount of morin dye in crude extracted dye.....	36
2.3.3.5 Sample preparation for ES-MS.....	37
2.4 Results and discussion.....	38
2.4.1 UV-Vis spectra of dyes in aqueous solution without pH control and at pH 4.5.....	38
2.4.2 Stoichiometry of dyes and alum in aqueous solution without pH control and at pH 4.5.....	42
2.4.3 Effect of alum concentration on morin in aqueous solution.....	47
2.4.4 Determination of the amount of morin in crude extracted dye.....	48
2.4.5 Electrospray mass spectrometry analysis.....	50
2.4.5.1 Al:M and Ser:Al:M complexes.....	50
2.4.5.2 Ga:M and Ser:Ga:M complexes.....	54
2.4.5.3 Al:Q and Ser:Al:Q complexes.....	58
2.4.5.4 Ga:Q and Ser:Ga:Q complexes.....	62
2.4.6 High resolution mass spectrometry.....	65
2.4.7 Computational modeling.....	66
2.5 Conclusion.....	71

CONTENTS (Continued)

	Page
2.6 References.....	71
III ADSORPTION OF MORIN AND EXTRACTED DYE FROM	
<i>MACLURA COCHINCHINENSIS</i> (LOUR.) CORNER DYEING	
ON SILK.....	
3.1 Abstract.....	76
3.2 Introduction.....	77
3.2.1 Physical chemistry of dyeing process.....	80
3.2.2 Kinetic models of adsorption.....	85
3.2.3 Adsorption isotherms.....	89
3.2.3.1 The Langmuir isotherm.....	89
3.2.3.2 The Freundlich isotherm.....	91
3.3 Experimental.....	93
3.3.1 Chemicals.....	93
3.3.2 Instruments.....	93
3.3.3 Experimental methods.....	94
3.3.3.1 Silk yarn preparation (Chairat, 2004).....	94
3.3.3.2 Stock solutions.....	94
3.3.3.3 Pre-, simultaneous and after-mordant for morin dyeing onto silk.....	94
3.3.3.4 Effect of pH.....	95
3.3.3.5 Batch kinetic of morin and alum-morin experiments.....	96

CONTENTS (Continued)

	Page
3.3.3.6 Batch equilibrium of alum-morin experiments.....	96
3.3.3.7 Adsorption and desorption studies of morin, alum-morin and alum-extracted dye onto silk.....	97
3.3.3.8 Extraction of dye.....	97
3.3.3.9 Batch kinetic studies of extracted dye onto silk.....	98
3.3.3.10 Batch equilibrium adsorption of extracted dye onto silk...	98
3.4 Results and discussion.....	99
3.4.1 Comparison of pre-, simultaneous and after-modant for morin dyeing onto silk.....	99
3.4.2 Optimal conditions of silk dyeing with morin and alum-morin....	102
3.4.2.1 The effect of pH on the adsorption of morin and alum-morin.....	102
3.4.2.2 The effect of material to liquor ratio (MLR) on the adsorption of alum-morin onto silk.....	104
3.4.2.3 The effect of contact time and initial morin concentration on the adsorption of alum-morin onto silk.....	107
3.4.2.4 The effect of temperature on the adsorption of alum-morin onto silk.....	110
3.4.2.5 Activation parameters of the adsorption of alum-morin on silk.....	114

CONTENTS (Continued)

	Page
3.4.2.6 Thermodynamic parameters for the adsorption of alum-morin on silk.....	116
3.4.2.7 Adsorption isotherm for the adsorption of alum-morin on silk.....	117
3.4.2.8 Adsorption-desorption of morin and alum-morin dye on silk.....	121
3.4.3 Optimal conditions of silk dyeing with alum-extracted dye.....	122
3.4.3.1 The effect of material to liquor ratio (MLR) on the adsorption of alum-extracted dye onto silk.....	122
3.4.3.2 The effect of contact time and initial extracted dye concentration on the adsorption of alum-extracted dye onto silk.....	125
3.4.3.3 The effect of temperature on the adsorption of alum-extracted dye onto silk.....	128
3.4.3.4 Activation parameters of the adsorption of alum-extracted dye on silk.....	132
3.4.3.5 Thermodynamic parameters of the adsorption of alum-extracted dye on silk.....	134
3.4.3.6 Adsorption isotherm of alum-extracted dye on silk.....	135
3.4.3.7 Adsorption-desorption of alum-extracted dye on silk.....	138

CONTENTS (Continued)

	Page
3.4.4 Comparison of activation, thermodynamic parameters and desorption between alum-morin and alum-extracted dye dyeing on silk.....	137
3.4.4.1 Comparison of activation parameters between alum-morin and alum-extracted dye dyeing on silk.....	137
3.4.4.2 Comparison of thermodynamics parameters between alum-morin and alum-extracted dyeing on silk.....	139
3.4.4.3 Comparison of adsorption-desorption of morin, alum-morin and alum-extracted dyeing on silk.....	140
3.5 Conclusion.....	141
3.6 References.....	142
IV AN ADSORPTION STUDY OF Al(III) IONS ONTO CHITOSAN.....	147
4.1 Abstract.....	147
4.2 Introduction.....	148
4.3 Experimental.....	150
4.3.1 Materials.....	150
4.3.2 Instruments.....	150
4.3.3 Batch adsorption experiments.....	151
4.3.3.1 Batch pH studies.....	151
4.3.3.2 Batch kinetic studies.....	152
4.3.3.3 Batch isotherm studies.....	152

CONTENTS (Continued)

	Page
4.4 Results and discussion.....	153
4.4.1 Effect of pH.....	153
4.4.2 Kinetics of adsorption.....	154
4.4.2.1 Effect of initial Al(III) concentration.....	154
4.4.2.2 Effect of temperature.....	156
4.4.3 Rate constant studies.....	156
4.4.4 Activation parameters	159
4.4.5 Adsorption isotherm.....	161
4.5 Conclusion.....	168
4.6 References.....	168
V CONCLUSION.....	172
APPENDIX.....	175
CURRICULUM VITAE.....	179

LIST OF TABLES

Table	Page
1.1 Natural dyes and pigments (Bhat <i>et al.</i> , 2005).....	2
1.2 Colours and application of flavonoid and related molecules (Bhat <i>et al.</i> , 2005)..	3
1.3 Natural quinones and anthraquinones dyes.....	5
1.4 Some examples of polyenes and their application.....	7
1.5 A summary of the characteristics of the main chemical classes of dyes (Christie <i>et al.</i> , 2000).....	12
1.6 Amino acid composition of sericin and fibroin (Karmakar, 1999).....	15
2.1 Exact mass measurements and elemental compositions for AlM ₂ , GaM ₂ , SerAlM, SerGaM, SerGaM ₂ , AlQ ₂ and SerAlQ complexes.....	65
2.2 Calculated heats of formation of Al:M, Ser:Al:M, Ga:M and Ser:Ga:M complexes.....	66
2.3 Calculated heats of formation of Al:Q, Ser:Al:Q, Ga:Q and Ser:Ga:Q complexes.....	67
3.1 Comparison of the first-order and second-order adsorption rate constants, calculated q_e and experimental q_e values for different MLR, initial morin dye concentrations and temperatures for alum-morin dyeing of silk.....	113
3.2 Activation parameters for the adsorption of morin and alum-morin onto silk at initial morin concentration 31 mg/L.....	114
3.3 Thermodynamic parameters for the adsorption of alum-morin dyeing at initial morin concentration 31 mg/L.....	116

LIST OF TABLES (Continued)

Table	Page
3.4 Langmuir and Freundlich isotherm constants for the adsorption of alum-morin onto silk at different temperatures.....	119
3.5 R_L values at different temperatures relating to the initial dye concentrations for alum-morin dyeing of silk.....	120
3.6 Comparison of the first-order and second order adsorption rate constants, calculated q_e and experimental q_e values for different MLR, initial extracted dye concentrations and temperatures for adsorption of extracted dye on silk..	131
3.7 Activation parameters for the adsorption of alum-extracted dye onto silk.....	133
3.8 Thermodynamic parameters for the adsorption of alum-extracted dye onto silk.....	134
3.9 Langmuir and Freundlich isotherm constants for the adsorption of alum-extracted dye onto silk at 30°C.....	135
3.10 R_L values at 30°C relating to the initial extracted dye concentrations.....	136
3.11 Activation parameters for the adsorption of alum-morin and alum-extracted dye dyeing on silk.....	138
3.12 Thermodynamic parameters for the adsorption of alum-morin and alum-extracted dye dyeing on silk.....	139
4.1 pH values of Al(III) solutions (V , 50 mL; W , 0.01 g; temp, 30°C; contact time 24 h); pH_a was adjusted by using 0.1 M NaOH or 0.1 M HNO ₃ and pH_e is the pH value of the aqueous solution after equilibration at concentration C_e	154

LIST OF TABLES (Continued)

Table	Page
4.2 Comparison of the pseudo first- and second-order adsorption rate constants and the calculated and experimental q_e values for different initial Al(III) concentrations and temperatures.....	158
4.3 Activation parameters for the adsorption of Al(III) onto chitosan.....	160
4.4 Langmuir and Freundlich isotherm constants for the adsorption of Al(III) onto chitosan at different temperatures.....	164
4.5 Thermodynamic parameters for the adsorption of Al(III) onto chitosan at different temperatures.....	165
4.6 Langmuir isotherm data for adsorption of Al(III) onto chitosan at different temperatures.....	166

LIST OF FIGURES

Figure	Page
1.1 A fundamental skeleton of porphyrins.....	8
1.2 Chemical structures of chlorophyll and heamin.....	9
1.3 Xanthopterin from the butterfly <i>Gonopterix rhamni</i> (Bhat <i>et al.</i> , 2005).....	10
1.4 An oxidation of indoxyl forms indigo.....	10
1.5 Examples of the structures of an azo dye, carbonyl dye and arycarbonium ion dye (a) C.I. Disperse Orange 25, monoazo dye; (b) C.I. Pigment Violet, quinacridone and (c) C.I. Basic Green 4, triphenylmethane dye (Christie <i>et al.</i> , 2000).....	11
1.6 General amino acid formula.....	13
1.7 Crystalline structure of polypeptide chains in fibroin (Karmakar, 1999).....	16
1.8 Molecular structure and configuration of cellulose (Karmakar, 1999).....	17
1.9 Examples of acid dyes; (a) C.I. Acid Blue 45 and (b) C.I. Acid Red 138.....	20
1.10 Mordant dye (C.I. Mordant Black 1).....	21
1.11 The chrome mordanting process.....	21
1.12 Premetallised dye (C.I. Acid Violet 78).....	22
2.1 Chemical structure of (a) morin and (b) quercetin.....	30
2.2 Molecular models of Al(III) complexation with morin and quercetin (Gutierrez and Gehlen, 2002).....	31
2.3 Chemical structure of (<i>S</i>)- <i>N</i> -acetylserine methyl ester (Ser).....	33

LIST OF FIGURES (Continued)

Figure	Page
2.4 Electronic absorption spectra of (a) morin (5.0×10^{-5} M) in aqueous solution in absence and in presence of alum (0-250 μ M) without pH control (pH 4.0-5.5), (b) quercetin (5.0×10^{-5} M) in aqueous solution absence and in presence of alum (0-500 μ M) without pH control (pH 4.0-5.8).....	40
2.5 Electronic absorption spectra of (a) morin (5.0×10^{-5} M) in aqueous solution absence and presence of alum (0-250 μ M) at pH 4.5, (b) quercetin (5.0×10^{-5} M) in aqueous solution absence and presence of alum (0-300 μ M) at pH 4.5.....	41
2.6 Absorbance versus (a) [alum]/[morin] molar ratios plots at 415 nm (b) [alum]/[quercetin] molar ratios plots at 420 nm without pH control.....	43
2.7 Absorbance versus (a) [alum]/[morin] (b) [alum]/[quercetin] molar ratios plots at pH 4.5.....	44
2.8 The proposed structures of Al(III) complexation (a) $Al_3(\text{morin})_2$, (b), (c) Al(morin) and (d), (e) Al(quercetin).....	46
2.9 The effect of alum concentrations on morin in aqueous solution (pH 4.0-5.5) Dash line is the [alum]/[morin] 1. Solid line is the [alum]/[morin] 2.....	47
2.10 UV-Vis spectra of crude extracted dye (100 mg/L), alum-extracted dye and alum-morin in water.....	49
2.11 Estimation of the amount of morin in the crude extracted dye.....	49

LIST OF FIGURES (Continued)

Figure	Page
2.12 (a) Full scan mass spectrum of the Al:morin complex, (b) MS ² spectrum of the <i>m/z</i> 629 ion in Figure 2.12(a), (c) MS ³ spectrum of <i>m/z</i> 629 in Figure 2.12(b) (629>573), (d) MS ² spectrum of the <i>m/z</i> 955 ion in Figure 2.12(a).....	51
2.13 (a) Full scan mass spectrum of Ser:Al:M complex, (b) MS ² spectrum of the <i>m/z</i> 488 ion in Figure 2.13(a), (c) MS ³ spectrum of the <i>m/z</i> 488 (488>458), (d) MS ⁴ spectrum of 488 (488>458>426), (e) MS ² spectrum of the <i>m/z</i> 790 ion in Figure 2.13(a).....	53
2.14 (a) Full scan mass spectrum of Ga:M complex, (b) MS ² spectrum of the <i>m/z</i> 672 ion in Figure 2.14(a), (c) MS ² spectrum of the <i>m/z</i> 1041 ion in Figure 2.14(a).....	56
2.15 (a) Full scan mass spectrum of the Ser:Ga:M complex, (b) MS ² spectrum of the <i>m/z</i> 530 ion in Figure 2.15(a), (c) MS ² spectrum of the <i>m/z</i> 832 ion in Figure 2.15(a).....	57
2.16 (a) Full scan mass spectrum of the Al:Q complex, (b) MS ² spectrum of the <i>m/z</i> 629 ion in Figure 2.16(a).....	59
2.17 (a) Full scan mass spectrum of Ser:Al:Q complex, (b) MS ² spectrum of the <i>m/z</i> 488 ion in Figure 2.17(a), (c) MS ² spectrum of the <i>m/z</i> 790.....	60
2.18 (a) Full scan (ES ⁺) mass spectrum of the Ga:Q complex, (b) MS ² spectrum of the <i>m/z</i> 672 ion in Figure 2.18(a).....	62

LIST OF FIGURES (Continued)

Figure	Page
2.19 (a) Full scan (ES^+) mass spectrum of the Ser:Ga:Q complex, (b) MS^2 spectrum of the m/z 530 ion in Figure 2.19(a), (c) MS^2 spectrum of the m/z 832 ion in Figure 2.19(a).....	63
2.20 Proposed structure of charged AlM_2 and Al_2M_3 complexes without water ligands.....	68
2.21 Proposed structure of charged SerAlM and SerAlM ₂ without water ligands.....	69
2.22 Possible ES(+)-MS-supported structures of charged AlQ ₂ , SerAlQ and SerAlQ ₂ complexes.....	70
3.1 Morphological illustration <i>Maclura cochinchinensis</i> (Lour.) Corner Brisbane Rainforest Action & Information Network. (2007) (left hand side) and its heartwood from Surin, Thailand (right hand side).....	79
3.2 Graphical representation of a dyeing process: kinetics (left) and equilibrium (right) (Zollinger, 1991).....	81
3.3 Rate of dyeing isotherms (Perkins, 1996).....	82
3.4 Comparison of morin alone, pre- and simultaneous mordanting for morin dyeing onto silk.....	100
3.5 Proposed Silk:Al:M coordination linkage structures.....	101
3.6 Effect of pH on morin and alum-morin dyeing on silk.....	103
3.7 Electrostatic map of morin (Spartan Program; AM1; Wavefunction Inc.; '02 Linux /Unix).....	104

LIST OF FIGURES (Continued)

Figure	Page
3.8 The effect of material to liquor ratio on the adsorption of alum-morin onto silk.....	105
3.9 Application of the pseudo first-order equation at different material to liquor ratios on the adsorption of alum-morin onto silk.....	106
3.10 Application of the pseudo second-order equation at different material to liquor ratios on the adsorption of alum-morin onto silk.....	106
3.11 The effect of contact time and initial dye concentration on the adsorption of alum-morin onto silk.....	108
3.12 The pseudo first-order equation at different initial dye concentrations on the adsorption of alum-morin onto silk.....	109
3.13 The pseudo second-order equation at different initial dye concentrations on the adsorption of alum-morin onto silk.....	109
3.14 The effect of temperature on the adsorption of alum-morin onto silk.....	111
3.15 The pseudo first-order equation at different temperatures on the adsorption of alum-morin onto silk.....	112
3.16 The pseudo second-order equation at different temperatures on the adsorption of alum-morin onto silk.....	112
3.17 Arrhenius plot for the adsorption of alum-morin onto silk.....	114
3.18 Plot of $\ln(k/T)$ against $1/T$ for the adsorption of alum-morin onto silk.....	115
3.19 Langmuir adsorption isotherm of alum-morin onto silk at 30, 50 and 70°C....	117

LIST OF FIGURES (Continued)

Figure	Page
3.20 A Langmuir plot of C_e/q_e against C_e for the adsorption of alum-morin onto silk at the initial dye concentration range 39-276 mg/L.....	118
3.21 Adsorption-desorption analysis of morin and alum-morin dye onto and off silk.....	121
3.22 The effect of material to liquor ratios (MLR) on the adsorption of alum-extracted dye onto silk.....	123
3.23 A plot of $\ln(q_e - q_t)$ versus time (pseudo first-order equation) at different MLR on the adsorption of alum-extracted dye onto silk.....	124
3.24 A plot of t/q_t versus time (pseudo second-order equation) at different MLR n the adsorption of alum-extracted dye onto silk.....	124
3.25 The effect of contact time and initial dye concentrations on the adsorption of alum-extracted dye onto silk.....	126
3.26 A plot of $\ln(q_e - q_t)$ versus time (pseudo first-order equation) at different initial dye concentrations on the adsorption of alum-extracted dye onto silk..	127
3.27 A plot of t/q_t versus time (pseudo second-order equation) at different initial dye concentrations on the adsorption of alum-extracted dye onto silk.....	127
3.28 The effect of temperature on the adsorption of alum-extracted dye onto silk.....	129
3.29 A plot of $\ln(q_e - q_t)$ versus time (pseudo first-order equation) at different temperatures on the adsorption of alum-extracted dye onto silk.....	130

LIST OF FIGURES (Continued)

Figure	Page
3.30 A plot of t/q_t versus time (pseudo second-order equation) at different temperatures on the adsorption of alum-extracted dye onto silk.....	130
3.31 Relationship between $\ln k$ and $1/T$ on activation energy of alum-extracted dye onto silk.....	132
3.32 Plot of $\ln (k/T)$ against $1/T$ for the adsorption of alum-extracted dye onto silk.....	133
3.33 Adsorption-desorption of alum-extracted dye on silk.....	137
3.34 Adsorption-desorption of morin, alum-morin alum-extracted dye on silk.....	140
4.1 The chemical structure of chitosan.....	150
4.2 Effect of initial pH (C_0 , 21 mg/L; W , 0.01 g; V , 50 mL; temp, 30°C; contact time 24 h) for Al(III) adsorption on chitosan.....	155
4.3 Adsorption kinetics for Al(III) onto chitosan at different initial Al(III) concentrations (W , 0.01 g; V , 50 mL; temperature 30°C; pH_a 4.0).....	155
4.4 Adsorption kinetics for Al(III) onto chitosan at different temperatures (C_0 , 20 mg/L; V , 50 mL; M , 0.01 g; pH_a 4.0).....	156
4.5 Langmuir adsorption isotherms for the adsorption of Al(III) onto chitosan (W , 0.01 g; V , 50 mL; C_0 , 5-40 mg/L; pH_a 4.0, contact time 24 h)....	162
4.6 The linearized Langmuir adsorption isotherms for the adsorption of Al(III) onto chitosan (W , 0.01 g; V , 50 mL; C_0 , 5-40 mg/L; pH_a 4.0, contact time 24 h)....	163
A.1 Calibration curve of morin dye solution.....	176
A.2 Calibration curve of alum-morin dye solution.....	177
A.3 Calibration curve of alum-extracted dye solution.....	178

LIST OF ABBREVIATIONS

mL	Millitre
L	Litre
g	gram
Wt.	Weight
m/z	mass to charge value
MS	Mass Spectrometry
HRMS	High Resolution Mass Spectroscopy
ESMS	Electrospray Mass Spectroscopy
M	Morin
Q	Quercetin
Al	Aluminium
Ga	Gallium
Ser	<i>N</i> -acetyl serine methyl ester
k_1	Rate constant of pseudo first-order adsorption
q_e	The amount of dye adsorbed per gram fibres at equilibrium
q_t	The amount of dye adsorbed per gram fibres at time t
k_2	Rate constant of pseudo second-order adsorption

LIST OF ABBREVIATIONS (Continued)

h_i	The initial dye adsorption rate
A	The pre-exponential factor
E_a	Activation energy
R	Gas constant
ΔH^\ddagger	Enthalpy of activation
ΔS^\ddagger	Entropy of activation
ΔG^\ddagger	Free energy of activation
k_b	Boltzmann's constant
h	Planck's constant
T	Temperature (K)
Q	Adsorption capacity of the Langmuir isotherm
b	Langmuir constant
Q_f	Adsorption capacity of the Freundlich isotherm
ΔH°	Enthalpy change
ΔS°	Entropy change
ΔG°	Gibbs free energy
K_c	Equilibrium constant
$C_{ad,e}$	Concentration of the dye adsorbed at equilibrium
C_e	Concentration of dye left in the dye bath at equilibrium
w/v	Weight by volume
v/v	Volume by volume

LIST OF ABBREVIATIONS (Continued)

t	Time
C_0	Initial dye concentration
C_t	Concentration of dye after dyeing time t
V	Volume of dye solution
W	Weight of fibre used
MLR	Material to Liquor Ratio
mg/L	Milligram per Litre
R^2	Correlation coefficient
Temp	Temperature
min	minute
q_{de}	The amount of dye desorbed from the fibres
λ_{max}	Maximum wavelength

CHAPTER I

GENERAL INTRODUCTION

From ancient times, mankind was enhanced by the marvelous colours arising from the treatment of cloth with extracted natural dyes. Natural colouring matters are dyes and pigments occurring in plants, animals, birds, insects, bacteria, fungi and minerals. A spectrum of beautiful colours ranging from yellow to black exists in the above sources (Bhat, Nagasampagi and Sivakumar, 2005). Up to the end of the nineteenth century natural dyes were the main colorants available for textile dyeing procedures. The development of synthetic dyes at the beginning of the twentieth century led to a more complete level of quality and more reproducible techniques of application (Bechtold, Turcanu, Ganglberger and Geissler, 2003). However, many colorants from synthetic sources can be harmful and cause allergies in humans and may also affect aquatic life and even the food chain (Chuah, Lin, Kawata, Hattori and Namba, 2005). The introduction of natural dyes into modern dyeing procedures can increase sustainability with regard, for example, to water, chemicals, and energy consumption. As a result of the use of natural products with low toxicity, a decrease in the overall reduction of exposure to harmful chemicals is expected for both textile workers and wearers of the material. The following sections discuss natural dyes including their classification, source and application.

1.1 Natural dyes

Generally the colouring matters from plants, insect and animals are referred to as natural dyes of which plant and insect dyes find their application in dyeing textiles, jute and leather. The chemical classification and the source and application of colourants is discussed below. Organic natural colourants can be nitrogenous and non-nitrogenous. Based on the skeleton and the chromophores they contain, broad classifications can be made as shown in Table 1.1.

Table 1.1 Natural dyes and pigments (Bhat *et al.*, 2005).

Skeleton type	Common colourants
Organic non-nitrogenous molecules	
a) Flavonoids	i. Flavones, flavonols, flavonones, isoflavones ii. Chalcones, aurones iii. Anthocyanins iv. Anhydrobases v. Xanthonenes vi. Tannins
b) Quinonoids	Benzoquinones, naphthoquinones, Anthraquinones, extended anthraquinones
c) Polyenes/carotenoids	Bixin, crocin, β -carotene, capsorubin
Organic-nitrogenous molecules	
a) Pyrrole	Porphyryns (chlorophyll, haeme, bilirubin)
b) Pyrimidine	Pteridines
c) Alkaloids	Indigo, betaine

A brief description of some of the common natural dyes is given below.

1.1.1 Organic non-nitrogenous molecules

Organic non-nitrogenous molecules can be divided into 3 groups; a) flavonoids, b) quinonoids and c) polyenes/carotenoids.

a) Flavonoids

Flavonoids are polyphenolic pigments widely present in plants. The term flavonoid has been derived from the Latin word *flavus* meaning yellow, as a large number of the flavonoids are yellow in colour. They also exhibit a range of biological activities in mammals, the most important one being antioxidant activity. The colours and application of flavonoid and related molecules are shown in Table 1.2.

Table 1.2 Colours and application of flavonoid and related molecules

(Bhat *et al.*, 2005).

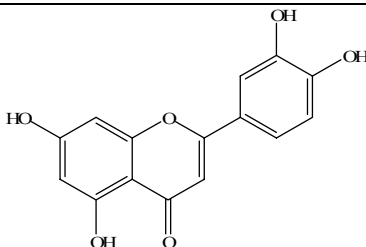
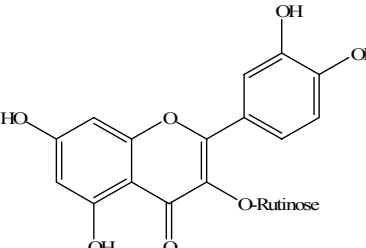
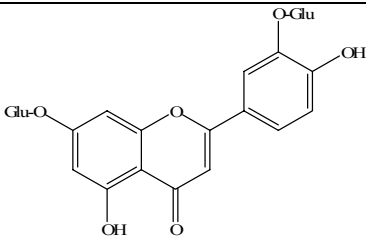
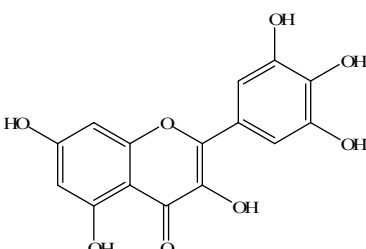
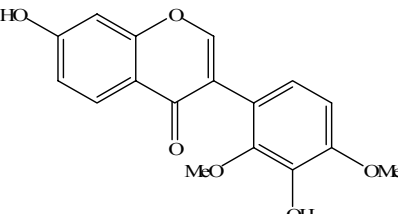
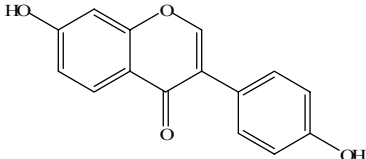
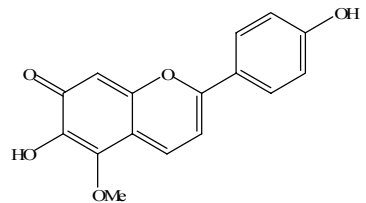
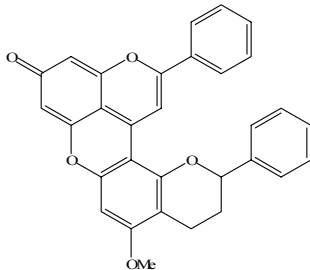
Natural dyes compound/class colour	Structure	Source/ Part/Application
Luteolin Flavone Yellow		<i>Reseda luteola</i> Leaves, seeds Dyeing silk, wool and textiles
Rutin Flavonol Yellow		<i>Sophora japonica</i> Flower buds threads, silk dyeing Embroidery

Table 1.2 (Continued).

Natural dyes compound/class colour	Structure	Source part/Application
Butrin Flavanone Yellow-orange		<i>Butea monosperma</i> Flowers Dyeing silk and cotton
Myricetin Dihydroflavonol Yellow		<i>Myrica rubra</i> Roots Tanning
Santal Isoflavone Red		<i>Pterocarpus santalinus</i> Wood Dyeing cotton, wool, leather, wood
Diadzein Isoflavone Yellow		<i>Glyciene max</i> Berries Food supplement
Carajurin Anhydro base Red		<i>Bignonia chika</i> Dyeing textiles
Dracorubin Anhydro base Red		<i>Dracaena draco</i> Dyeing textiles

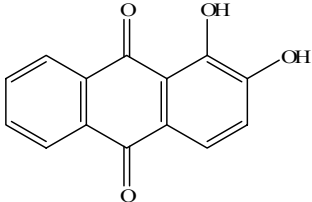
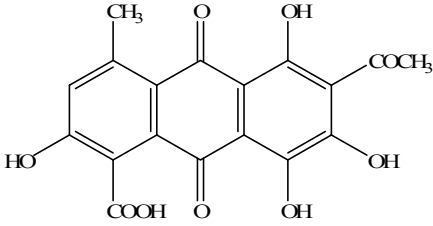
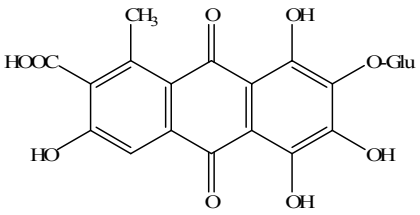
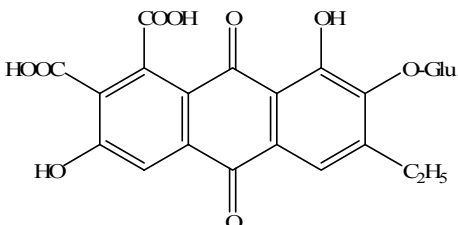
b) Quinonoids

Quinonoids contain a quinone moiety which contributes to the yellow-red range of colours. Four types of quinonoid dyes such as benzoquinones, naphthoquinones, anthraquinones and extended quinones are known. Table 1.3 shows some natural quinones and anthraquinones dyes and their application.

Table 1.3 Natural quinones and anthraquinones dyes.

Name	Structure	Source/Application
Perezone Benzoquinone Orange		<i>Trixis pipitzahue</i> Roots Dyeing textile
Polyporic acid Benzoquinone Bronze		<i>Polyporus fries</i> Fungus
Phoenicin Di-benzoquinone Yellow		<i>Penicillium phoeniceum</i> Bacteria
Lapachol Naphthoquinone Yellow		<i>Tecoma leucoxydon</i>
Alkannin Naphthoquinone Red		<i>Anchusa tinctori</i> Root Red dye, cosmetic and food

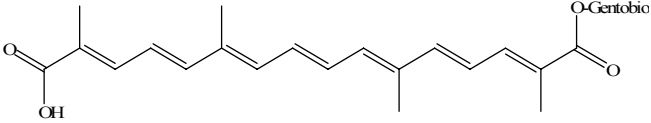
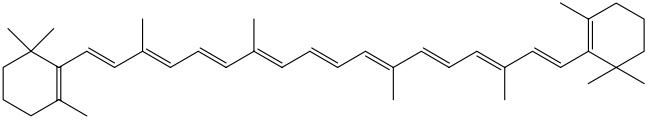
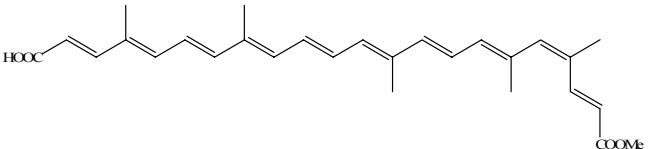
Table 1.3 (Continued).

Name	Structure	Source/Application
Alizarin Anthraquinone Red		<i>Rubia cordifolia</i> Dyeing cloth
Kermesic acid Anthraquinone Red		<i>Coccus ilici</i> (Insect) Dyeing cloth
Carminic acid Anthraquinone Red		<i>Coccus Spp</i> (Insect) Dyeing cloth
Laccaic acid Anthraquinone Red		<i>Coccus laccae</i> (Insect) Dyeing wood

c) Polyenes/carotenoids

Polyene dyes contain a series of conjugated double bonds, usually terminating in aliphatic or alicyclic groups. The best-known group of polyene dyes is the carotenoids, which are widely encountered natural colourants. Some examples and their application are given in Table 1.4.

Table 1.4 Some examples of polyenes and their application.

Plant original Compound class Colour	Structure	Source/Part/ Application
Crocin Apocarotenoid Golden yellow		<i>Crocus sativus</i> Pistil Food
β -Carotene Carotenoid Orange red		<i>Daucus carota</i> Tuber Food
Bixin Apocarotenoid Golden yellow		<i>Bixus Orellana</i> Seedcoat Food

1.1.2 Organic-nitrogenous molecules

Organic-nitrogenous natural pigments are a chemically heterogeneous group of basic nitrogen containing substances. They can be divided into 3 groups; a) pyrrole, b) pyrimidine and c) alkaloids.

a) Pyrrole

Pyrrole is a heterocyclic aromatic organic compound with a five-membered nitrogen-containing ring. Pyrroles are components of larger aromatic rings, including the porphyrins of heme, the chlorins and bacteriochlorins of chlorophyll, and the corrin ring of vitamin B12. There are 3 major groups of pyrrole dyes namely porphyrinoids, porphyrins, and chlorophyll/hemoglobin.

Porphyrinoids, tetrapyrrole macrocycles are natural pigments displaying beautiful range of colours, which occur in many living organisms such as plants, animals, marine organism, birds, bacteria, fungi, etc. They have important roles to play in nature, which include electron transfer, oxygen transfer and photosynthesis.

Porphyrins are the substituted porphins, which are macrocyclic compounds formed by joining four pyrrole rings with four methine bridges (Figure 1.1).

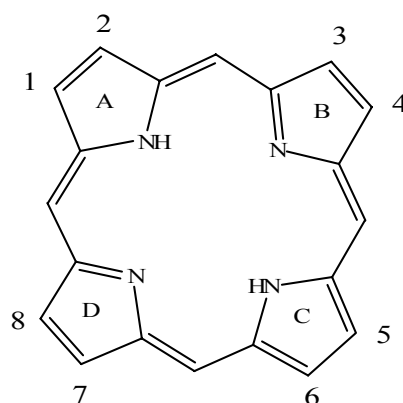


Figure 1.1 A fundamental skeleton of porphyrins.

Chlorophyll and hemoglobin (Figure 1.2) form two important porphyrins containing magnesium and iron metal-complexes respectively. Chlorophyll is the green pigment occurring in the leaves and green stems of various plants. It acts as catalyst for absorption of the light energy from the sun to convert carbon dioxide and water into carbohydrates in plants and this process is known as photosynthesis.

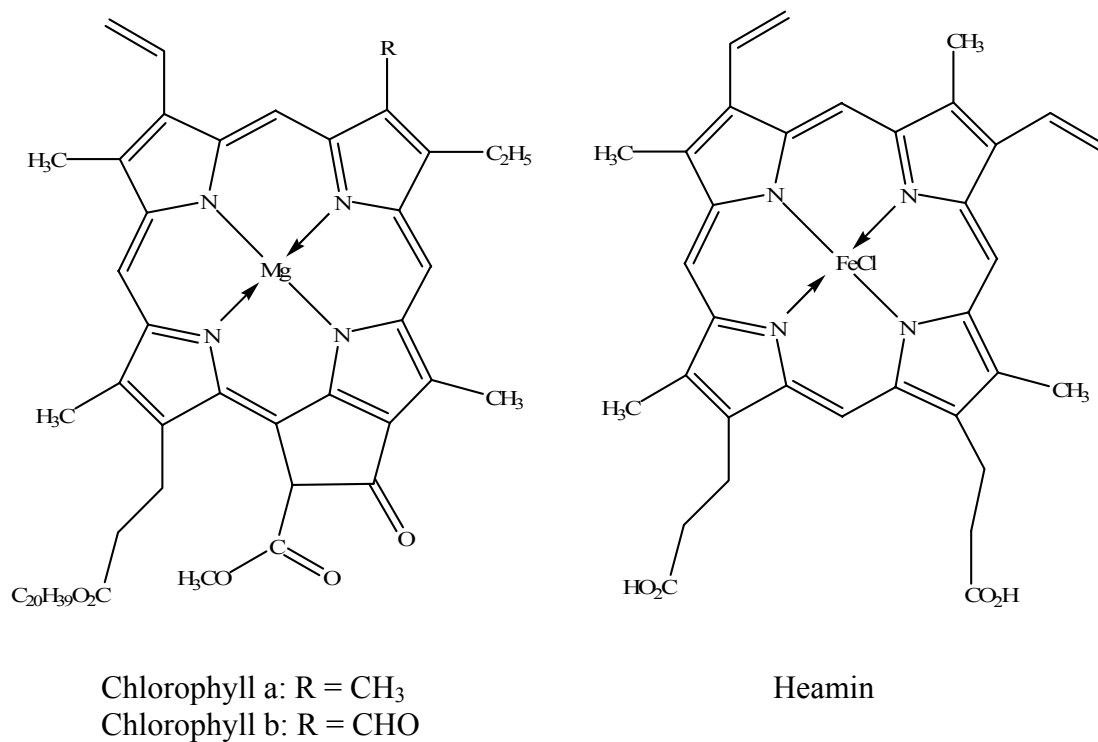


Figure 1.2 Chemical structures of chlorophyll and heamin.

b) Pyrimidine

Pyrimidine is a heterocyclic aromatic organic compound similar to benzene and pyridine, containing two nitrogen atoms at positions 1 and 3 of the six-membered ring. Pteridines are pyrimidine-based natural pigments that are widely distributed in butterflies (e.g. *Gonopterix rhamni*) and insects (Figure 1.3). Most of them are derived from xanthopterin, which contains a pyrimidine ring fused to a piperazine moiety.

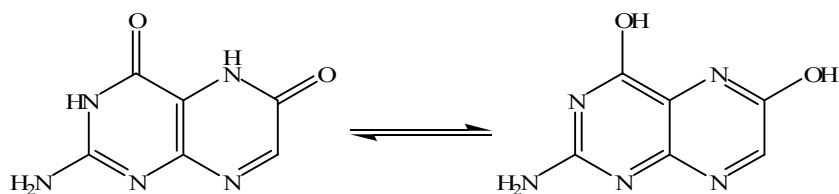


Figure 1.3 Xanthopterin from the butterfly *Gonopteryx rhamni* (Bhat *et al.*, 2005).

c) Alkaloid

Alkaloids are naturally-occurring amines (and derivatives) produced mainly by plants, but also by animals and fungi. Many alkaloids have pharmacological effects on humans and animals. The name derives from the word alkaline; originally, the term was used to describe any nitrogen-containing base.

The famous blue dye, indigo, used to dye burial clothes during ancient times and denims in recent times, is an alkaloid occurring in the form of its glucoside, indicant, in the leaves of *Indigofera tinctoria* and *Isatis tinctoria*. The leaves, on maceration with water, release an enzyme which hydrolyses the glucoside to give indoxyl and glucose. Air oxidation of two molecules of indoxyl forms indigo (indigotin), which is insoluble in water (Figure 1.4).

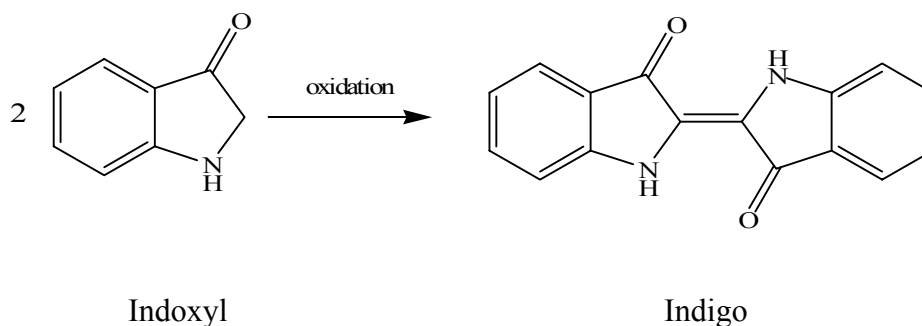


Figure 1.4 An oxidation of indoxyl forms indigo.

1.2 Synthetic dyes

Synthetic dyes for textile fibres may be classified according to chemical structure features or according to the method of application (Christie, Mather and Wardman, 2000). The classification of synthetic dyes according to chemical structure can be grouped into thirteen dye classes as shown in Table 1.5. Examples of the structures of azo dye, carbonyl dye and arycarbonium ion dye are illustrated in Figure 1.5.

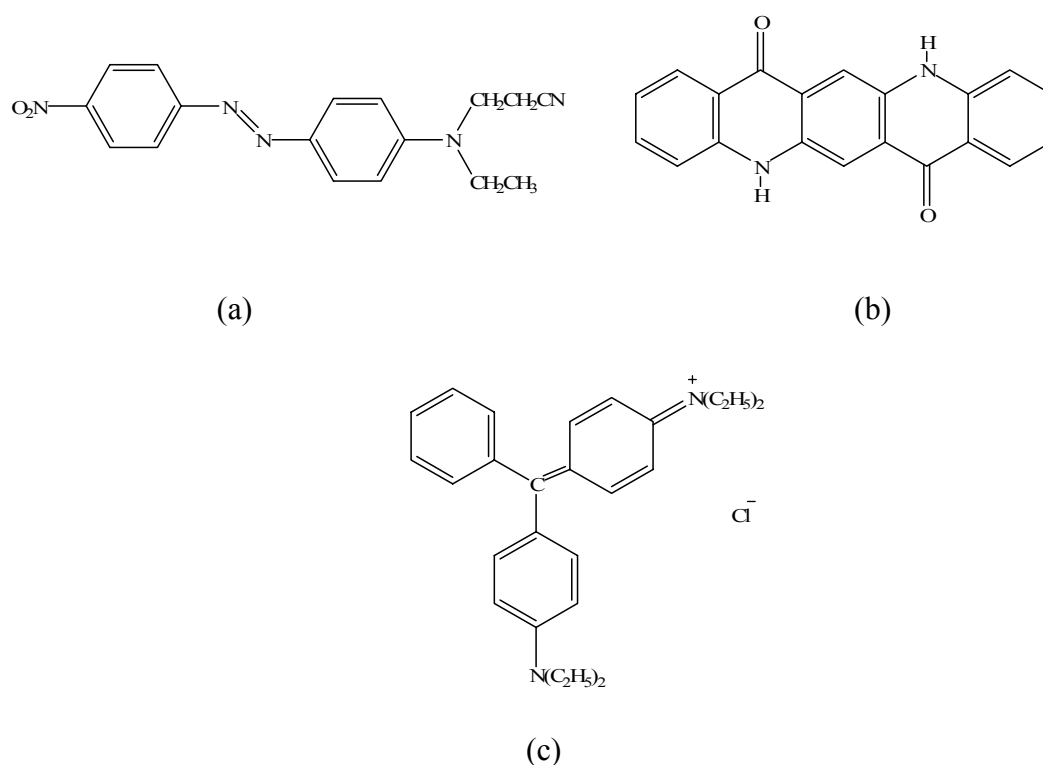


Figure 1.5 Examples of the structures of an azo dye, carbonyl dye and arycarbonium ion dye (a) C.I. Disperse Orange 25, monoazo dye; (b) C.I. Pigment Violet, quinacridone and (c) C.I. Basic Green 4, triphenylmethane dye (Christie *et al.*, 2000).

Table 1.5 A summary of the characteristics of the main chemical classes of dyes
(Christie *et al.*, 2000).

Chemical class	Distinctive structural feature	General characteristics	Main application class(es)
Azo	-N=N-	All hues, but yellow to red most important	Dominate most, but not vat dyes
Carbonyl	C=O	All hues, but blue most important	Important in most applications
Phthalocyanine	16-membered heterocyclic ring, metal complex	Blue and green only	Most important in pigments
Triarycarbonium ion	Positively-charged carbon atom	All hues, but reds and blues most important	Cationic dyes and pigments
Sulfur dyes	Complex polymeric S-containing species	Mostly dull colours, such as blacks and browns	Often considered as an application class itself
Methine dyes	-C=	All hues, but yellows most important	Disperse, cationic
Nitro	-NO ₂	Mainly yellows	Disperse, hair dyes
Inorganic colorants	Range of inorganic types	All hues, white and metals	Exclusive pigments

1.3 Textile fibres

Textile fibres have been, and continue to be, derived from an enormous range of materials (Carr, 1995). The classification of textile fibres is based on the principal origin of the fibre (natural or man-made), chemical type (cellulosic, man-made cellulosic), generic term (seed, hair, rayon) and common names and trade names of the fibres (cotton, viscose, rayon) (Karmakar, 1999). For the application of dyes, a simpler classification into three broad categories is often used (Christie, Mather and Wardman, 2000):

- Protein fibres e.g. silk and wool;
- Cellulosic fibres e.g. cotton, viscose rayon, and flax (linen);
- Synthetic and cellulose acetate fibres e.g. polyester, polyamide, acrylic and cellulose acetate.

1.3.1 Natural protein fibres

Natural protein fibres are generally obtained from animal hair and animal secretions. They have poor resistance to alkalis but have good resiliency and elastic recovery (Needles, 1981). The most prominent protein fibres are wool and silk. Protein molecules are polypeptides, derived from different naturally occurring α -amino acids, most of which can be represented by the general formula (Figure 1.6).

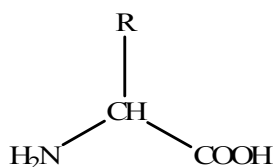


Figure 1.6 General amino acid formula.

Silk is a natural protein fibre excreted by the moth larva *Bombyx mori* (Truter, 1973; Lewin and Pearce, 1998). The silk fibre is almost a pure protein fibre composed of two types of proteins, namely, fibroin and sericin. It also contains small quantities of carbohydrate, wax and inorganic components which also play a significant role as structural elements during the formation of silk fibres.

1.3.1.1 Physical properties

Silk is one of the strongest fibres, only slightly less strong than steel wires, but at the same time also one of the lightest (2000 m of silk thread unwound from a cocoon weigh about 0.250 g) (Ganga, 2003). Silk is a tough fibre with tenacity in the range of 3.0 to 4.5 grams per denier. At the same time it is very elastic fibre with an elongation value of 18-22%. It is very hygroscopic and absorbs about 11% moisture under standard atmospheric conditions of 65% RH and 27°C. As well as this, its unique thermal properties make silk a fabric suitable for wear in all seasons. It is used for making winter jackets, comforters and sleeping bags because it wraps the body in a layer of warm air that acts as an insulator against radiation of heat from the body to the cold surroundings. During summer, its hygroscopic nature makes it a cool body cover (Ganga, 2003).

1.3.1.2 Chemical properties

The actual fibre protein in silk is called fibroin and the protein sericin is the gummy substance that holds the filament together. Raw silk has an average composition of 70-75% fibroin ($C_{15}H_{23}N_5O_8$), 20-25% sericin, 2-3% waxy material and 1-1.7% mineral matter (Karmakar, 1999). Sericin is amorphous and can be selectively removed by dissolution in hot soap solution. Both fibroin and sericin are protein substances built up from 16-18 amino acids out of which glycine, alanine,

serine and tyrosine make up the largest part of the silk fibre, and the remaining amino acids containing bulky side groups are not significant (Karmakar, 1999). The composition of fibroin and sericin with respect to the four main amino acids is shown in Table 1.6; the side groups R refer to the general structure in Figure 1.6.

Table 1.6 Amino acid composition of sericin and fibroin (Karmakar, 1999).

Amino acids	Side groups R	Sericin (% mol)	Fibroin (% mol)
Glycine	H –	14.75	45.21
Alanine	CH ₃ –	4.72	29.16
Serine	HOCH ₂ –	34.71	11.26
Tyrosine	<i>p</i> -OHPhCH ₂ –	3.35	5.14

The structures of *Bombyx mori* silk fibroin has been studied by using solid state ¹³C- and ¹⁵N-NMR spectroscopies (Kaplan *et al.*, 1994; Karmakar, 1999). This work indicated that the main amino acid sequence of silk fibroin is Gly–Ala–Gly–Ala–Gly–Ser where Gly, Ala and Ser denote glycine, alanine and serine respectively (Kaplan *et al.*, 1994). In addition, the X-ray crystal structure of silk fibroin has been reexamined by using newly collected intensity data. It was found that the crystalline region of silk is composed of rather irregular stacks of the antipolar-antiparallel beta sheets with varying orientations. The crystal structure of the polypeptide chains in silk fibroin is shown in Figure 1.7.

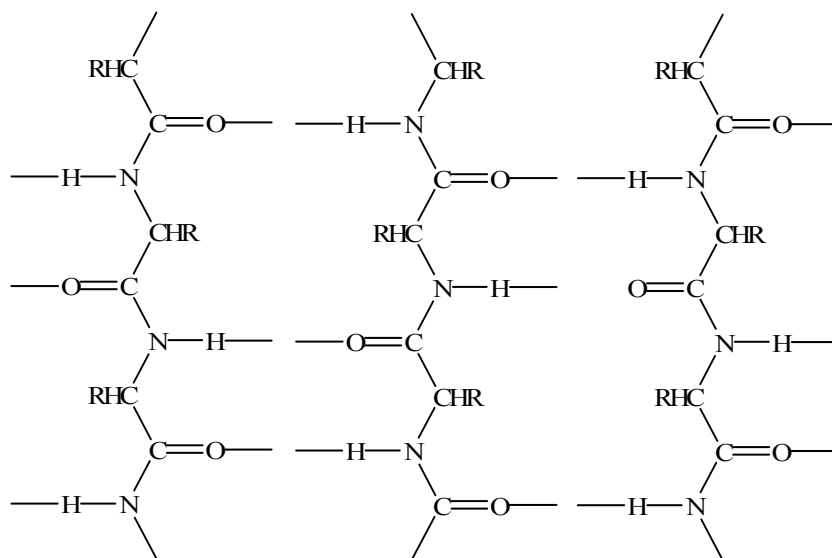


Figure 1.7 Crystalline structure of polypeptide chains in fibroin (Karmakar, 1999).

1.3.2 Cellulosic fibres

Cellulose fibres are natural fibres derived from plant sources. The most important cellulosic fibres are cotton, viscose, linen, jute, hemp and flax. Cotton accounts for half of the world's consumption of fibres (Horrocks and Anand, 2000). The principal component of cotton fibres is cellulose (88-96%), a high molar mass, linear polymeric sugar or polysaccharide. The polymer is formed (Christie *et al.*, 2000) from molecules of the monosaccharide, β -D-glucose, linked through carbon atoms in the 1- and 4-positions. Cotton may be described chemically as poly (1,4- β -D-anhydroglucopyranose) (Karmakar, 1999) (Figure 1.8). Large dye molecules can penetrate easily into the fibre because cellulose has a fairly open structure (Christie, 2001). There are three hydroxy groups in each glucose unit of the cellulose structure, two of which are secondary and one primary, and these give the cellulose molecule a considerable degree of polar character (Christie, 2001).

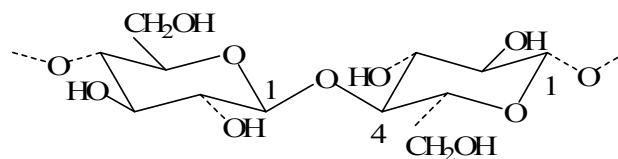


Figure 1.8 Molecular structure and configuration of cellulose (Karmakar, 1999).

1.4 Natural dyes for fibres

Natural dyes were the main source of textile colourants until the mid- to late-19th century. From the application point of view these dyes are classified as: (i) direct dyes, (ii) vat dyes, or (iii) mordant dyes (Bhat *et al.*, 2005).

1.4.1 Direct dyes

For direct dyes no pretreatment is required either to the dyestuff or to the fabric. These dyes form hydrogen bonds with the hydroxyl groups of appropriate fibres, and an example of such a dye is curcumin (from tumeric) which is a yellow dyestuff.

1.4.2 Vat dyes

Vat dyes are used mainly on cellulosic fibres, but some can be applied to protein fibres (Perkins, 1996). They are usually classified into three groups such as indigoid, anthraquinone, and fused ring polycyclic dyes.

1.4.3 Mordant dyes

The word mordant is from the Latin word *mordere*, which means to “bite” or “fasten”. The main reason for using a mordant in dyeing is to make the dyestuff stick to the fibre, which it does through various mechanisms. The most commonly used mordant dyes have hydroxyl and carboxyl groups and are negatively charged, i.e. anionic. A mordant dye forms a lake with a metal, there is a strong colour change.

The incorporation of metals which have low energy atoms into the delocalised electron system of the dye causes a bathochromic shift in the absorption. Since different metal atoms have differing energy levels, the colour of the lakes may also differ.

A second reason for using a mordant is that the mordant can affect the colour of the dyestuff that is used. It can deepen and intensify the colour, or it can lighten it, or it can completely change the colour. Thirdly, use of a mordant can positively influence the fastness of the dye (Bechtold *et al.*, 2003; Moeyes, 1993). The basic principle of mordanting (with metal ions) is the formation of metal ion bonds with the electron donating chromophores of dyes. For this bond formation a range of ligand groups are important, including orthodihydroxy, 3-hydroxy-4-keto-, 4-keto-5-hydroxy-, carboxyl group or sulfonyl groups.

Mordants are of two types: (i) Natural or organic and (ii) Inorganic (Bhat *et al.*, 2005).

(i) Natural mordants consist of tannic acid, ellagic acid, tannins and sulfated and sulfonated oil obtained from vegetable oil.

(ii) Inorganic mordants include alum or potash alum $\text{Al}_2\text{K}_2(\text{SO}_4)_4$, ammonia alum $(\text{Al}_2\text{NH}_4)_2(\text{SO}_4)_4 \cdot 24\text{H}_2\text{O}$, soda alum $\text{Al}_2(\text{Na}_2((\text{SO}_4)_4 \cdot 24\text{H}_2\text{O}))$, chrome alum $\text{Cr}_2(\text{SO}_4)_4 \cdot 24\text{H}_2\text{O}$, ferric alum $\text{Fe}_2(\text{NH}_4)_2(\text{SO}_4)_4 \cdot 24\text{H}_2\text{O}$, potassium dichromate $\text{K}_2\text{Cr}_2\text{O}_7$, ferrous sulfate $\text{FeSO}_4 \cdot 7\text{H}_2\text{O}$, Cupric sulfate $\text{CuSO}_4 \cdot 5\text{H}_2\text{O}$, stannous chloride and stannic chloride.

In the actual dyeing process, there are four ways of using mordant (Bechtold *et al.*, 2003; Moeyes, 1993) as follows:

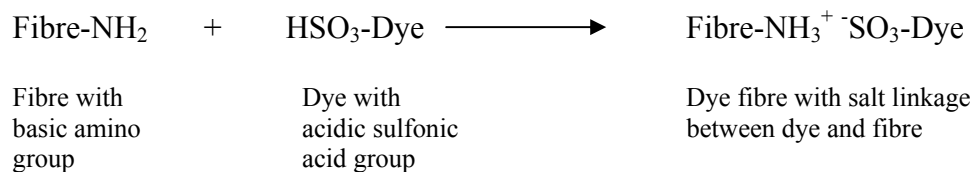
- (a) Mordanting before dyeing, or pre-mordanting;
- (b) Mordanting and dyeing at the same time, called stuffing;
- (c) Mordanting after dyeing, or after-mordanting or post-mordanting;
- (d) A combination of pre-mordanting and after-mordanting.

1.5 Synthetic dyes for protein fibres

Classification of dyes by application method is most useful to the technologist concerned with colouration of textile products. There are eight major classes according to the method of application. Protein fibres may be dyed using a number of application classes of dyes, the most important of which are acid, mordant, pre-metallised and reactive dyes.

1.5.1 Acid dyes

Acid dyes contain acidic groups in their structure; these are usually sulfonate ($-\text{SO}_3^-$) groups, either as $-\text{SO}_3\text{Na}$ or $-\text{SO}_3\text{H}$ groups, although $-\text{COOH}$ groups can sometimes be incorporated (Horrocks and Anand, 2000). The most common structural types of acid dyes are monoazo and anthraquinone dyes. They have been used to dye protein fibres such as wool and silk. Wool, silk and other protein-based natural fibers have basic amino groups that can interact with acid dyes. The protein molecules carry a positive charge which attracts the acid dye anion by ionic forces. Van der Waal's forces, dipolar forces and hydrogen bonding between appropriate functional groups of the dye and fibre molecules may also play a part in the acid-dyeing of protein fibres (Perkins, 1996; Christie *et al.*, 2000).



The most common structural types of acid dyes are anthraquinone and monazo dyes as shown in Figures 1.9(a) and (b), respectively (Perkins, 1996).

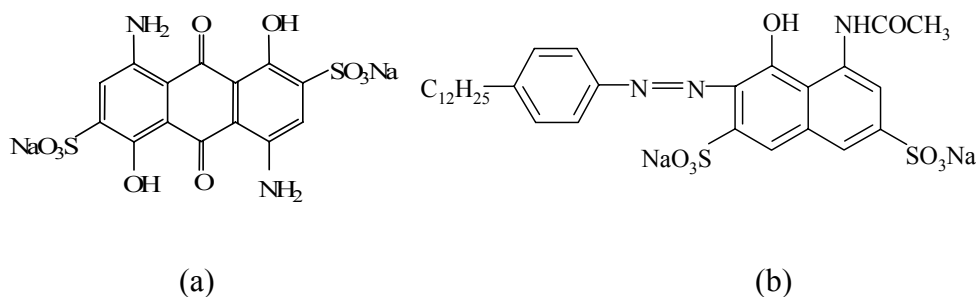


Figure 1.9 Examples of acid dyes; (a) C.I. Acid Blue 45 and (b) C.I. Acid Red 138.

1.5.2 Mordant dyes

Mordant dyes generally have the characteristics of acid dyes but with the additional ability to form stable complexes with chromium (III) ions. Most commonly, this takes the form of two hydroxyl (OH) groups on either side of (*ortho* to) the azo group of a monoazo dye as shown in Figure 1.10. The dye is generally applied to the fibre as an acid dye and then treated with a source of chromium. As a result, a chromium complex of the dye is formed within the fibre as shown in Figure 1.11. The chromium atom in complexes of this type always bonds to six atoms and the complexes show octahedral geometry. It is not established with certainty how the remaining three valencies of chromium are satisfied in the mordant dyeing of protein

fibres, although the possibilities include bonding with water molecules, or coordinating groups on the fibre or with a second dye molecule.

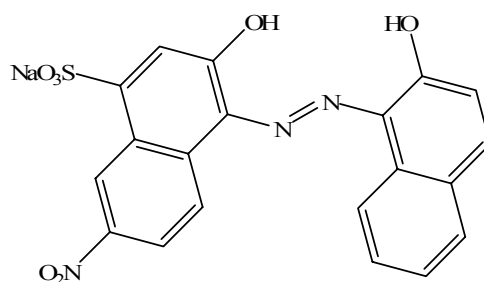


Figure 1.10 Mordant dye (C.I. Mordant Black 1)

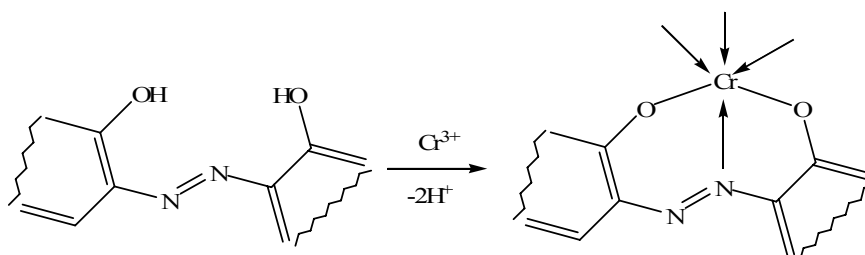


Figure 1.11 The chrome mordanting process.

1.5.3 Premetallised dyes

Premetallised dyes are pre-formed metal complex dyes. They are usually six-coordinate complexes of chromium with octahedral geometry as exhibited in Figure 1.12. They are applied to protein fibres as acid dyes and, because of the special stability of chromium complexes, provide dyeing with excellent light fastness.

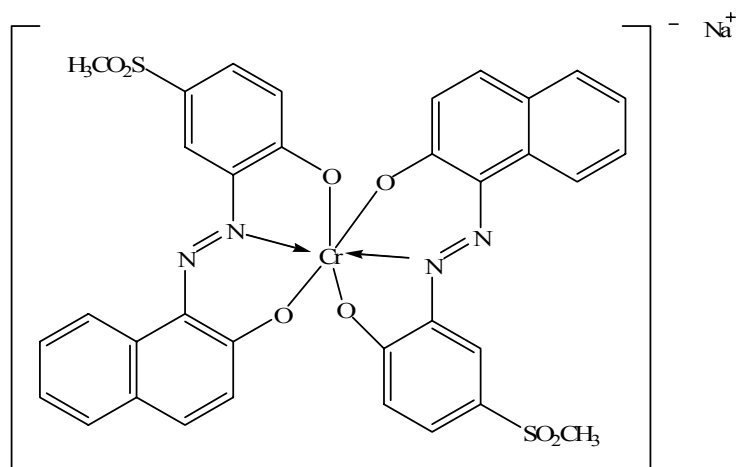


Figure 1.12 Premetallised dye (C.I. Acid Violet 78).

1.6 Natural organic dyes

As an alternative to synthetic dyes, natural dyes continue to hold a place in the dyeing industry. These dyes were the focus of this research project and in particular dyes from the plant *Maclura cochinchinensis* (Lour.) Corner, a plant in the Moraceae family (Lemmens and Wulijarni-Soetjipto, 1992); its synonyms are *Cudrania javanensis*, *Maclura javanica*, and *Cudrania cochinchinensis* (Lour.). It is a subscandent or small tree which is widely distributed. It is found from the Himalayas in Nepal and India to Japan, Southeast Asia and eastern Australia. The heartwood of this plant is used to dye textiles yellow and it is used in mixtures of dyes. In addition, the wood has been used to treat fever. A decoction of the roots is used to alleviate coughing. The young leaves are sometimes eaten raw and the fruit is edible (Lemmens and Wulijarni-Soetjipto, 1992).

In Thailand, *M. cochinchinensis* is widely used by the villagers, especially in the northeast, for dyeing of fibres which yields a beautiful yellow colour (Moeyes, 1993). The flavonoid yellow colouring substance in the wood is morin, which is the major component of the heartwood of this plant (Dechsree, 1998). Other substances found in the bark, root and wood (Murti, Seshadri and Sivakumaran, 1972; Sun, Chang and Cassady, 1988; Chang, Lin, Kawata, Hattori and Namba 1989; Hou, Fukai, Shimazaki, Sakagami, Sun and Nomura 2001; Fukai, Yonekawa, Hou, Nomura, Sun and Uno, 2003) include cudranixanthone, butyrospermol acetate, kaempferol, aromadendrin, populnin, quercetin, taxifolin, cudraiso flavone-A, gerontoxanthone A, B, C, D, E, G, H and I, benzophenones and xanthenes.

A disadvantage of natural yellow dyes, however, is a tendency to “poor fastness” properties. To obtain a wash-fastness in dyeing onto keratin fibres, the flavonoids are usually mordanted with metal ions. In the northeast of Thailand, the villagers have used some metal ion mordants with the silk dyeing by trial and error (Moeyes, 1993) and examples of these mordants include alum, iron oxide and copper sulfate. However, data concerning the thermodynamics of the dyeing of extracted dye from heartwood of *M. cochinchinensis* onto silk are still lacking. Such data on the adsorption process could help to solve some of the dyeing problems associated with extracts of this plant. The improvement of the dyeing process using natural dyes should improve the economics and well-being of villagers in the northeastern part of Thailand who are mostly poor.

The aims of this research were thus to study the interaction of flavonoid and extracted dyes from the heartwood of *M. cochinchinensis* with metal ions. The thermodynamics and kinetics of adsorption of morin and extracted dyes from the heartwood of *M. cochinchinensis* onto silk were also to be investigated in order to obtain the kinetic and thermodynamic parameters of dyeing. In addition, a study of the removal of Al(III) ions in the aqueous solution from dyeing by using chitosan was also undertaken.

1.7 Research objectives

- (a) To study the interaction of morin and quercetin with metal ions.
- (b) To study the thermodynamics and kinetics of adsorption of morin and extracted dyes from heartwood of *M. cochinchinensis* onto silk.
- (c) To investigate the removal of metal ions in the wastewater after dyeing by using chitosan.

1.8 Scope and limitations of the study

Heartwood of *M. cochinchinensis* will be collected from Surin province, Thailand. The interaction of morin and quercetin with metal ions will be investigated by using spectroscopic techniques. Kinetics and thermodynamics aspects of the adsorption of morin and extracted dyes from heartwood *M. cochinchinensis* on silk will be performed using UV-visible spectroscopy. Chitosan will also be used to remove aluminium ions in wastewater after dyeing.

1.9 References

- Bechtold, T., Turcanu, A., Ganglberger, E. and Geissler, S. (2003). Natural dyes in modern textile dyehouses-how to combine experiences of two centuries to meet the demands of the future? **Journal of Cleaner Production** 11: 499-509.
- Bhat, S. V., Nagasampagi, B. A. and Sivakumar, M. (2005). **Chemistry of natural products**. New Delhi: Narosa Publishing House.
- Carr, C. M. (1995). **Chemistry of the textiles industry** Glasgow: Blackie Academic & Professional.
- Chang, C. H., Lin, C. C., Kawata, Y., Hattori, M. and Namba, T. (1989). Prenylated xanthenes from *Cudrania cochinchinensis*. **Phytochemistry** 28: 2823-2826.
- Christie, R. M., Mather, M. M. and Wardman, R. H. (2000). **The Chemistry of Colour Application**. Oxford: Blackwell Science.
- Chuah, T. G., Jumariah, A., Azni, I., Katayon, S. and Thomas Choong, S.Y. (2005). Rice husk as a potentially low-cost biosorbent for heavy metal and dye removal: an overview. **Desalination** 175: 305-316.
- Dechsree, S. (1998). **Isolation of active components against herpes simplex virus from *Maclura cochinchinensis* (Lour.) Corner heartwood**. M.Sc. Thesis, Mahidol University.
- Fukai, T., Yonekawa, M., Hou, A. J., Nomura, T., Sun, H. D. and Uno, J. (2003). Antifungal agents from the roots of *Cudrania cochinchinensis* against *Candida*, *Cryptococcus*, and *Aspergillus* species. **Journal of Natural Product** 66: 1118-1120.

- Ganga, G. (2003). **Comprehensive sericulture Volume 2 Silkworm rearing and silk reeling**. New Hampshire: Science Publishers.
- Hou, A. J., Fukai, T., Shimazaki, M., Sakagami, H., Sun, H. D. and Nomura, T. (2001). Benzophenones and xanthenes with isoprenoid groups from *Cudrania cochinchinensis*. **Journal of Natural Product** 64: 65-70.
- Kaplan, D., Adam, W. W., Farmer, B. and Viney, C. (1994). **Silk polymers: Materials science and Biotechnology**. Washington: American Chemical Society.
- Karmakar, S. R. (1999). **Chemical technology in the pre-treatment processes of textiles**. Amsterdam: Elsevier Science B.V.
- Lemmens, R. H. M. J. and Wulijarni-Soetjipto, N. (1992). **Plant Resources of South-East Asia 3: Dye and Tannin-Producing Plants**. Bogor Indonesia: Prosea.
- Lewin, M. and Pearce, E. M. (1998). **Handbook of fiber chemistry**. New York: Marcel Dekker.
- Moeyes, M. (1993). **Natural Dyeing in Thailand**. Bangkok: White Lotus.
- Murti, V. V. S., Seshadri, T. R. and Sivakumaran, S. (1972). Cudraniaxanthone and butyrospermol acetate from the roots of *Cudrania javanensis*. **Phytochemistry** 11: 2089-2092.
- Needles, H. O. (1981). **Handbook of Textile Fibres, Dyes, and Finishes**. New York: Garland STPM Press.
- Perkins, W. S. (1996). **Textile coloration and finishing**. North Carolina: Carolina Academic Press.

Sun, N. J., Chang, C. J. and Cassady, J. M. (1988). A cytotoxic isoflavone from *Cudrania cochinchinensis*. **Phytochemistry** 27: 951-952.

Truter, E. V. (1973). **Introduction to natural protein fibres: Basic chemistry**. London: Elek Science.

CHAPTER II

CHARACTERIZATION OF DYE-METAL COMPLEXES AND DYE-METAL-AMINO ACID COMPLEXES

2.1 Abstract

The formation of complexes between alum with morin and quercetin in aqueous solution with and without pH control have been studied by UV-visible spectroscopy. The stoichiometries of the complexes were evaluated using the molar ratio method. The association ratio of alum with morin and quercetin without pH control were 3:2 and 1:1, respectively. In the buffer system pH 4.5, the stoichiometry of alum with morin and quercetin were 1:1 and 1:1, respectively.

Al(III) and Ga(III) complexes formed by morin (M) and quercetin (Q) in aqueous solution were investigated by means of electrospray mass spectrometry (ESI-MS). In the full scan mass spectra, Al:M and Al:Q showed major 1:2 stoichiometric ratios. When (*S*)-*N*-acetyls erine methyl ester (Ser), as a partial mimic of the serine residue in silk, was added to Al:M, Ga:M, Al:Q and Ga:Q complexes in aqueous solution, the mass spectra of Ser:Al:M and Ser:Al:Q showed 1:1:1 and 1:1:2 stoichiometric ratios. The patterns of the mass spectra of Ga:M, Ser:Ga:M, Ga:Q and Ser:Ga:Q complexes were similar to those for the corresponding Al(III) complexes. Calculated heats of formation of potential structures of the complexes, with and without bound water, were obtained using semiempirical PM3 calculations.

2.2 Introduction

The yellow flavonoid, morin, is a major component of the heartwood of the plant *Maclura cochinchinensis* (Lour.) Corner (family Moraceae) (Lemmens and Wulijarni-Soetjpto, 1992). In Thailand, especially in the Northeast, aqueous extracts of the wood of this plant are used for the dyeing of silk (Moeyes, 1993). The dye extract, which has morin (3,5,7,2',4'-pentahydroxyflavone) (Figure 2.1(a)) as a major component together with quercetin (3,3',4',5,7-pentahydroxyflavone) (Figure 2.1(b)), imparts a beautiful yellow colour to the silk. However, the use of this natural dye mixture is often linked to poor fastness properties and thus metal-based mordants are used to increase fastness (e.g. wash fastness) properties. One such mordant used by villagers in Northeast Thailand is alum (Moeyes, 1993). Alum is widely used as a mordant for dyeing silk fibres with polyphenolic dyes to obtain a bright colour rendition and wash-fast finish (Raisanen, Nousiainen and Hynninen, 2001; Bechtold, Turcanu, Ganglberger and Geissler, 2003; Bhuyan and Saikia, 2005; Shanker and Vankar, 2007). However, problems with fastness are still encountered. Thus detailed information on the molecular basis of the dye-mordant-silk interaction is required in order to help solve some of the dyeing problems.

A traditional analytical method (UV-Visible absorption spectroscopy) has been used to elucidate structural information on the Al(III)-flavonoid complex or complexes formed in solution (Boudet, Cornard and Merlin, 2000; Cornard, Boudet and Merlin, 2001; Cornard and Merlin, 2001; Cornard and Merlin, 2002; Cornard and Merlin, 2002; Gutierrez and Gehlen, 2002; Cornard and Merlin, 2003; Castro and Blanco, 2004).

It was found that flavonoids form complexes with Al(III) with various Al:flavonoid stoichiometries such as 2:1, 1:1 and 1:2, either through the 4-keto and neighbouring hydroxyl (3-, 5-OH, or both) groups or through adjacent hydroxyl groups on the B ring (i. e. 3'-OH and 4'-OH).

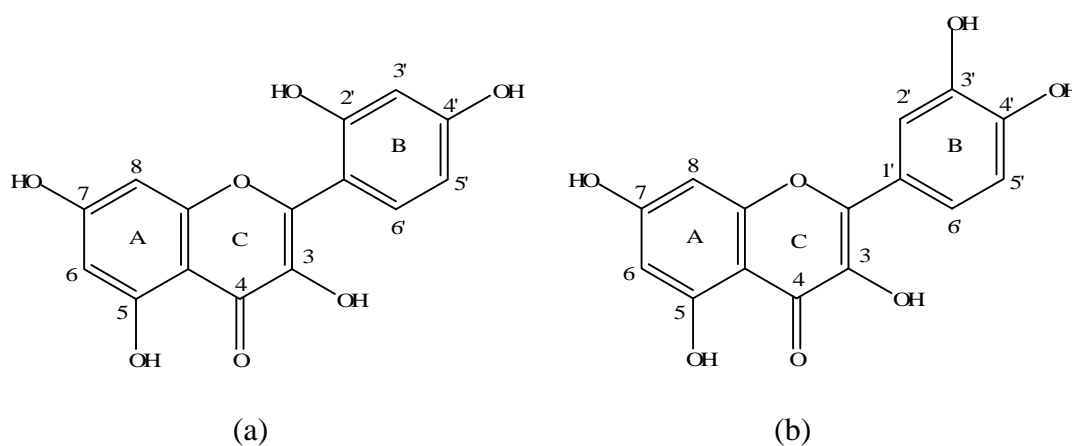


Figure 2.1 Chemical structure of (a) morin and (b) quercetin.

Boudet *et al.* (2000) have studied conformational and spectroscopic aspects of 3-hydroxyflavone (3HF)-aluminium chelates. Spectrophotometric methods have shown that the 3-hydroxyflavone molecule forms a $\text{Al}(\text{3HF})_2$ complex in pure methanol. Structural and spectroscopic studies of 5-hydroxyflavone (5HF) and its complex with aluminium were also investigated (Cornard and Merlin, 2001) and a 1:1 complex with Al(III) in methanol was reported.

The structure, stability and molar absorptivity of the complex formed between AlCl_3 and 5,7-dihydroxyflavone in methanol was investigated using UV-Vis spectroscopy and the AM1 method (Castro and Blanco, 2004). The molar ratio method and Job's method of continuous variation were applied to ascertain the

stoichiometric composition of the complex in methanol at constant ionic strength. It was shown that a 1:2 complex was indicated by both methods.

Spectroscopic and structural studies of complexes of quercetin with Al(III) have been investigated by the combined use of spectroscopic measurements and quantum chemical calculations (Cornard and Merlin, 2002). UV-visible spectroscopy has confirmed the successive formation of two complexes of stoichiometry Al(III):quercetin of 1:2 and 2:1 respectively.

Time resolved fluorescence spectroscopic analysis of quercetin and morin complexes with Al(III) has been reported (Gutierrez and Gehlen, 2002). It was found that the association of Al(III) with morin gives rise to two complexes with 1:1 and 2:1 (morin:Al(III)) stoichiometries, and in both species the association of the cation involved the carbonyl and 3-hydroxyl groups of the pyrone ring. The association of Al(III) with quercetin forms preferentially two complexes with 1:1 and 1:2 (quercetin:Al(III)) stoichiometries where the first cation binds to the site of the pyrone ring but the second one is bound to the catechol group of the molecule (Figure 2.2).

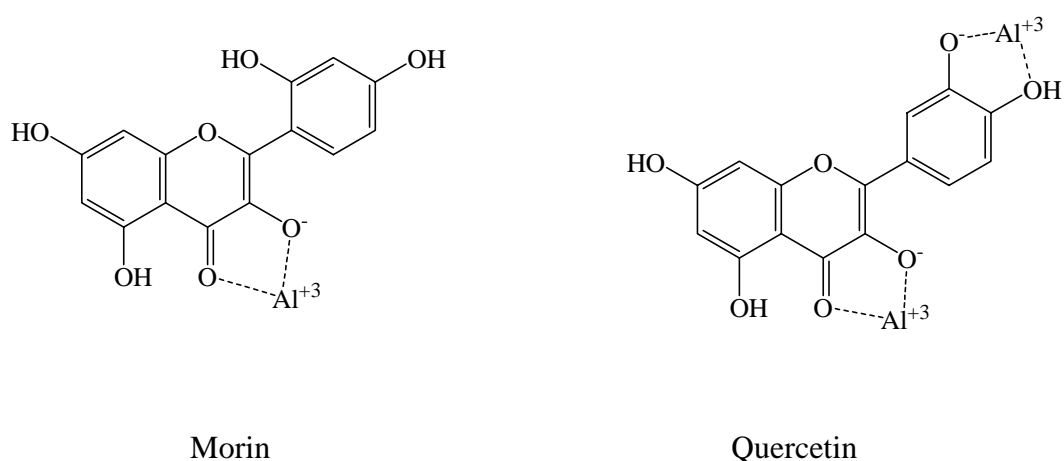


Figure 2.2 Molecular models of Al(III) complexation with morin and quercetin (Gutierrez and Gehlen, 2002).

In addition, a comparison of the chelating power of hydroxyflavones has been investigated (Cornard and Merlin, 2003). The chelating power of 3-hydroxy-4-keto, 5-hydroxy-4-keto and catechol functional groups have been compared in methanol solution, firstly when these binding sites were isolated, and then when they were in competition on the same ligand. It was found that the 3-hydroxy-4-keto group had the strongest chelating power in acidic and neutral media whereas the catechol group presents the greatest ability to chelate Al(III) in alkaline solution.

To better understand Al(III)-flavonoid complexation, a method other than the traditional means of spectrophotometry and fluorescence is warranted. One such method is NMR spectroscopy and ^{27}Al -NMR studies on the complexation of aluminium(III) with phosphinate and phosphate ions has been investigated (Miyazaki, Hiramatsu, Miura and Sakashita, 1999). Also, the emergence of electrospray mass spectrometry (ES-MS) in recent years has greatly enhanced the application of mass spectrometry in this type of analysis (Deng and Van Berkel, 1998; Satterfield and Brodbelt, 2000; Satterfield and Brodbelt, 2001; Pikulski and Brodbelt, 2003; Bai, Song, Chen, Xing, Liu, Z. and Liu, S., 2004; Zhang, Brodbelt and Wang, 2004; Zhang, Wang and Brodbelt, 2005). An electrospray mass spectrometric study of iron and copper flavonoids has been investigated (Frenandez, Mira, Florêncio and Jennings, 2002). It was found that complexes with a range of stoichiometries of metal:flavonoid, 1:1, 1:2, 2:2, 2:3, were observed.

Rutin-metal complexation was characterized by electrospray ionization tandem mass spectrometry (Bai *et al.*, 2004). In addition, aluminium complexes of the type $[\text{Al}^{\text{III}}(\text{flavonoid-H})_2]^+$ are generated by electrospray ionization in order to allow differentiation of isomeric flavonoids by tandem mass spectrometry. The dominant

species observed from the aluminium complexation reaction has a 1:2 aluminium(III):flavonoid stoichiometry (Zhang *et al.*, 2005). The structural requirements necessary for aluminium complexation are that flavonoids must have a 4-keto group and at least one neighboring (3- or 5-) hydroxyl group.

In this study we investigated the complexing of morin with Al(III) in methanolic aqueous solutions and undertook comparative studies with the related Ga(III) ion. One aspect of this investigation has involved the use of electrospray mass spectrometry. The two stable isotopes of Ga [^{71}Ga (39.9%) and ^{69}Ga (60.1%)] were expected to assist with the identification of metal ion-containing complex peaks by ES-MS. This study was also extended to a preliminary assessment of potential interactions of the metal ion-flavonoid complexes with the silk protein fibres, the study of complexing of a serine analog with the complexes by ES-MS, and associated molecular modeling. Serine is a significant component of silk protein (Kaplan, Adam, Farmer and Viney, 1994; Karmakar, 1999) and is a possible site for Al(III) mordant complexing in view of the primary hydroxyl group in its side chain. A partial mimic of the serine residue, (*S*)-*N*-acetylserine methyl ester (Figure 2.3), was thus used in these initial complexing studies by ES-MS, the results of which are presented in this study.

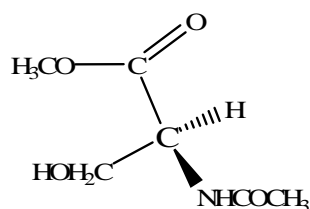


Figure 2.3 Chemical structure of (*S*)-*N*-acetylserine methyl ester (Ser).

2.3 Experimental

2.3.1 Chemicals

- (a) Morin (FW 302.24) [480-16-0], Sigma
- (b) Quercetin (FW 302.24), Acros Organics
- (c) Alum ($\text{KAl}(\text{SO}_4)_2 \cdot 12\text{H}_2\text{O}$) (MW 474.38), UNIVAR
- (d) Aluminium nitrate ($\text{Al}(\text{NO}_3)_3 \cdot 9\text{H}_2\text{O}$) (MW 375.14) 99.997%, Aldrich
- (e) Gallium nitrate ($\text{Ga}(\text{NO}_3)_3 \cdot x\text{H}_2\text{O}$) (MW 255.74) 99.999%, Aldrich
- (f) *N*-acetylserine methyl ester (MW 161.16) Purity > 99%, BACHEM
- (g) Methanol HPLC grade, UNICHROM
- (h) Milli-Q water

2.3.2 Instruments

(a) An Agilent 8453 UV-Vis spectrophotometer was employed for absorbance measurements using quartz cells of path length 1 cm.

(b) A pH meter (Schott) was used to measure the pH values of dye solutions.

(c) Electrospray mass spectrometry

A Thermo Finnigan LTQ quadrupole ion trap (QIT) instrument equipped with an electrospray ionization (ESI) source was used. The flow-rate of the solutions was set at $10 \mu\text{L min}^{-1}$. The heated capillary temperature was kept at 275°C . The ESI spray voltage was set at +4.5 kV. The injection time was set at 50 ms. The other instrumental parameters were tuned to optimize the relative abundance of the aluminium-morin or gallium-morin complex. All spectra were obtained in the positive mode. The scan mode was positive and the isolation width for MS^n was 1.0-6.0 Da.

(d) High-resolution mass spectrometry

High-resolution mass spectrometry for the determination of the accurate masses of the complexes was performed on QTOF Ultima fitted with a lockspray source. Samples were loop injected (10 μ L) using 50% aqueous acetonitrile(v/v). The mass scale was calibrated with polyethylene glycol (PEG) and masses compared with a leucine enkephalin lock mass (m/z 566.2771).

(e) Computational modeling

For computational modeling, PC Spartan Pro (Wavefunction, Irvine, CA) was used. Lowest energy conformers were determined by molecular modeling using MMFF94 force fields. The semi-empirical PM3 is used for calculating the approximate heats of formation of the probable structure of the complexes.

2.3.3 Experimental methods

2.3.3.1 Determination of the mole ratio for Al(III) ion with morin and quercetin complexes

The molar ratio method has allowed us to determine the composition of the complex in solution from spectrophotometric spectra. For this method, the morin stock solution (1.0×10^{-3} M) is prepared successively in 50% (v/v) methanol. Alum stock solution (1.0×10^{-3} M) is prepared in deionized water. A required concentration of 5.0×10^{-5} M of morin in deionized water was diluted from stock solution and kept constant and then mixed well with alum at various concentration ranging from 0 to 250 μ M. Quercetin stock solution (1.0×10^{-3} M) is prepared successively in methanol. The stoichiometry of alum and quercetin were performed in a similar manner with morin. For the study in buffer system, 5% v/v of 1.0 M ammonium acetate-acetic acid buffer (pH 4.5) were added into mixture of alum and dyes.

In order to reach the complexation equilibrium, the absorption spectra of each solution was recorded after standing for 30 minutes by using UV-Vis spectrophotometer for absorbance measurements.

2.3.3.2 Effect of alum concentration on morin in aqueous solution

A concentration of 5.0×10^{-5} M, 7.5×10^{-5} M, 10.0×10^{-5} M of morin was diluted from stock solution and kept constant whereas alum was varied from 0 to 500 μ M of each concentration of morin. In order to reach the complexation equilibrium, the absorbance of each solution was recorded after standing for 30 minutes at 415 nm by using UV-Vis spectrophotometer.

2.3.3.3 Extraction of dye

Heartwood of *M. cochinchinensis* was collected from Surin Province, Thailand. The heartwood was chopped into a small piece. A weighed amount of heartwood was extracted with deionized water in a beaker. In the standard procedure the ratio of mass of material to the volume of liquid was 1:20; extraction was performed for 60 minutes at 85-95°C. The extracted dye solution was filtered and the filtrate concentrated under reduced pressure (rotary evaporator) and then dried by using a Freeze dryer to give a crude extracted dye 10% w/w powder which was then used without further purification.

2.3.3.4 Determination of the amount of morin dye in crude extracted dye

Stock extracted dye (1000 mg/L) was prepared in 50% of methanol/H₂O (v/v). In order to estimate the amount of morin dye in crude extracted dye, Crude extracted dye 100 mg/L from the stock solution was mixed with alum (95 mg/L). The alum-extracted dye mixture was analysed by measurement of the λ_{\max}

using Agilent 8453 UV-Vis spectrophotometer. The amount of morin dye in crude extracted dye was determined with alum-morin calibration curve.

2.3.3.5 Sample preparation for ES-MS

The stock solutions were prepared of 1.0×10^{-3} M morin and 1.0×10^{-3} M quercetin and 1.0×10^{-3} M (*S*)-*N*-acetylserine methyl ester in methanol, 1.0×10^{-3} M alum, aluminium nitrate and gallium nitrate in Milli-Q water. The 1.0×10^{-3} M solution of morin was mixed separately with solutions of alum, aluminium nitrate and gallium nitrate in volumetric flasks (10 mL) and the volume adjusted with water in each case to give a 3:2 mole ratio; the final concentration of the sample was 100 μ M. Pre-mixed solutions of morin-aluminium nitrate and morin-gallium nitrate were each added to separate solutions of *N*-acetylserine methyl ester in volumetric flasks (10 mL) and the volume adjusted with water to give a 3:2:3 mole ratio in each case. In case of quercetin, 1.0×10^{-3} M solution of quercetin was mixed separately with solutions of alum, aluminium nitrate and gallium nitrate in volumetric flasks (10 mL) and the volume adjusted with water in each case to give a 2:1 mole ratio; the final concentration of the sample was 100 μ M. Pre-mixed solutions of quercetin-aluminium nitrate and morin-gallium nitrate were each added to separate solutions of *N*-acetylserine methyl ester in volumetric flasks (10 mL) and the volume adjusted with water to give a 2:2:1 mole ratio in each case.

2.4 Results and discussion

2.4.1 UV-Visible spectra of dyes in aqueous solution without pH control and at pH 4.5

The UV-Vis spectrum of morin in aqueous solution without pH control (pH 4.0-5.5) (Figure 2.4(a)) is characterized by two major absorption bands with maxima at 378 nm (band I) and 261 nm (band II). Band I is considered to be associated with the absorption due to the B-ring cinnamoyl system, and band II with the absorption involving the A ring system (Castro and Blanco, 2004) (Figure 2.1(a)). With alum, morin containing hydroxyl groups at C-3 and C-5 form stable complexes between C-4 keto function and either the 3- or 5-hydroxyl group, producing a large bathochromic shift of band I. As seen in Figure 2.4(a), the absorbance of band I of morin decreases at 378 nm and a new band, which increases with the amount of added alum, appears at 415 nm.

The addition of alum to quercetin aqueous solution without pH control (pH 4.0-5.8) results in significant change of the absorbance spectrum with the appearance of a new band centered on 420 nm with bathochromic shift of about 58 nm from the original band in the absence of alum. A typical example of the spectral changes observed upon addition of alum to quercetin solution is shown in Figure 2.4(b).

Absorption spectra of morin in aqueous solution at pH 4.5 with different concentration of alum are shown in Figure 2.5(a). The absorbance of the band I of morin at 355 nm decreased and a new band, which increased with the amount of alum added, appeared at 413 nm. For quercetin, the absorbance of the band I of quercetin at 368 nm decreased and a new band, which increased with the amount of alum added,

appeared at 425 nm (Figure 2.5(b)) and isobestic points were shown for both morin (at 380 nm) and quercetin (at 395 nm).

The results of the study of the effect of alum on the visible spectra (λ_{max}) of morin and quercetin are presented in Figure 2.4 and Figure 2.5 which show a large bathochromic shift of morin and quercetin as the alum concentration increases. The higher alum concentration results in higher amount of the morin and quercetin complex in solution and the intensity of the absorption band at the longer wavelength is increased.

It is probable that the bathochromic shift occurs as a result of coordination by the lone pair electrons on the O donor atoms with the aluminium ion site, thus stabilizing the excited state relative to the ground state leading to longer wavelength absorption maxima (Christie, 2001; Zollinger, 2003).

Commonly, the transition metal complexes of a coloured organic ligand exhibit light fastness which is significantly better than that of the free ligand. An explanation that has been offered for this effect is that coordination with a transition metal ion reduces the electron density at the chromophore, which in turn leads to improved resistance to photochemical oxidation (Christie, 2001).

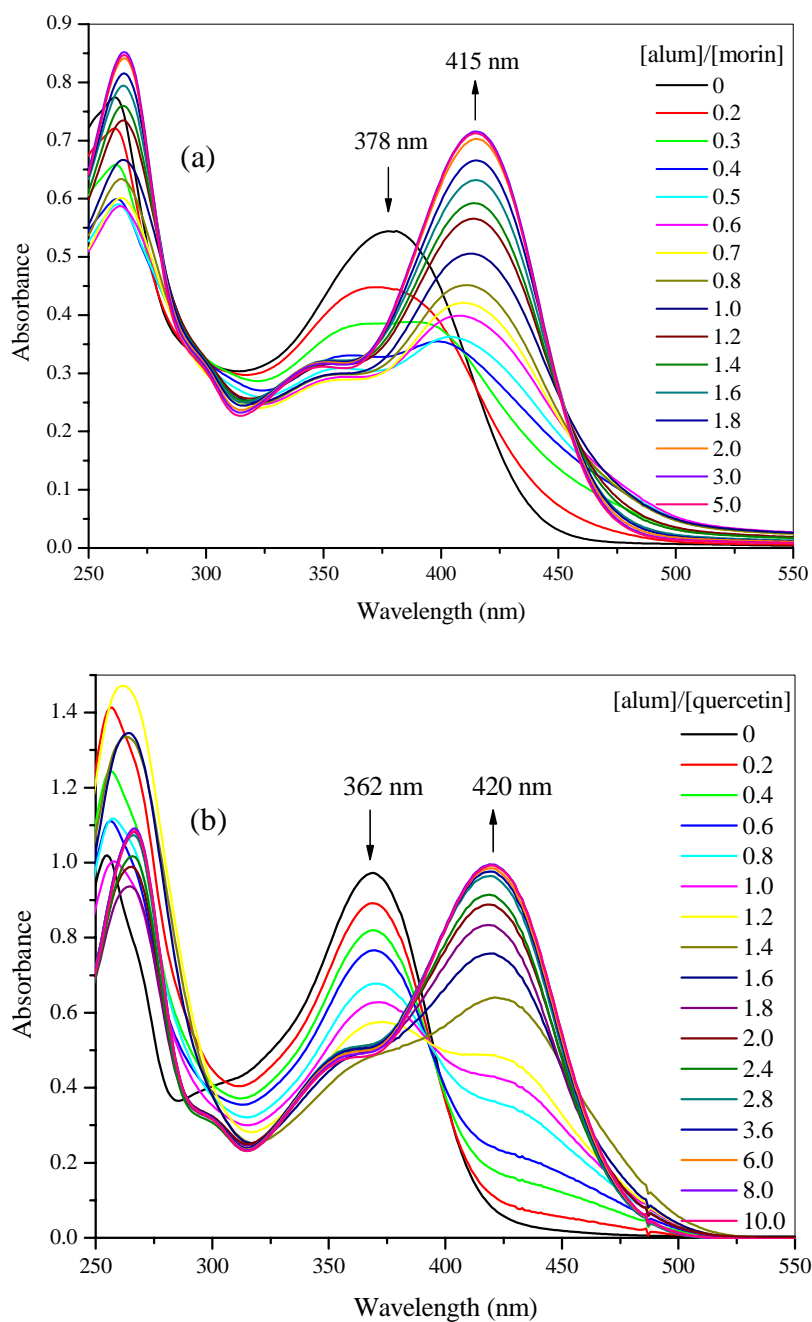


Figure 2.4 Electronic absorption spectra of (a) morin (5.0×10^{-5} M) in aqueous solution in the absence and in the presence of alum (0-250 μ M) without pH control (pH 4.0-5.5), (b) quercetin (5.0×10^{-5} M) in aqueous solution in the absence and presence of alum (0-500 μ M) without pH control (pH 4.0-5.8).

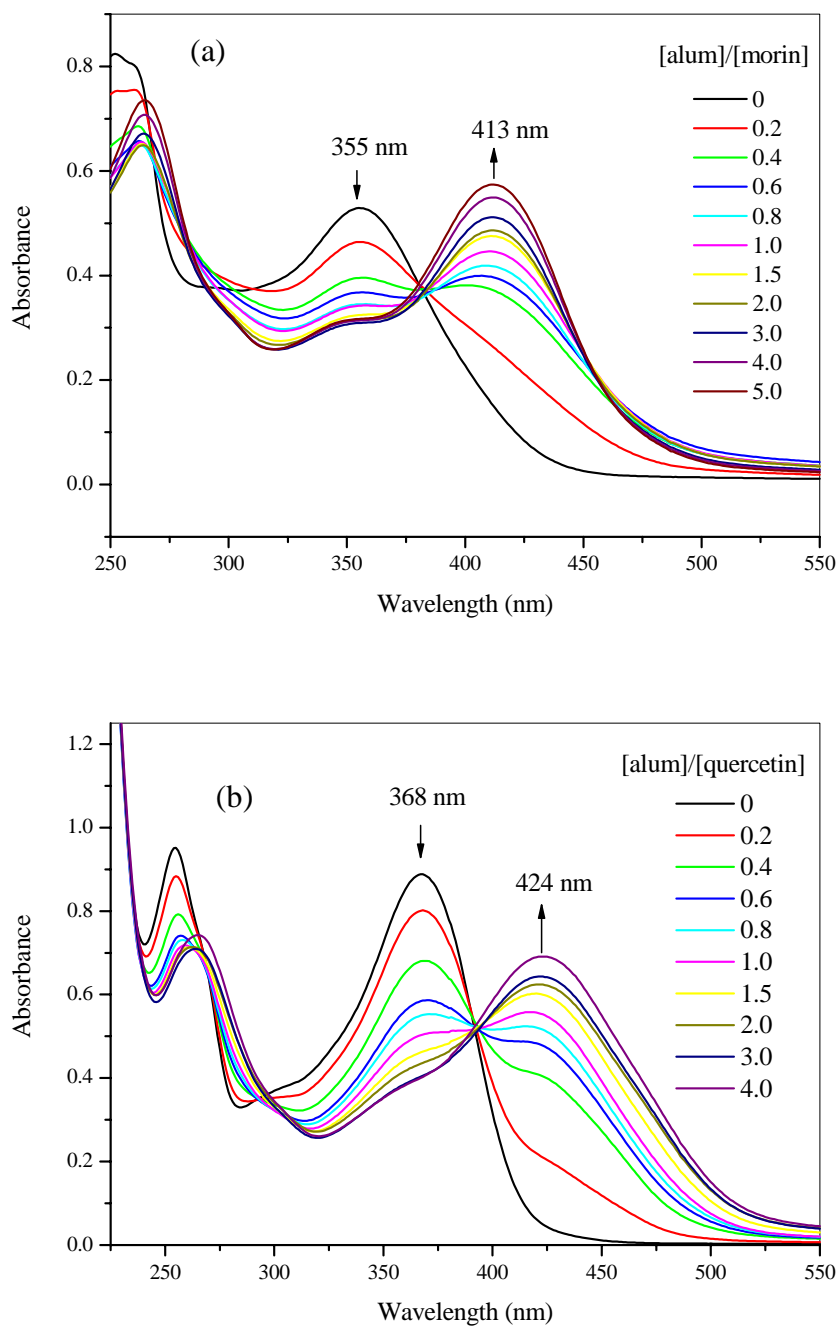


Figure 2.5 Electronic absorption spectra of (a) morin (5.0×10^{-5} M) in aqueous solution absence and presence of alum (0-250 μ M) at pH 4.5, (b) quercetin (5.0×10^{-5} M) in aqueous solution absence and presence of alum (0-200 μ M) at pH 4.5.

2.4.2 Stoichiometry of dyes and alum in aqueous solution without pH control and at pH 4.5

The stoichiometric ratio of Al:morin complexes depends on the nature and properties of the media such as solvent and pH. The association of Al(III) ion with morin gives rise to two complexes with 1:1 and 1:2 (Al(III):morin) stoichiometries in methanol solution and 1:1 in acidic methanol solution (Gutierrez and Gehlen, 2002). In this study the stoichiometry of the complex was determined using the molar ratio method. The molar ratio plots at 415 nm without pH control (pH 4.0-5.5) (λ_{\max} of complex) show an inflection at [alum]/[morin] 1.5, indicating a stoichiometry ratio of alum:morin, i.e. $\text{Al}_3(\text{morin})_2$ (Figure 2.6(a)). The proposed structure of $\text{Al}_3(\text{morin})_2$ in water is shown in Figure 2.8(a). In addition, at pH 4.5, the molar ratio plots of [alum]/[morin] at 355 nm and 413 nm (Figure 2.7(a)) show an inflection at [alum]/[morin] 1 which indicates the formation of an alum:morin 1:1 complex, i.e. Al(morin). Two proposed structures of Al(morin) in aqueous solution are shown in Figures 2.8(b) and (c). These structures had the largest negative heats of formation of those assessed using the PM3 program.

Morin possesses two possible chelating sites, 3-hydroxy-4-oxo and 5-hydroxy-4-oxo systems. In addition, the 3,2'-dihydroxy system in morin is a potential chelating site, which is so placed that a seven-membered chelate ring can be formed on binding Al(III) ion. An Al(III) ion bridges 2'- and 3-hydroxy groups rather than 4-keto- and 3-hydroxy groups, and makes another Al(III) ion binding with the 5-hydroxy-4-oxo system possible, resulting in the 3:2 complex (Figure 2.8(a))

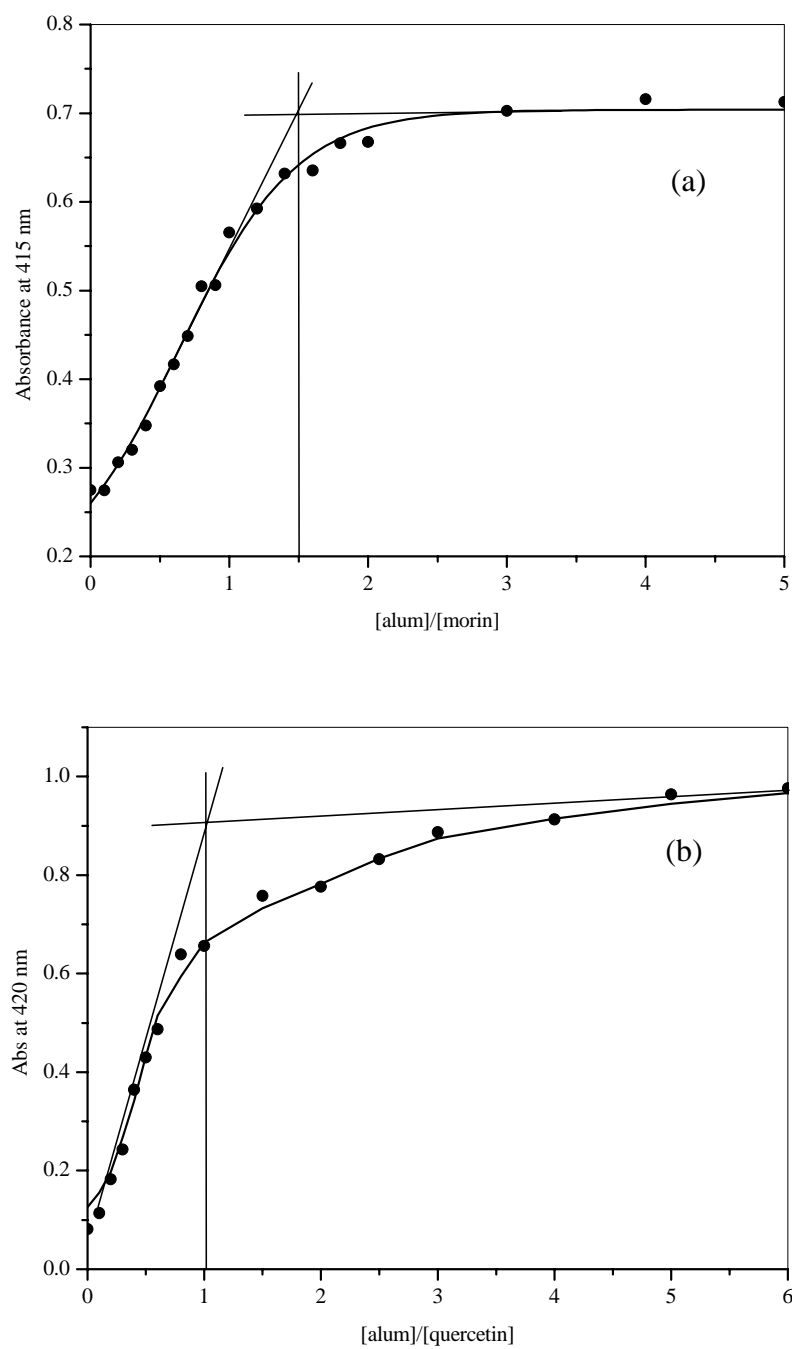


Figure 2.6 Absorbance versus (a) [alum]/[morin] molar ratio plots at 415 nm
(b) [alum]/[quercetin] molar ratio plots at 420 nm without pH control.

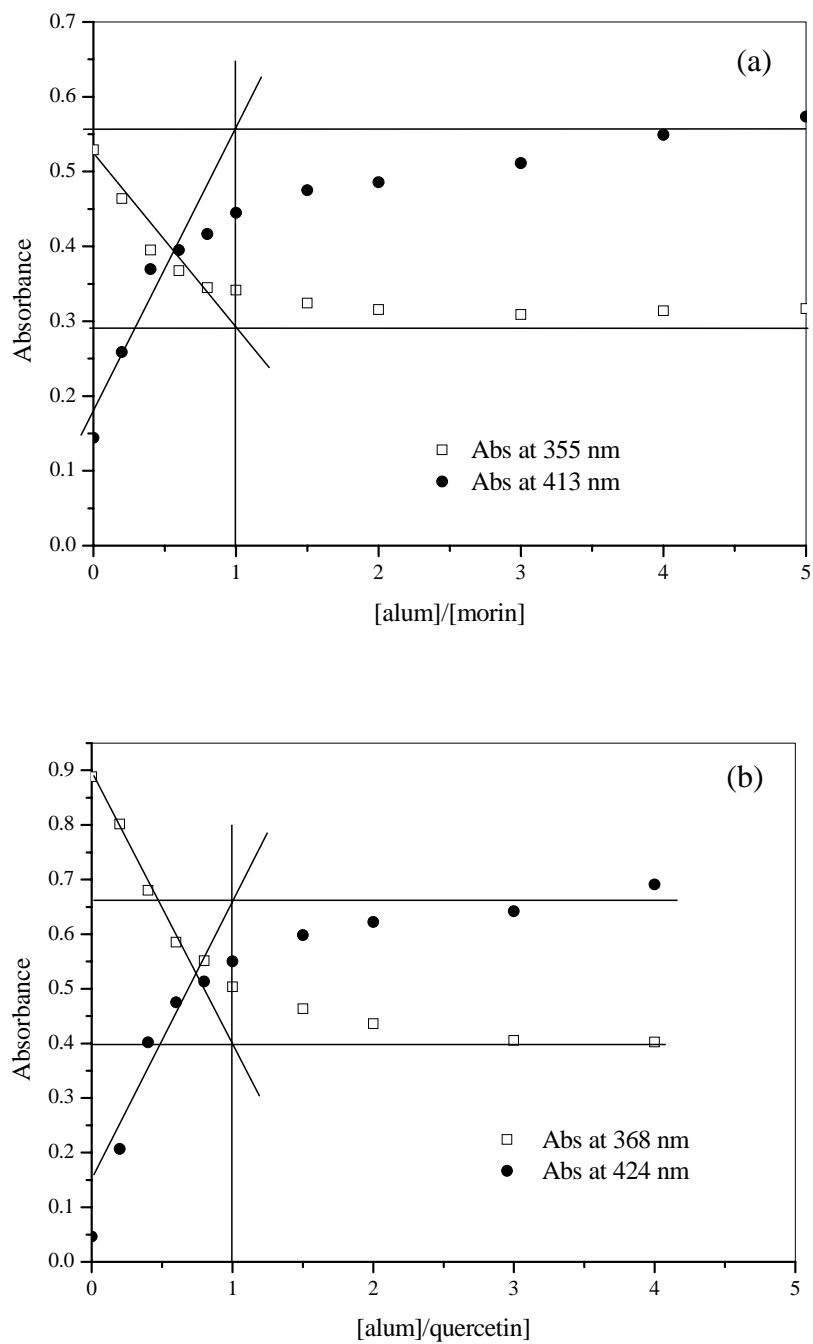


Figure 2.7 Absorbance versus (a) $[\text{alum}]/[\text{morin}]$ (b) $[\text{alum}]/[\text{quercetin}]$ molar ratios plots at pH 4.5.

The stoichiometry of alum and quercetin in aqueous solution without pH control (pH 4.0-5.8) was also investigated. A molar ratio plot of the results is presented in Figure 2.6(b) and it was found that the alum:quercetin ratio was 1:1. The molar ratio plots obtained at pH 4.5 of [alum]/[quercetin] in aqueous solution at 368 nm and 424 nm are shown in Figure 2.7(b). In this case also an [alum]/[quercetin] ratio of 1 was noted.

Quercetin possesses three competing chelating sites: the 3-hydroxychromone, 5-hydroxychromone and the 3',4'-dihydroxy sites (Cornard and Merlin, 2002). The proposed preferred structures of Al(III) complexation with quercetin in aqueous media are shown in Figures 2.8(d) and (e).

The Al(III) ion has a coordination number of six and forms a complex with an octahedral configuration. It can form complexes with six monodentate ligands, or three bidentate ligands. In the case of quercetin as the ligand, the 3-hydroxychromone (Figure 2.8(d)) or 5-hydroxychromone (Figure 2.8(e)) sites appear to be preferred on the basis of the calculated heats of formation. In each case, water is the ligand at the remaining co-ordination sites.

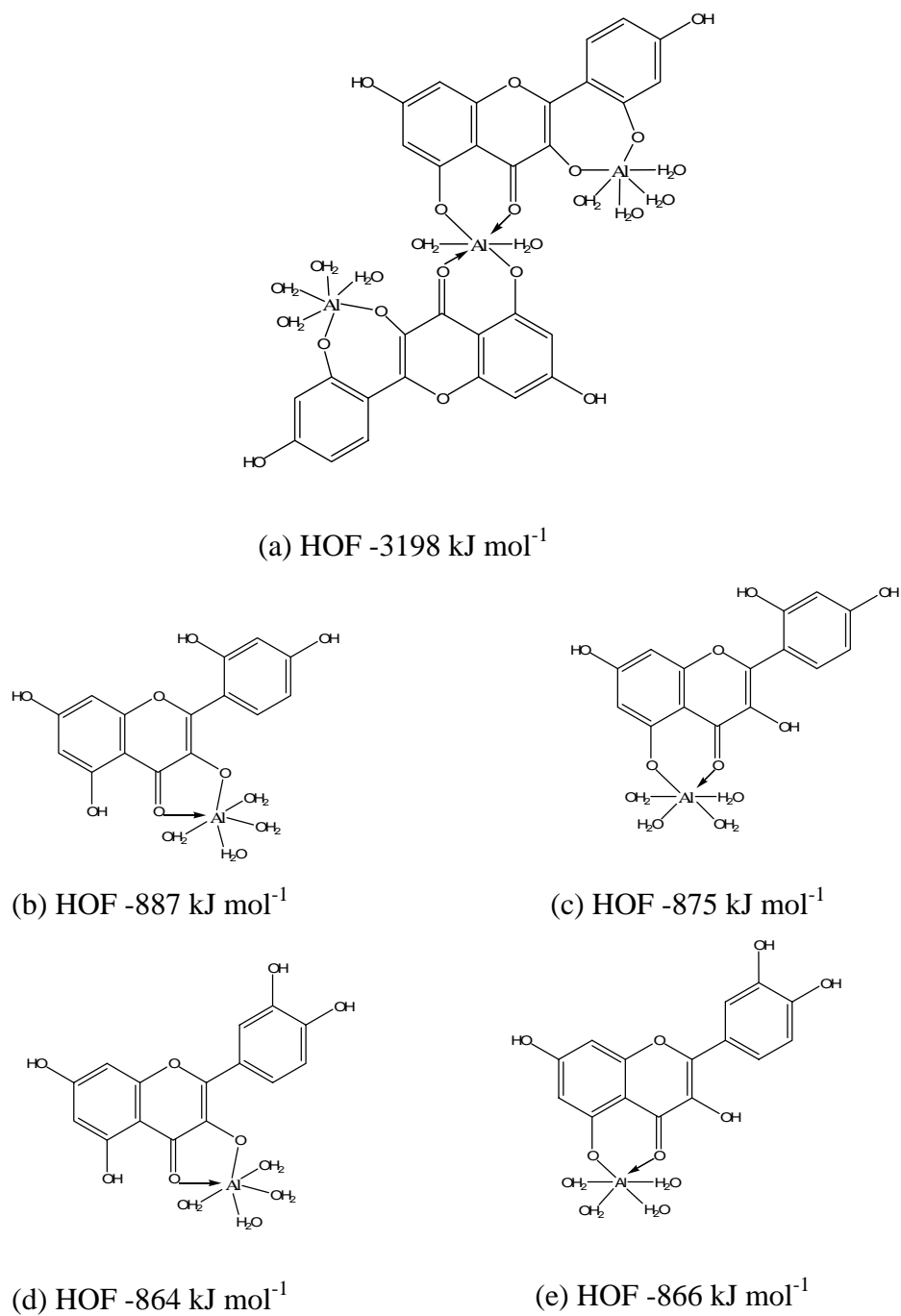


Figure 2.8 The proposed structures of Al(III) complexation (a) $\text{Al}_3(\text{morin})_2$, (b), (c) $\text{Al}(\text{morin})$ and (d), (e) $\text{Al}(\text{quercetin})$.

2.4.3 Effect of alum concentration on morin in aqueous solution

Morin is a major component in *M. cochinchinensis* and an adsorption of morin and extracted dye from heartwood of *M. cochinchinensis* will be studied in Chapter III. In order to minimize the ratio of alum-morin, optimization the amount of alum used for dyeing were investigated. Alum was mixed with morin solution at different morin concentrations ($5.0\text{-}10.0\times 10^{-5}$ M). It was found that the absorbance of alum-morin at wavelength 415 nm still keep increasing with increased alum concentration at the ratio $[\text{alum}]/[\text{morin}]$, 1:1 (dash line in Figure 2.9) and start to be constant at $[\text{alum}]/[\text{morin}]$ 2 stoichiometry in $5.0\text{-}10.0\times 10^{-5}$ M morin concentrations (solid line in Figure 2.9). Thus $[\text{alum}]/[\text{morin}]$, 2:1 stoichiometry was fixed to study alum-morin complex dyeing on silk in Chapter III.

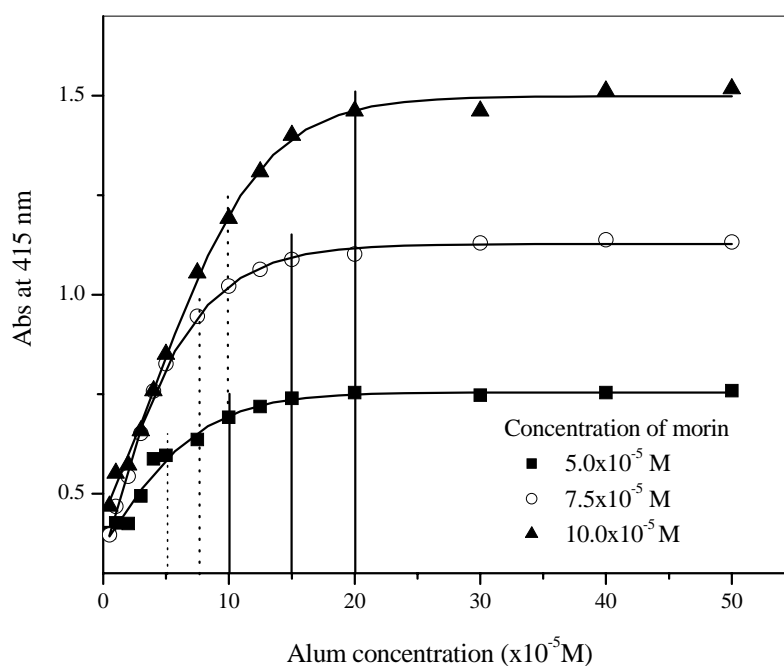


Figure 2.9 The effect of alum concentrations on morin in aqueous solution (pH 4.0-5.5). Dash line is the $[\text{alum}]/[\text{morin}]$, 1:1. Solid line is the $[\text{alum}]/[\text{morin}]$, 2:1.

2.4.4 Determination of the amount of morin in crude extracted dye

There are several methods to determine aluminium in water samples (Trai, Butler, Haddad and Bowie, 2007) such as atomic spectrometry, voltammetry, electrocaper detection-gas chromatography, UV-vis spectrophotometry and fluorometry. Morin is one of reagent can selectively form complex with aluminium and has been widely used as a reagent for both fluorometric and spectrophotometric determinations (Trai *et al.*, 2007; Ahmed and Hossan, 1995). As mentioned in Chapter I, *M. cochinchinensis* is the plant which is contain mainly morin dye. Estimation the amount of morin in the crude extracted dye from *M. cochinchinensis*, alum-morin complex was used to evaluate the amount of dye from this plant.

Crude extracted dye 100 mg/L alone and the alum-extracted dye mixture were analysed by measurement of the appropriate λ_{\max} values by UV-vis spectrophotometry. It was found that the λ_{\max} values of extracted dye alone and alum-extracted dye were 380 and 415 nm (Figure 2.10), respectively. In addition, the absorbance at 415 nm of 100 mg/L of extracted dye was 0.6393, which indicated about 17% morin in this extract, assuming Beer's Law holds and no other interfering absorbing species at this wavelength were present. An adsorption behaviour of extracted dye onto silk, adsorption kinetics and thermodynamics will be investigated in the Chapter III.

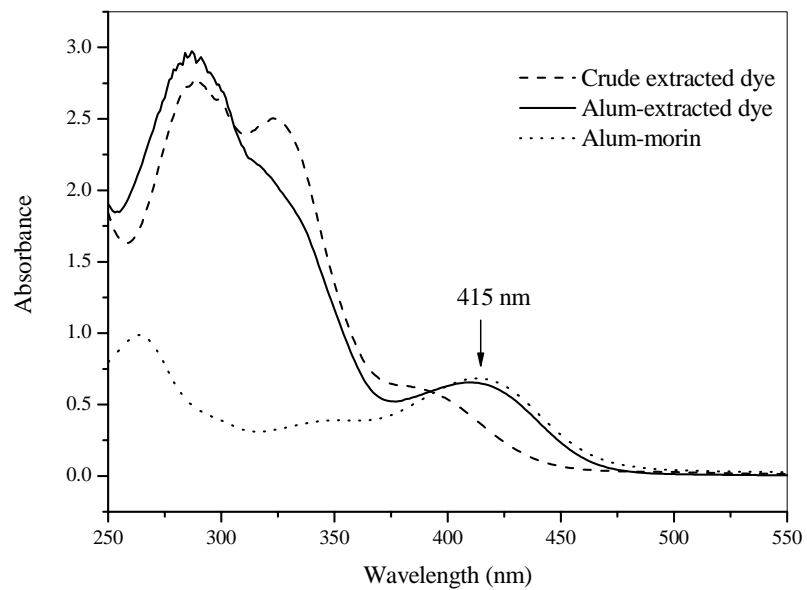


Figure 2.10 UV-Vis spectra of crude extracted dye (100 mg/L), alum-extracted dye and alum-morin in water.

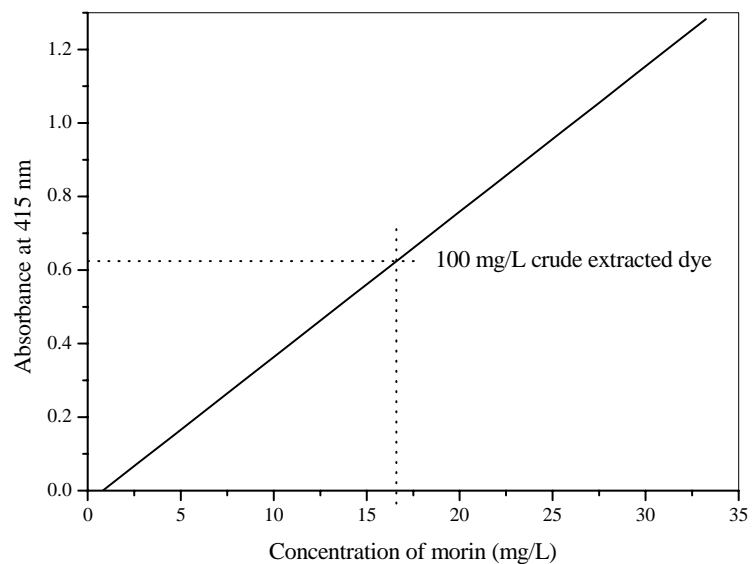


Figure 2.11 Estimation of the amount of morin in the crude extracted dye.

2.4.5 Electrospray mass spectrometry analysis

Aluminium(III) and gallium(III) ions were used to form complexes with morin and quercetin (Figure 2.1) in methanolic aqueous solution. (*S*)-*N*-acetylserine methyl ester (Figure 2.3) was mixed with aluminium-morin and gallium-morin solutions. The positive scan mode was used for all the electrospray mass spectrometric experiments. In order to elucidate the structure of the complexes and the fragmentation mechanism of aluminium- and gallium-morin complexes, multistage tandem mass spectrometry was performed to produce abundant fragments.

2.4.5.1 Al:M and Ser:Al:M complexes

The full-scan ESI mass spectrum of the Al and M complexing is shown in Figure 2.12(a). In this spectrum, two Al:M complexes were found, with peaks at m/z 629 and m/z 955. On the basis of molecular mass and assuming a single positive charge, the complexes were assigned as $[\text{Al}(\text{M}-\text{H})_2]^+$ and $[\text{Al}_2(\text{M}-\text{H})_2(\text{M}-3\text{H})]^+$, respectively. In order to obtain more structural information on the Al:M complexes, further analyses using multistage tandem mass spectrometry (MS^n) were performed. Three ions at m/z 611, 600 and 573 were present in the MS^2 spectrum of m/z 629 (Figure 2.12(b)). The ion at m/z 611 is from the neutral loss of H_2O (-18 Da), while the ion at m/z 600 corresponds to the neutral loss of CHO (-29 Da). The most intense fragment ion (m/z 573) resulted from the neutral loss of $\text{C}_3\text{H}_4\text{O}$ (-56 Da). Figure 2.12(c) shows the MS^2 spectrum of m/z 955, in which it was found that the most intense fragment ion (m/z 653) resulted from the neutral loss of $\text{C}_{15}\text{H}_7\text{O}_7$ (morin; 302 Da).

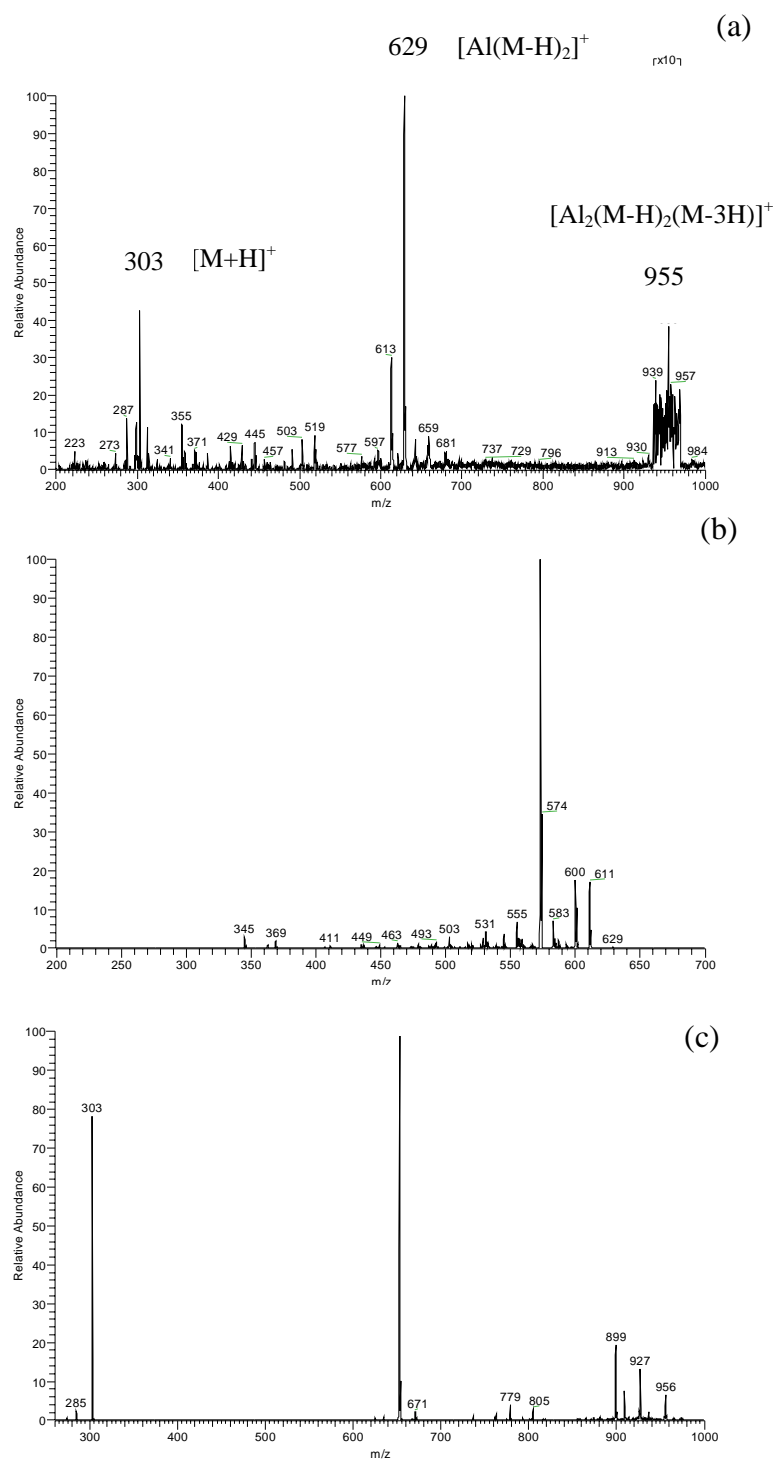


Figure 2.12 (a) Full scan mass spectrum of the Al:M complex, (b) MS^2 spectrum of the m/z 629 ion in Figure 2.12(a), (c) MS^3 spectrum of m/z 629 in Figure 2.12(b) ($629 > 573$), (d) MS^2 spectrum of the m/z 955 ion in Figure 2.12(a).

The full-scan ESI mass spectrum of the Ser:Al:M solution is shown in Figure 2.13. In this spectrum, two Ser:Al:M complexes were detected. The ions for these complexes appeared at m/z 488 and m/z 790, consistent with $[(\text{Ser-H})\text{Al}(\text{M-H})]^+$ and $[\text{SerAl}(\text{M-H})_2]^+$, respectively. Multistage tandem mass spectrometry (MS^n) was also used to study these complexes and provided further structural confirmation. Ions at m/z 458 and 359 were present in the MS^2 spectrum of m/z 488 (Figure 2.13(b)). The m/z 458 ion is formed from neutral loss of CH_2O (-30 Da) and the signal at m/z 359 corresponds to the ion $[\text{Al}(\text{OCH}_3)(\text{M-H})]^+$. Figure 2.13(c) shows the MS^3 spectrum of the m/z 488 ion ($488 > 458$) in which the m/z 426 ion results from loss of CH_3OH from m/z 458. In addition, an MS^n experiment was employed on the m/z 426 fragment ion; the resulting spectrum is shown in Figure 2.13(d) (MS^4 spectrum of m/z 488 ($488 > 458 > 426$)). In this last spectrum, the m/z 426 ion cleaved to produce the m/z 398 ion as a result of the neutral loss of CO (-28 Da). The ions at m/z 629 and 488 were present in the MS^2 spectrum of m/z 790 (Figure 2.13(e)). The ion at m/z 629 most likely resulted from neutral loss of *N*-acetyl serine methyl ester (-161 Da) and the m/z 488 ion from the neutral loss of morin (-302 Da).

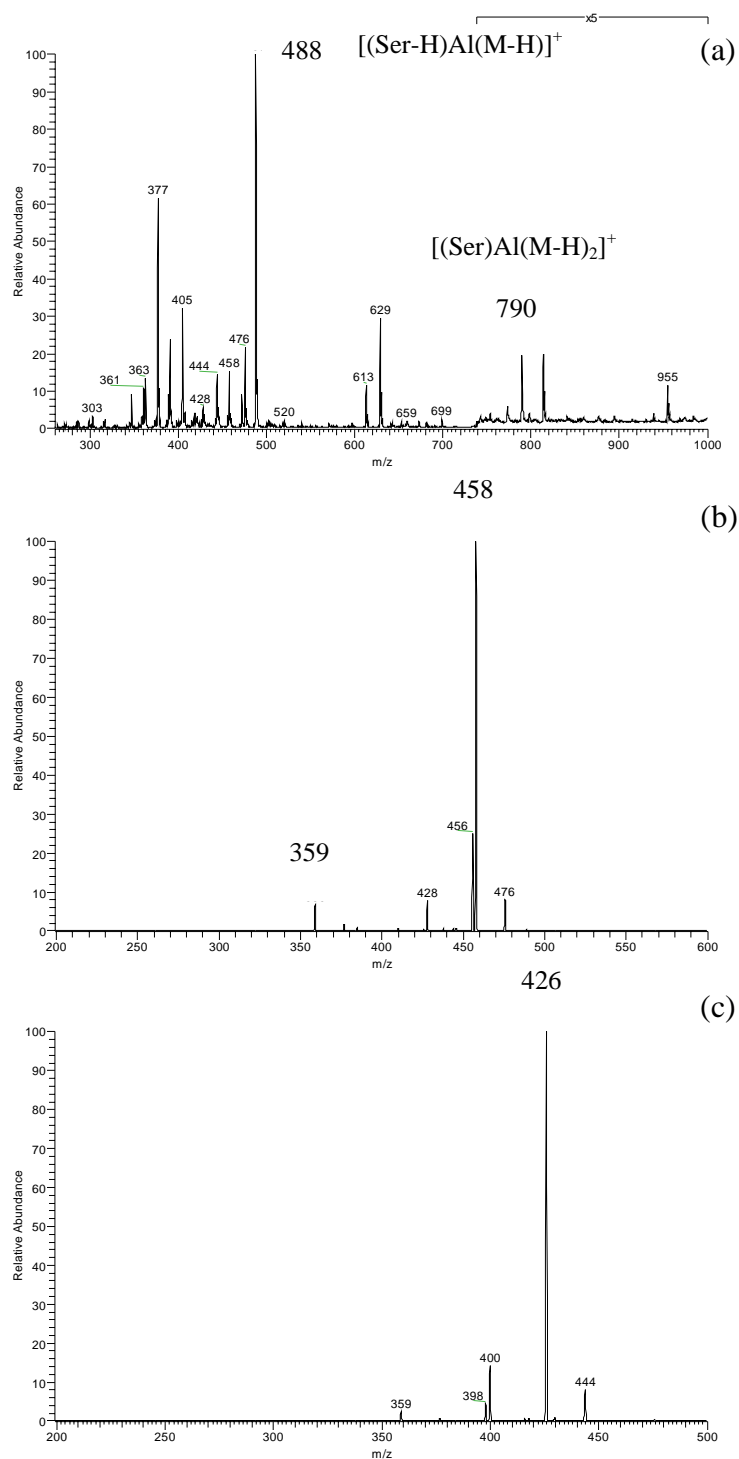


Figure 2.13 (a) Full scan mass spectrum of Ser:Al:M complex, (b) MS² spectrum of the m/z 488 ion in Figure 2.13(a), (c) MS³ spectrum of the m/z 488 (488>458), (d) MS⁴ spectrum of 488 (488>458>426), (e) MS² spectrum of the m/z 790 ion in Figure 2.13(a).

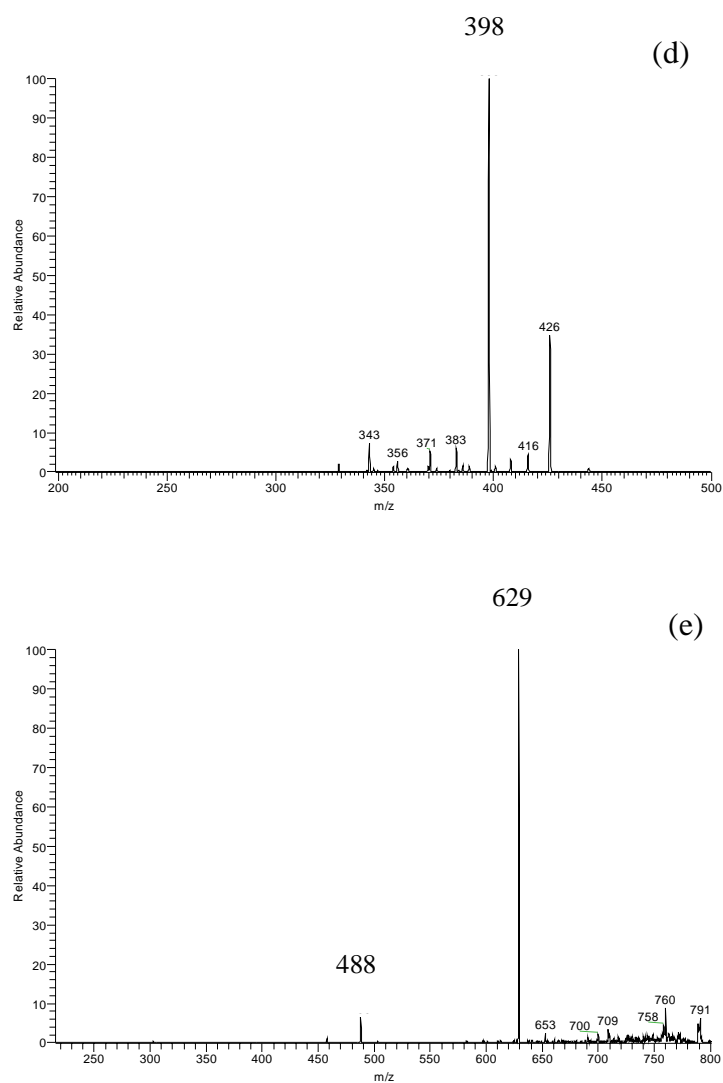


Figure 2.13 (Continued).

2.4.5.2 Ga:M and Ser:Ga:M Complexes

In order to gain further corroboration for the presence of the Al:M and Ser:Al:M complexes, the analogous Ga complexes were assessed. The full-scan ESI mass spectrum of Ga and M complex is shown in Figure 2.14(a). In this spectrum,

two clear Ga:morin complexes were detected with isotopic signature ions at m/z 671, 673 and m/z 1039,1041,1042. High resolution ES-MS substantiated these complex assignments as $[\text{Ga}(\text{M-H})_2]^+$ and $[\text{Ga}_2(\text{M-H})_2(\text{M-3H})]^+$, respectively. The MS^2 spectrum of m/z 672 (Figure 2.14(b)) indicated fragment ions for the neutral loss of H_2O (-18 Da), CHO (-29 Da) and $\text{C}_3\text{H}_4\text{O}$ (-56 Da) at m/z 653, 655; m/z 642, 644 and m/z 615, 617, respectively. The same fragmentation pattern was observed with the corresponding Al:M complex. In addition, in the MS^2 spectrum of m/z 1041 (Figure 2.14(c)), it was found that the most intense fragment ion (m/z 739) resulted from the neutral loss of $\text{C}_{15}\text{H}_{10}\text{O}_7$ (morin).

The full-scan ESI mass spectrum of the Ser:Ga:M solution is shown in Figure 2.15(a). In this spectrum, two Ser:Ga:M complexes were apparent from the ion peaks at m/z 530, 532 and m/z 831, 833. The high resolution ES-MS analysis indicated these complexes were most likely to have the compositions $[(\text{Ser-H})\text{Ga}(\text{M-H})]^+$ and $[\text{SerGa}(\text{M-H})_2]^+$, respectively. The ions at m/z 500, 502 and 401, 403 were present in the MS^2 spectrum of m/z 531 (Figure 2.15(b)). The m/z 500, 502 ions are most likely from the neutral loss of CH_2O (-30 Da), and m/z 401, 403 from the neutral loss of $\text{C}_5\text{H}_7\text{NO}_3$ from the serine analog component resulting in $[\text{Ga}(\text{OCH}_3)(\text{M-H})]^+$. The ions at m/z 671, 673 and 530, 532 were present in the MS^2 spectrum of m/z 833 (Figure 2.15(a)). The gallium containing ions at m/z 671, 673 ion are likely to arise from neutral loss of *N*-acetyl serine methyl ester (-161 Da) and the m/z 530, 532 ions from the neutral loss of morin (-302 Da).

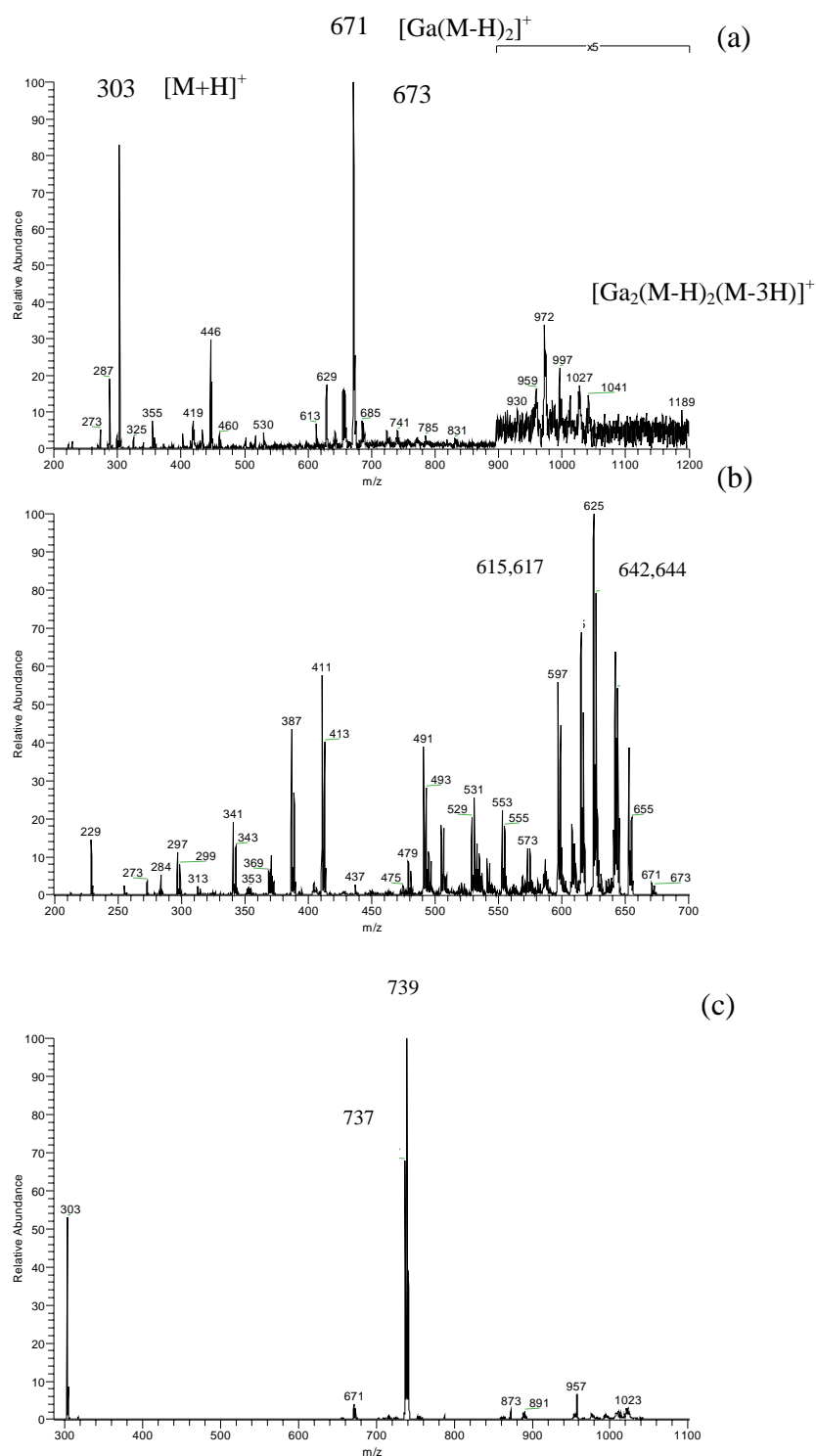


Figure 2.14 (a) Full scan mass spectrum of Ga:M complex, (b) MS^2 spectrum of the m/z 672 ion in Figure 2.14(a), (c) MS^2 spectrum of the m/z 1041 ion in Figure 2.14(a).

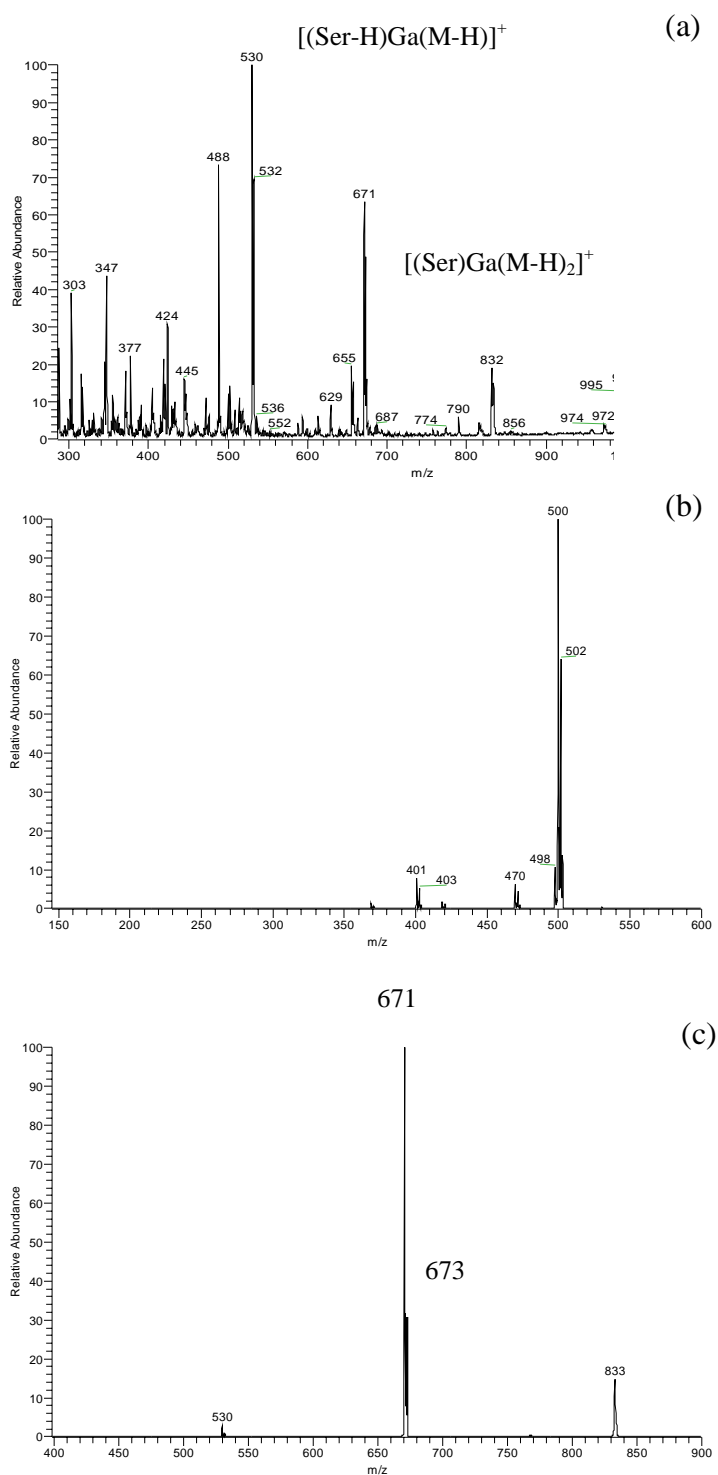


Figure 2.15 (a) Full scan mass spectrum of the Ser:Ga:M complex, (b) MS² spectrum of the m/z 530 ion in Figure 2.15(a), (c) MS² spectrum of the m/z 832 ion in Figure 2.15(a).

2.4.5.3 Al:Q and Ser:Al:Q complexes

The full-scan ESI mass spectrum for the Al and Q complexing is shown in Figure 2.16(a). In this spectrum, an Al:Q complex was apparent, with a peak at m/z 629. On the basis of molecular mass and assuming a single positive charge the complex ion was assigned as $[\text{Al}(\text{Q-H})_2]^+$. In order to obtain more structure information on this Al:Q complexes further analysis using multistage tandem mass spectrometry (MS^n) were performed. Three ions at m/z 611, 601 and 573 were present in the MS^2 spectrum of m/z 629 (Figure 2.16(b)). The ion at m/z 611 most likely arises from the neutral loss of H_2O (-18 Da). The ion at m/z 601 is from the neutral loss of CO (-28 Da). The most intense fragment ion (m/z 573) is consistent with the neutral loss of $\text{C}_3\text{H}_4\text{O}$ (-56 Da), a fragment loss which was also dominant with the Al:M complex.

The full-scan ESI mass spectrum of Ser Al and Q complexing is shown in Figure 2.17(a). In this spectrum, two Ser:Al:Q complexes are obviously found, which are at m/z 488 and m/z 790. According to the molecular weight and assuming a single positive charge, it is proposed that the complexes are most probably $[(\text{Ser-H})\text{Al}(\text{Q-H})]^+$ and $[\text{SerAl}(\text{Q-H})_2]^+$, respectively. Multistage tandem mass spectrometry (MS^n) was also used to study these complexes. The ions at m/z 458 and 359 were present in the MS^2 spectrum of m/z 488 (Figure 2.17(b)). The m/z 458 ion is from neutral loss of CH_2O (-30 Da) and m/z 359 is most likely to be $[\text{Al}(\text{OCH}_3)(\text{M-H})]^+$. Figure 2.17(c) shows the MS^2 spectrum of the m/z 790 ion ($790 > 759$) in which the ion at m/z 426 results from neutral loss of CH_3O from m/z 790.

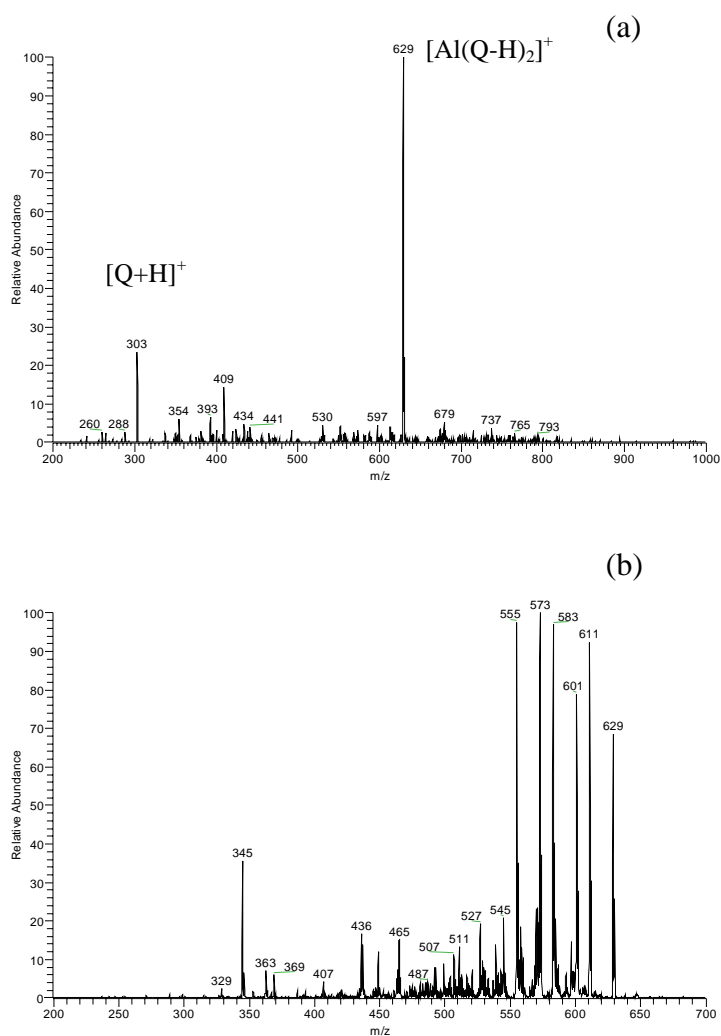


Figure 2.16 (a) Full scan mass spectrum of the Al:Q complex, (b) MS² spectrum of the m/z 629 ion in Figure 2.16(a).

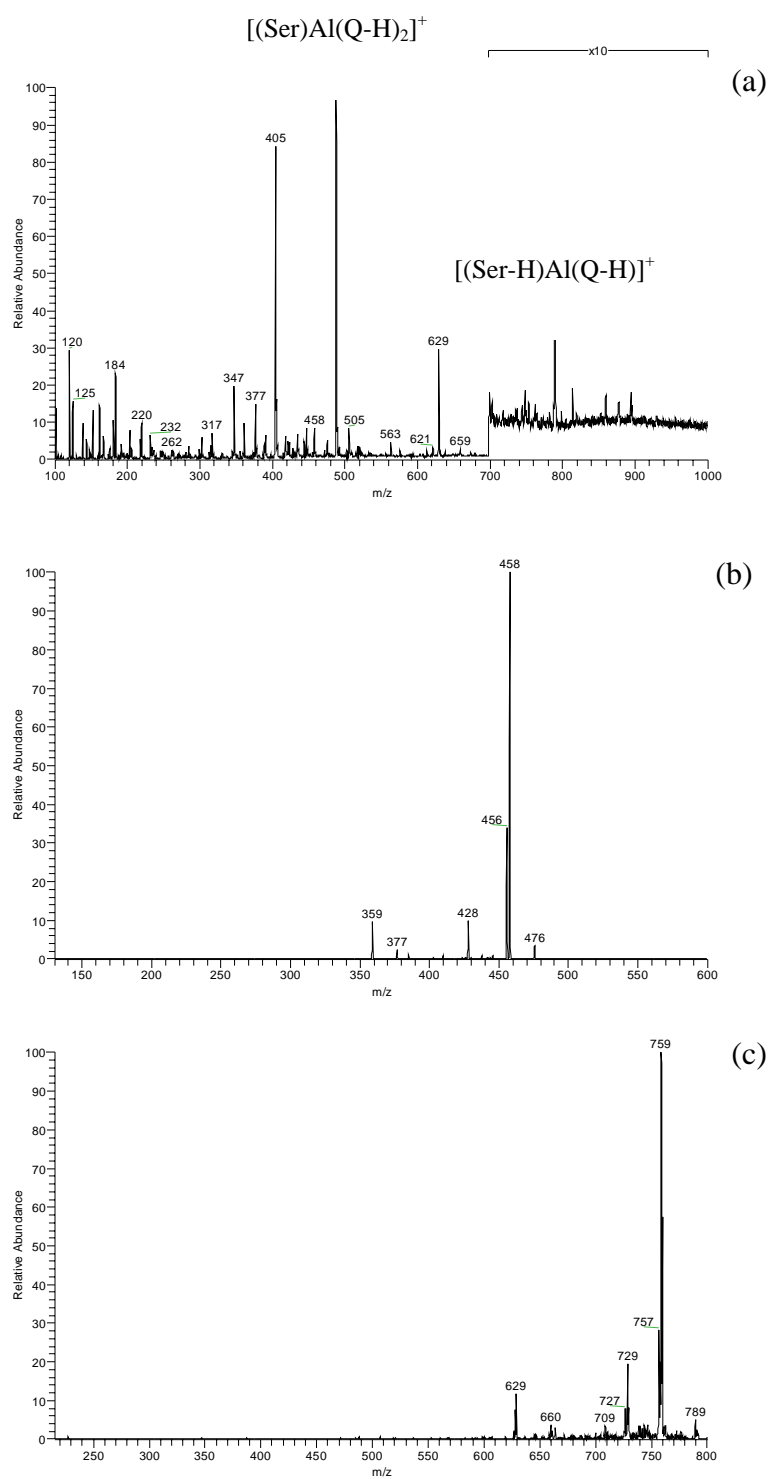


Figure 2.17 (a) Full scan mass spectrum of Ser:Al:Q complex, (b) MS^2 spectrum of the m/z 488 ion in Figure 2.17(a), (c) MS^2 spectrum of the m/z 790.

2.4.5.4 Ga:Q and Ser:Ga:Q complexes

For comparison purposes and in order to obtain possible confirmatory evidence for the Al:Q and Ser:Al:Q complexes, the related Ga(III) ion (referred to as Ga subsequently) was employed in the same experimental. The full-scan ESI mass spectrum resulting from Ga and Q complexing is shown in Figure 2.18(a). In this spectrum, one Ga:Q complexes was found, with ions at m/z 671, 673, corresponding to the two Ga isotopes (^{69}Ga and ^{71}Ga). According to the molecular weight and the single charge, it was demonstrated that the complex ion was $[\text{Ga}(\text{Q-H})_2]^+$. The MS^2 spectrum of m/z 672 (Figure 2.18(b)) showed a neutral loss of H_2O (-18 Da), CHO (-29 Da) and $\text{C}_3\text{H}_4\text{O}$ (-56 Da) with resultant ions at m/z 653, 655; m/z 642, 644 and m/z 615, 617, respectively. The same fragmentation pattern was evident with Al:Q.

The full-scan ESI mass spectrometric analysis of the Ser Ga and Q complexing is shown in Figure 2.19(a). In this spectrum, two Ser:Ga:Q complexes were detected on the basis of Ga-isotopic ions at m/z 530, 532 and m/z 831, 833. According to the molecular weight, it is most likely that the complexes are $[(\text{Ser-H})\text{Ga}(\text{Q-H})]^+$ and $[\text{SerGa}(\text{Q-H})_2]^+$, respectively. Ions at m/z 500, 502 and 401, 403 were present in the MS^2 spectrum of m/z 531 (Figure 2.19(b)). The m/z 500, 502 ions correspond to the neutral loss of CH_2O (-30 Da), while those at m/z 401, 403 were attributed to the species $[\text{Ga}(\text{OCH}_3)(\text{Q-H})]^+$ in which the methoxide ligand was derived from the serine methyl ester derivative. Ions at m/z 671, 673 and 530, 532 were present in the MS^2 spectrum of the ion at m/z 833 (Figure 2.19(c)). The ions at m/z 671, 673 ion are from neutral loss of *N*-acetyl serine methyl ester (-161 Da) and the m/z 530, 532 ion are from the neutral loss of quercetin (-302 Da), providing further support for the complex composition proposed.

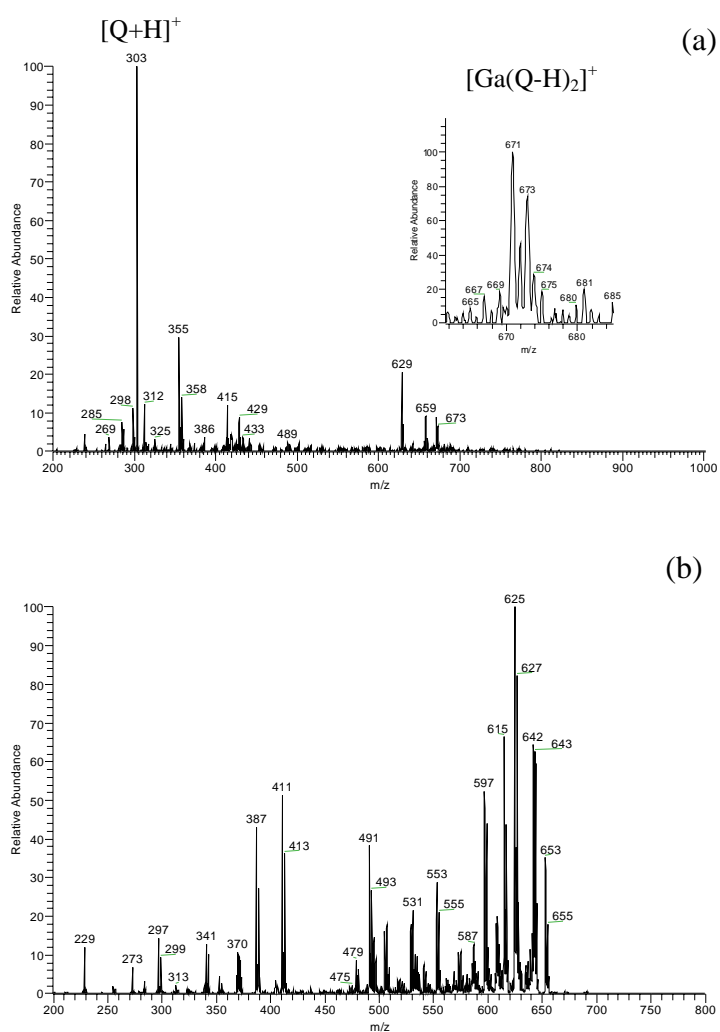


Figure 2.18 (a) Full scan (ES⁺) mass spectrum of the Ga:Q complex, (b) MS² spectrum of the m/z 672 ion in Figure 2.18(a).

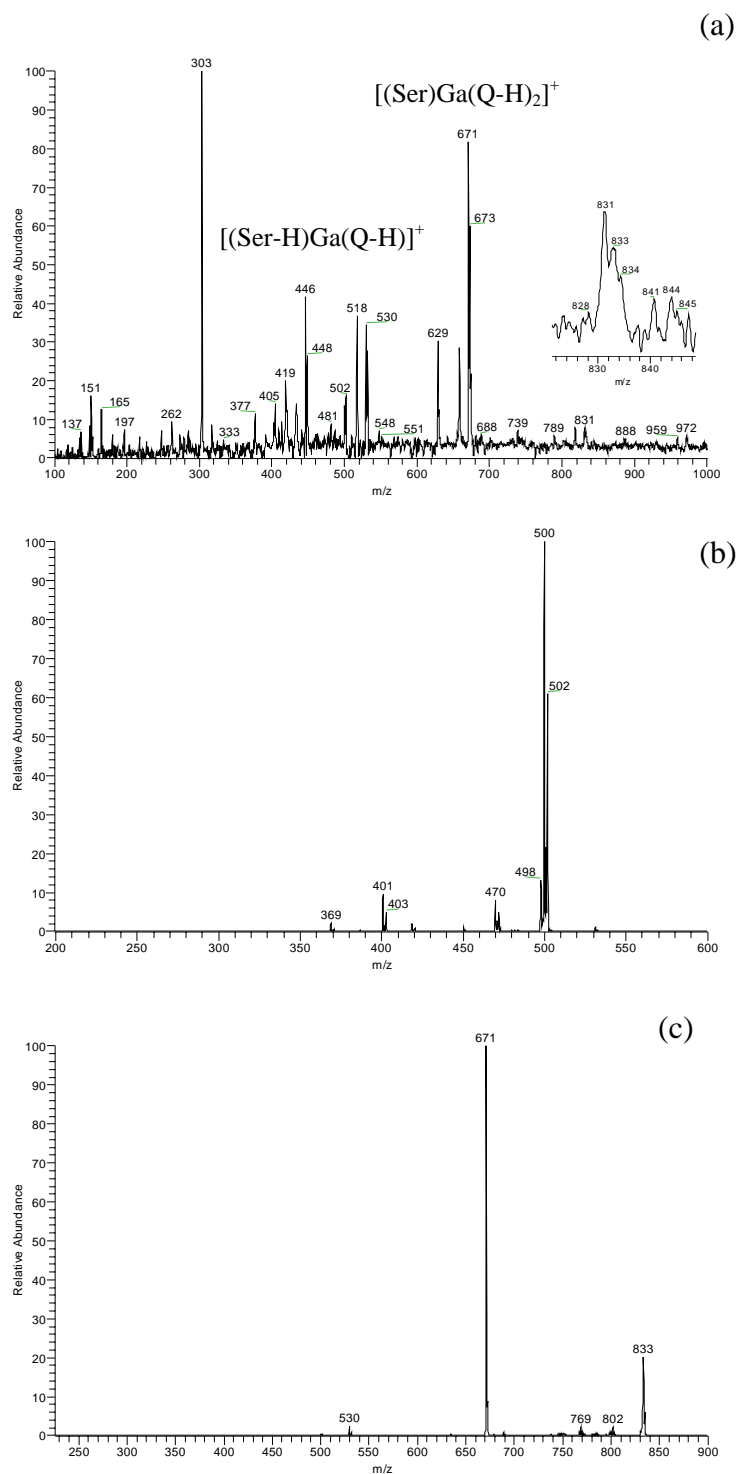


Figure 2.19 (a) Full scan (ES^+) mass spectrum of the Ser:Ga:Q complex, (b) MS^2 spectrum of the m/z 530 ion in Figure 2.19(a), (c) MS^2 spectrum of the m/z 832 ion in Figure 2.19(a).

2.4.6 High resolution mass spectrometry

High-resolution mass spectrometry for the determination of the accurate masses of AlM₂, GaM₂, SerAlM, SerGaM, SerGaM₂, AlQ₂ and SerAlQ complexes was performed on a QTOF Ultima mass spectrometer fitted with a lockspray source. The obtained exact mass measurements for all complexes, listed in Table 2.1, were between -2.9 and 5.2 ppm, well within the commonly accepted 5 ppm error limit. Based on this information, corroborating formulae were then obtained for all the proposed complex ions as shown in Table 2.1. No exact mass was obtained for the very low abundance Ga:Q ion, and similarly for the very weak ion for Ser:Ga:Q₂. The exact mass for the ion from Ser:Ga:Q was not determined.

Table 2.1 Exact mass measurements and elemental compositions for ions derived from AlM₂, GaM₂, SerAlM, SerGaM, SerGaM₂, AlQ₂ and SerAlQ complexes.

Complex	Ion	<i>m/z</i>	Elemental composition	Theoretical value	Experimental value	Δ (ppm)
AlM ₂	[Al(M-H) ₂] ⁺	629	C ₃₀ H ₁₈ O ₁₄ Al	629.0512	629.0539	4.3
GaM ₂	[Ga(M-H) ₂] ⁺	671	C ₃₀ H ₁₈ O ₁₄ Ga	670.9952	670.9952	-0.1
SerAlM	[(Ser-H)Al(M-H)] ⁺	488	C ₂₁ H ₁₉ O ₁₁ NAI	488.0774	488.0795	4.4
SerGaM	[(Ser-H)Ga(M-H)] ⁺	530	C ₂₁ H ₁₉ O ₁₁ NGa	530.0229	530.0214	2.8
SerGaM ₂	[SerGa(M-H) ₂] ⁺	832	C ₃₆ H ₂₉ O ₁₈ NGa	832.0640	832.0616	-2.9
AlQ ₂	[Al(Q-H) ₂] ⁺	629	C ₃₀ H ₁₈ O ₁₄ Al	629.0512	629.0535	3.7
SerAlQ	[(Ser-H)Al(Q-H)] ⁺	488	C ₂₁ H ₁₉ O ₁₁ NAI	488.0774	488.0799	5.2

2.4.7 Computational modeling

Molecular modeling was carried out on Al:M, Ga:M, Ser:Al:M, Ser:Al:M Al:Q, Ga:Q, Ser:Al:Q and Ser:Al:Q complexes by semiempirical PM3 calculations to determine the most probable structure of the complexes (Figure 2.20-2.22). Water

molecules bound to aluminium *via* oxygen were added to obtain an octahedral environment of the complex ions which are the most likely structure of Al(III) complexes in aqueous solution. Table 2.2 shows heat of formation values of Al:M, Ga:M, Ser:Al:M and Ser:Al:M complexes with and without water molecules. In the case of Al:M with water molecules, the opportunity exists to form 3 different dimer structures, and it was found that the heat of formation of the structure (i) (Table 2.2, Al:M) was possibly due to the influence of steric factors (Deng and Van Barkel, 1998). Therefore, in the case of Ga:M the heat of formation of the structure (iii) is the most favored. However, in the case of Al:M without bound water, the heats of formation of AlM₂ complexes (i), (ii) and (iii) are very similar (Table 2.2, Figure 2.20). The computer modeled structures with the serine analog as a co-ligand are shown in Figure 2.21.

Table 2.3 shows heats of formation values of Al:Q, Ga:Q, Ser:Al:Q and Ser:Al:Q complexes with and without water molecule. In the case of Al:Q with water, the heats of formation of AlQ₂ structures for structure (i) is the most favored with the same reason to AlM₂ complexes. Also in case of Ga:Q the heats of formation of the structure (iii) is the most favored. In addition, in case of Al:Q without water the heats of formation of AlQ₂ complexes (i), (ii) and (iii) are very similar. The computer modeled structures with the serine analog as co-ligand are shown in Figure 2.22.

Table 2.2 Calculated heats of formation of Al:M, Ser:Al:M, Ga:M and Ser:Ga:M complexes.

Complex	Ratio	Heat of formation	
		(kJ/mol)	
		With H ₂ O	Without H ₂ O
Al:M	(i) 1:2	-2,296	-1,705
	(ii) 1:2	-2,259	-1,705
	(iii) 1:2	-2,272	-1,704
	(i) 2:3	-4,091	-2,985
	(ii) 2:3	-4,085	-2,989
	(iii) 2:3	-4,094	-2,984
	(iv) 2:3	-4,084	-2,985
Ser:Al:M	(i) 1:1:1	-1,975	-1,453
	(ii) 1:1:1	-1,983	-1,449
	(i) 1:1:2	-	-2,469
	(ii) 1:1:2	-	-2,483
	(iii) 1:1:2	-	-2,452
Ga:M	(i) 1:2	-2,351	-1,605
	(ii) 1:2	-2,368	-1,638
	(iii) 1:2	-2,384	-1,672
	(i) 2:3	-4,424	-2,932
	(ii) 2:3	-4,395	-3,222
	(iii) 2:3	-4,402	-2,961
	(iv) 2:3	-4,463	-2,986
Ser:Ga:M	(i) 1:1:1	-2,206	-1,545
	(ii) 1:1:1	-2,228	-1,575
	(i) 1:1:2	-	-2,690
	(ii) 1:1:2	-	-2,716
	(iii) 1:1:2	-	-2,736

Table 2.3 Calculated heats of formation of Al:Q, Ser:Al:Q, Ga:Q and Ser:Ga:Q complexes.

Complex	Ratio	Heat of formation (kJ/mol)	
		With H ₂ O	Without H ₂ O
Al:Q	(i) 1:2	-2,272	-1,689
	(ii) 1:2	-2,262	-1,687
	(iii) 1:2	-2,260	-1,688
Ser:Al:Q	(i) 1:1:1	-2,002	-1,445
	(ii) 1:1:1	-1,997	-1,442
	(i) 1:1:2	-	-2,449
	(ii) 1:1:2	-	-2,459
	(iii) 1:1:2	-	-2,460
Ga:Q	(i) 1:2	-2,321	-1,590
	(ii) 1:2	-2,358	-1,619
	(iii) 1:2	-2,650	-1,650
Ser:Ga:Q	(i) 1:1:1	-2,207	-1,540
	(ii) 1:1:1	-2,210	-1,566
	(i) 1:1:2	-	-2,656
	(ii) 1:1:2	-	-2,697
	(iii) 1:1:2	-	-2,847

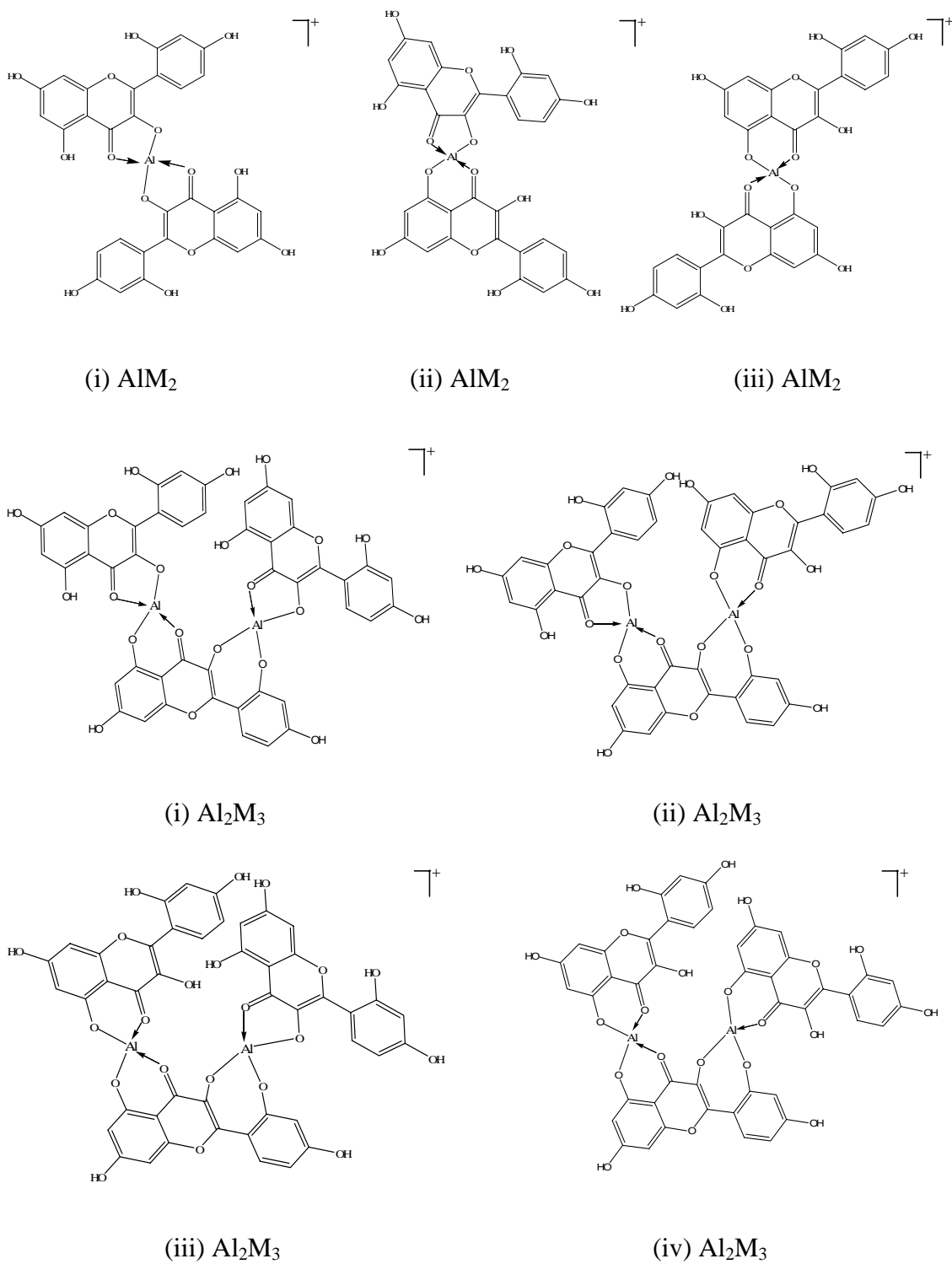


Figure 2.20 Proposed structures of charged AlM_2 and Al_2M_3 complexes without water ligands.

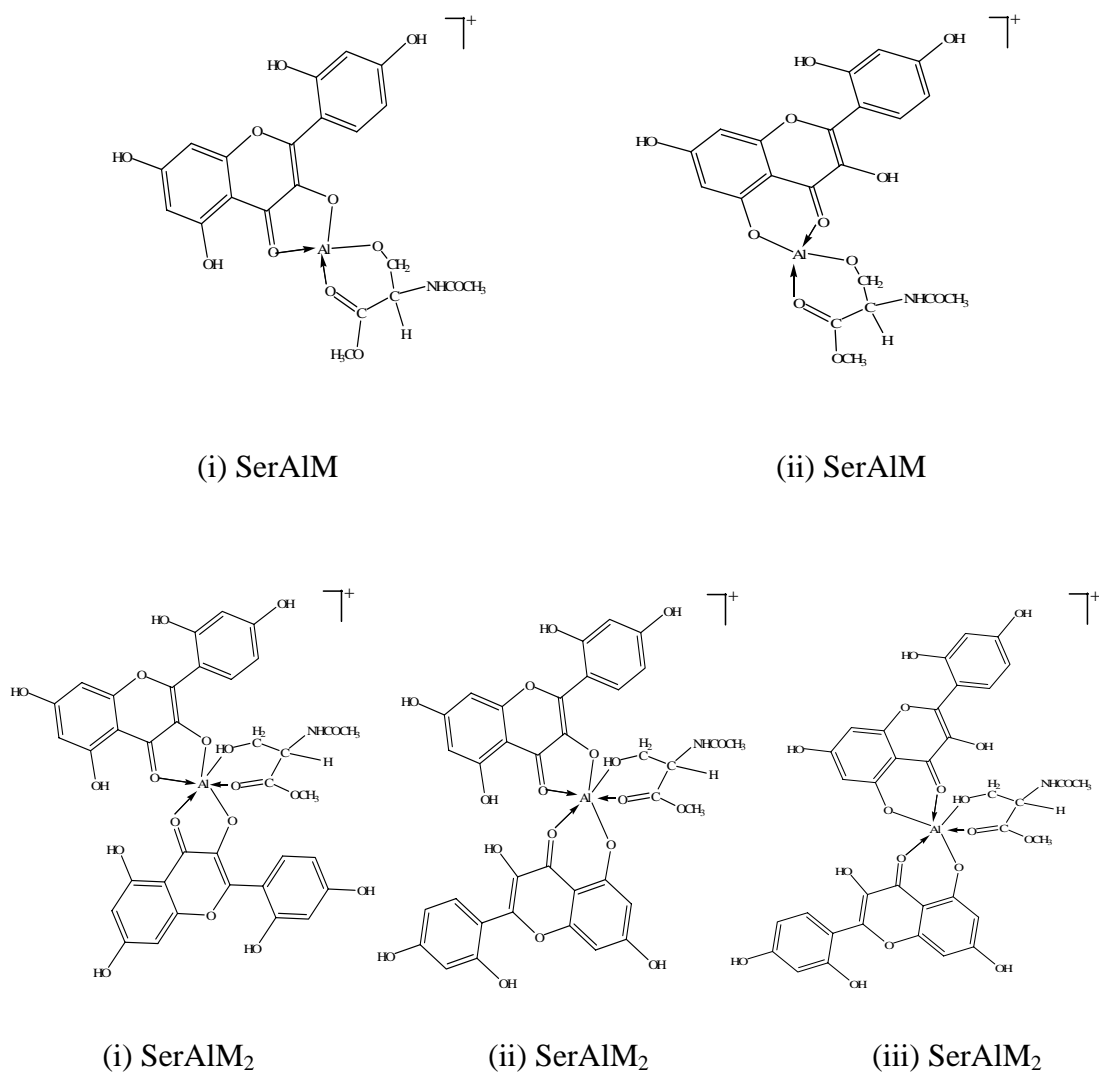


Figure 2.21 Proposed structures of charged SerAlM and SerAlM₂ complexes without water ligands.

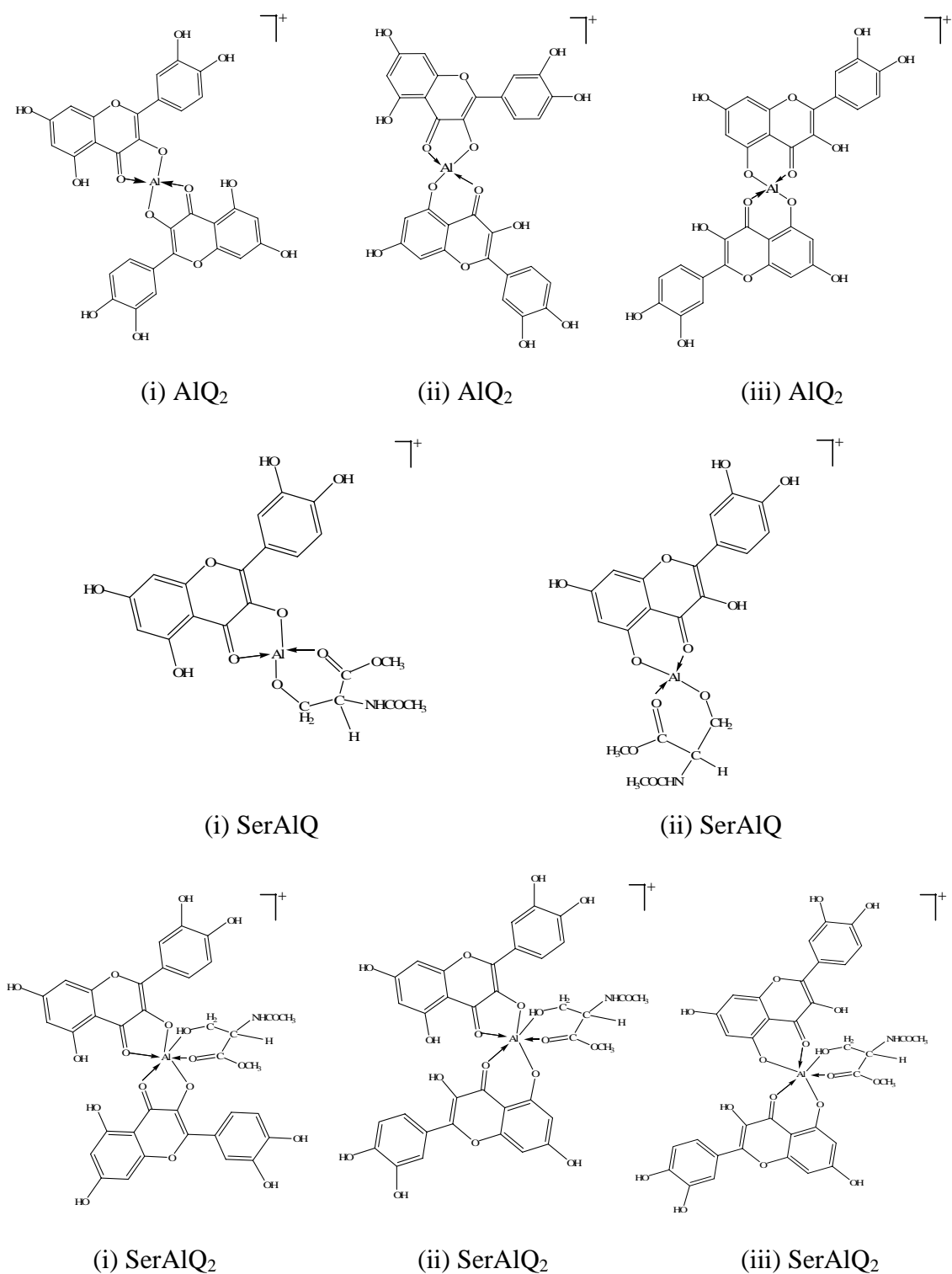


Figure 2.22 Possible ES(+)-MS-supported structures of charged AIQ₂, SerAIQ and SerAIQ₂ complexes.

2.5 Conclusion

Applying the molar ratio method, it was determined that stoichiometric composition of complex formed is Al_3M_2 , AlM and AlQ in aqueous solution. Alum caused a bathochromic shift of the visible absorption bands in morin and quercetin. The bathochromic shifts observed are consistent with the lone pair electrons in the donor atoms (O in the dyes) participating in metal ion coordination and stabilizing the excited state relative to the ground state.

Electrospray mass spectra of $Al:M$, $Ga:M$, $Al:Q$ and $Ga:Q$ complexes show 1:2 stoichiometry for the major complex formed in each case. Calculated heats of formation of complexes were reasonable for both these complexes and indicated possible structures. In aqueous solution the preferred complexes were $AlM_2 \cdot 2H_2O$, $GaM_2 \cdot 2H_2O$, $AlQ_2 \cdot 2H_2O$ and $GaQ_2 \cdot 2H_2O$. The stoichiometries of the Ser: $Al:M$, Ser: $Ga:M$, Ser: $Al:Q$ and Ser: $Ga:Q$ complexes observed mass spectrometrically were 1:1:1 and 1:1:2. These water-excluded structures may have some relevance to those formed in part on interaction with silk.

2.6 References

- Ahmed, M. J. and Hossan, J. (1995). Spectrophotometric determination of aluminium by morin. **Talanta** 42: 1135-1142.
- Bai, Y., Song, F., Chen, M., Xing, J., Liu, Z. and Liu, S. (2004). Characterization of the rutin-metal complex by electrospray ionization tandem mass spectrometry. **Analytical Science** 20: 1147-1151.

- Bechtold, T., Turcanu, A., Ganglberger, E. and Geissler, S. (2003). Natural dyes in modern textile dyehouses-how to combine experiences of two centuries to meet the demands of the future? **Journal of Cleaner Production** 11: 499-509.
- Bhuyan, R. and Saikia, C. N. (2005). Isolation of colour components from native dye-bearing plants in northeastern India. **Bioresource Technology** 96: 363-372.
- Boudet, A. C., Cornard, J. P. and Merlin, J. C. (2000). Conformational and spectroscopic investigation of 3-hydroxyflavone-aluminium chelates. **Spectrochimica Acta Part A: Molecular and Biomolecular Spectroscopy** 56: 829-839.
- Castro, G. T. and Blanco, S. E. (2004). Structural and spectroscopic study of 5,7-dihydroxy-flavone and its complex with aluminum. **Spectrochimica Acta Part A: Molecular and Biomolecular Spectroscopy** 60: 2235-2241.
- Christie, R. M., Mather, M. M. and Wardman, R. H. (2000). **The Chemistry of Colour Application** Oxford: Blackwell Science.
- Cornard, J. P. and Merlin J. P. (2002). Complexes of aluminium(III) with isoquercitrin: spectroscopic characterization and quantum chemical calculations. **Polyhedron** 21: 2801-2810.
- Cornard, J. P., Boudet, A. C. and Merlin, J. C. (2001). Complexes of Al(III) with 3'4'-dihydroxy-flavone: characterization, theoretical and spectroscopic study. **Spectrochimica Acta Part A: Molecular and Biomolecular Spectroscopy** 57: 591-602.
- Cornard, J. P. and Merlin, J. C. (2002). Complexes of aluminium(III) with isoquercitrin: spectroscopic characterization and quantum chemical calculations. **Polyhedron** 21: 2801-2810.

- Cornard, J. P. and Merlin, J. C. (2002). Spectroscopic and structural study of complexes of quercetin with Al(III). **Journal of Inorganic Biochemistry** 92: 19-27.
- Cornard, J. P., and Merlin, J. C. (2003). Comparison of the chelating power of hydroxyflavones. **Journal of Molecular Structure** 651-653: 381-387.
- Cornard, J. P. and Merlin, J. C. (2001). Structural and spectroscopic investigation of 5-hydroxyflavone and its complex with aluminium. **Journal of Molecular Structure** 569: 129-138.
- Deng, H. and Van Berkel, G. J. (1998). Electrospray mass spectrometry and UV/Visible spectrophotometry studies of complexes aluminum(III)-flavonoid complexes. **Journal of Mass Spectrometry** 33: 1080-1087.
- Frenandez, M. T., Mira, M. L., Florêncio, M. H. and Jennings, K. R. (2002). Iron and copper chelation by flavonoids: an electrospray mass spectrometry study. **Journal of Inorganic Biochemistry** 92: 105-111.
- Gutierrez, A. C. and Gehlen, M. H. (2002). Time resolved fluorescence spectroscopy of quercetin and morin complexes with Al³⁺. **Spectrochimica Acta Part A: Molecular and Biomolecular Spectroscopy** 58: 83-89.
- Kaplan, D., Adam, W. W., Farmer, B. and Viney, C. (1994). **Silk polymers: Materials science and Biotechnology**. Washington: American Chemical Society.
- Karmakar, S. R. (1999). **Chemical technology in the pre-treatment processes of textiles**. Amsterdam: Elsevier Science B.V. Hall.
- Lemmens, R. H. M. J. and Wulijarni-Soetjipto, N. (1992). **Plant Resources of South-East Asia 3: Dye and Tannin-Producing Plants**. Bogor Indonesia: Prosea.

- Miyazaki, Y., Hiramatsu, E., Miura, Y. and Sakashita, H. (1999). ²⁷Al NMR studies on the complexation of aluminium(III) with phosphinate and phosphite ions. **Polyhedron** 18: 2041-2045.
- Moeyes, M. (1993). **Natural Dyeing in Thailand**. Bangkok: White Lotus.
- Pikulski, M. and Brodbelt, J. S. (2003). Differentiation of flavonoid glycoside isomer by using metal complexation and electrospray ionization mass spectrometry. **American Society for mass spectrometry** 14: 1437-1453.
- Raisanen, R., Nousiainen, P. and Hynninen, P. H. (2001). Emodin and dermocybin natural anthraquinones as mordant dyes for wool and polyamide. **Textile Research Journal** 71: 1016-1022.
- Satterfield, M. and Brodbelt, J. S. (2001). Structural characterization of flavonoid glycosides by collisionally activated dissociation of metal complexes. **American Society for mass spectrometry** 12: 537-549.
- Satterfield, M. and Brodbelt, J. S. (2000). Enhanced detection of flavonoids by metal complexation and electrospray ionization mass spectrometry. **Analytical Chemistry** 72: 5898-5906.
- Shanker, R. and Vankar, P. S. (2007). Dyeing cotton, wool and silk with *Hibiscus mutabilis* (Gulzuba). **Dyes and Pigments** 74: 464-469.
- Trai, J., Butler, E. C. V., Haddad, P. R. and Bowie, A. R. (2007). Determination of aluminium in natural water samples. **Analytica Chimica Acta** Article in press doi:10.1016/j.aca.2007.02.048.
- Zhang, J., Brodbelt, J. S. and Wang, J. (2004). Threshold dissociation and molecular modeling of transition metal complexes of flavonoids. **American Society for mass spectrometry** 16: 139-151.

Zhang, J., Wang, J. and Brodbelt, J. S. (2005). Characterization of flavonoids by aluminum complexation and collisionally activated dissociation. **Journal of Mass Spectrometry** 40: 350-363.

Zollinger, H. (2003). **Colour Chemistry**. Weinheim: Wiley-VCH.

CHAPTER III

ADSORPTION OF MORIN AND EXTRACTED DYE

FROM *MACLURA COCHINCHINENSIS* (LOUR.)

CORNER DYEING ON SILK

3.1 Abstract

The adsorption kinetic and thermodynamic studies of alum-morin and alum-extracted dye from *M. cochinchinensis* dyeing onto silk fibres indicated that the adsorption capacities are significantly affected by pH, the material to liquor ratio (MLR), the initial dye concentration, and temperature. The initial dye adsorption rates of alum-morin and alum-extracted dye on silk before equilibrium time was reached increased at higher dyeing temperature. The pseudo second-order kinetic model was indicated for both alum-morin and alum-extracted dye dyeing of silk at pH 4.0 with activation energies (E_a) of 45.26 and 18.73 kJ/mol respectively. The values of the enthalpy for the alum-morin and alum-extracted dye dyeing on silk at pH 4.0 were -31.29 and -14.16 kJ/mol, respectively. Also, the free energy (ΔG°) and entropy changes (ΔS°) for the alum-morin and alum-extracted dye dyeing on silk were determined. The experimental isotherm data were analyzed using the Langmuir and Freundlich equations. Additionally, adsorption-desorption of morin, alum-morin and alum-extracted dye dyeing onto silk were investigated.

3.2 Introduction

Natural dyes were the main source of textile colour until the mid- to late- 19th century. Flavonoids (flavones and flavonols) are the main chromophores in the most commonly used yellow dyes. The most common yellow dyes were extracted from several kinds of plants such as *Reseda luteola*, *Sophora japonica*, *Butea monosperma*, etc as mentioned in section 1.1.1.1.

Morin is the flavonoid yellow colouring substance in the wood, which is the major component of the heartwood of *M. cochinchinensis* (Dechsree, 1998). In Thailand, it is widely used by the villagers, especially in the northeast, for dyeing of fibres which yields a beautiful yellow colour (Moeyes, 1993).

Silk fibres are made up of a protein called fibroin. This protein is constructed from layers of anti-parallel beta pleated sheets which run parallel to the silk fibre axis. Each chain of fibroin is made up of multiple repeats of the sequence (Gly-Ser-Gly-Ala-Gly-Ala)_n, where Gly, Ala and Ser refer to glycine, alanine and serine respectively (Kaplan *et al.*, 1994). Like wool, silk fibres contain carboxyl and protonated amino groups which result in its amphoteric characteristics (Carr, 1995). Under acid conditions the carboxyl groups are unionized, leaving a net positive charge which enables dye anions to be adsorbed (Carr, 1995). Many studies have been undertaken to investigate protein fibres dyeing. For instance, the crude water extract of saffron stigmas and crocin were used for dyeing wool fibre after enzymatic treatment (Tsatsaroni, Liakopoulou-Kyriakides and Elefthiadis, 1998). The results showed that wash and light fastness values were satisfactory. In addition, emodin and dermocybin natural anthraquinones as mordant dyes for wool and polyamide have

been investigated (Raisanen, Nousiainen and Hynninen, 2001). It was found that the wool and polyamide have a high uptake for the pure natural anthraquinones.

To understand the silk dyeing process, the adsorption kinetic and thermodynamics of dyeing have been studied. An adsorption and kinetic studies of lac dyeing on silk were investigated (Chairat, Rattanaphani, S., Bremner and Rattanaphani, V., 2005). It was found that the experimental data fitted well to the Langmuir and Freundlich isotherms with a high correlation coefficient (R^2). The pseudo second-order kinetic model was indicated with the activation energy of 47.5 kJ/mol. It is suggested the overall rate of lac dye adsorption is likely to be controlled by the chemical process. The kinetics of wool dyeing with acid dye have also studied (Bruce and Broadwood, 2000). They found that the uptake rate of the acid dye is likely to be a second order reaction. The kinetics can be explained in terms of the rate controlling step, which in this case is the reaction between the dye anion and the attachment site, rather than diffusion of the dye to the attachment site. In addition, thermodynamics of adsorption of laccaic acid on silk were investigated (Kongkachuichay, Shitangkoon and Chinwongamorn, 2002). It was found that the adsorption isotherm obtained was identified to be a Langmuir type. The values of heat and entropy of dyeing were also reported.

In the north and the northeast of Thailand, extracted dye from *M. cochinchinensis* is used as a natural yellow dyestuff for silk dyeing but the fastness properties and reproducibility to give consistency in production are still problems to be solved. As part of the approach to tackle these problems, fundamental physical studies on the dyeing process are important.



Figure 3.1 Morphological illustration *Maclura cochinchinensis* (Lour.) Corner
Brisbane Rainforest Action & Information Network. (2007)
(left hand side) and its heartwood from Surin, Thailand (right hand side).

As mentioned in Chapter II, morin is a major component of the heartwood of the plant *M. cochinchinensis* and aqueous extracts of the wood of this plant are used for the dyeing of silk. However, the use of this natural dye mixture is often linked to poor fastness properties and thus metal-based mordants are used to increase fastness (e.g. wash fastness) properties. The aluminium and morin complexes have been investigated. In addition, aluminium-morin complexes were mixed with *N*-acetyl serine methyl ester which is derivative of component in silk fibre and these complexes were proposed the possible structure by computational modeling. Therefore, the

adsorption of morin and extracted dye from *M. cochinchinensis* on silk yarn will be measured and determined quantitatively in relation to dye solution pH values, contact time, initial dye concentration, and material to liquor ratio (MLR) in this research. In addition, the Langmuir and Freundlich equations will be used to fit the equilibria of dyeing on silk yarn. The scientific results from this study will hopefully give a better understanding of the adsorption mechanism in this dyeing process. Since quercetin is a minor component in this plant. The study of this dye will not be followed in this section.

3.2.1 Physical chemistry of dyeing process

The scientific investigation of the dyeing processes involves two experimental methods which can be described by dyeing kinetics and dyeing equilibria (Zollinger, 2003). The dyeing process involves the distribution of a dye between at least two phases, namely dye bath and substrate. The distribution process is called adsorption if the substance which is to be distributed is retained by a surface (e.g. gas on a solid). If the substance does not stay at the surface but enters the interior of a body (e.g. gas in liquid), the process is termed sorption. Dyeing processes of water soluble dyes in aqueous dye baths with any substrate always requires a distribution process between two phases (dye bath and substrate) (Perkins, 1996). The kinetics of dyeing are represented by dye uptake curves which give the rate of transfer of dye in solution from the dye bath into the substrate. The position of sorption versus desorption after infinite time is represented by the dyeing equilibria of the dyeing process. Graphical representations of a dyeing process are shown in Figure 3.2, by the dye uptake curves (left hand side) and dyeing isotherms (right hand side).

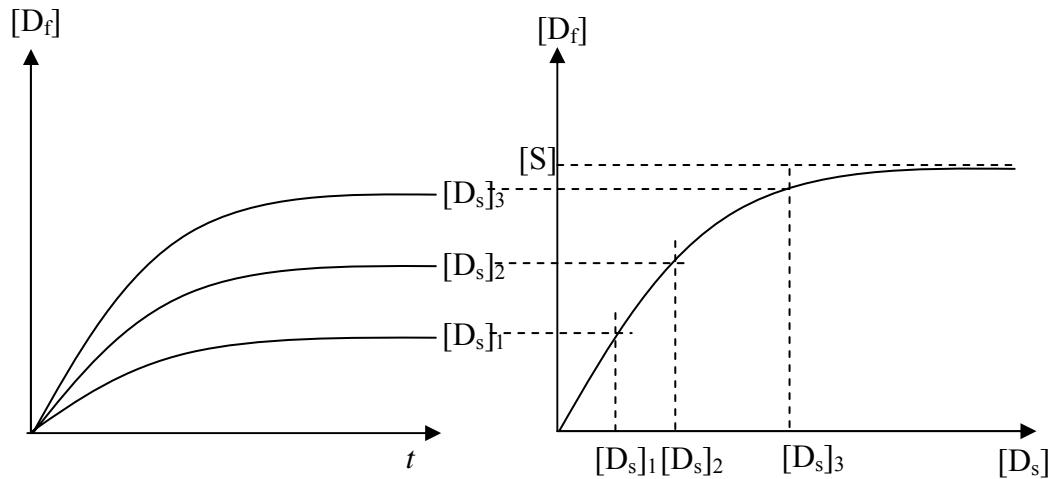


Figure 3.2 Graphical representation of a dyeing process: kinetics (left) and equilibrium (right) (Zollinger, 1991).

$[D_s]$: concentration of dye in solution $[D_f]$: concentration of dye in substrate
 t : time $[S]$: saturation value

If the dyeing process was done under different isothermal conditions, a series of curves (Perkins, 1996) are given, as shown in Figure 3.3. The initial adsorption rate increases with an increasing in dyeing temperature. This can be explained by the fact that the dye adsorption by fibres at higher temperature is faster than that at lower temperature and hence leads to increase the initial rate constant. The slope of curve varies depending on the temperature, type of fibre, type of dye, amount of agitation of the dye bath, amount and type of dyeing auxiliaries used and other factors. As the amount of dye on the fibres increases, the sites being covered, and as a result the dye

must leave the surface and diffuse toward the interior of the fibre before additional dye molecules can be adsorbed from the dye bath.

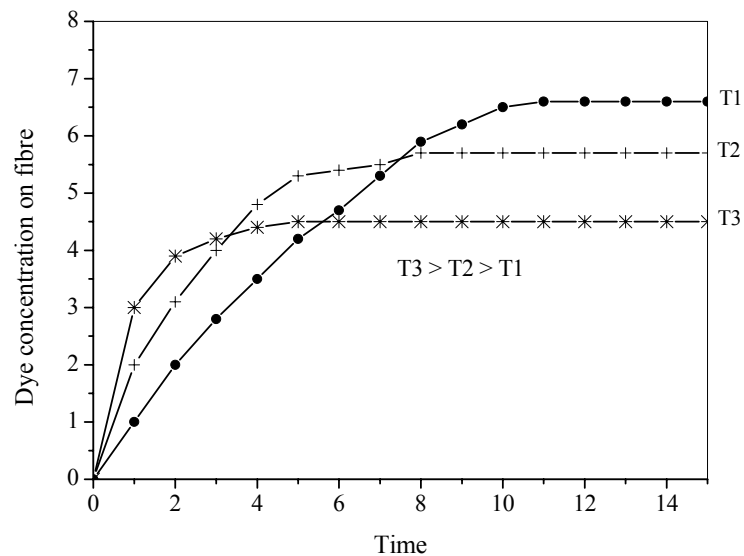


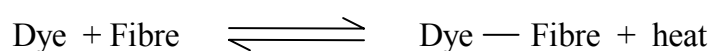
Figure 3.3 Rate of dyeing isotherms (Perkins, 1996).

The kinetic behaviour of a dye in the dyeing of a textile material comprises at least four stages (Zollinger, 2003):

- (a) convectional diffusion to the fibre surface, occurring in the dye bath;
- (b) molecular diffusion through the hydrodynamic boundary layer;
- (c) adsorption at the outer surface;
- (d) molecular diffusion into the fibre (sorption).

The stages (a), (c) and (d) are important for the kinetics of the overall dyeing process. After some period of time, the slope of the isotherm becomes flat indicating that the system has reached equilibrium. The time required to reach equilibrium is always shorter at higher dyeing temperature. It is mainly due to the fibres containing

more dye at higher temperatures in the early stages but less dye in the latter stages of dyeing. Therefore, an increasing in the temperature leads to an increase in the dyeing rate but a decrease in the ultimate exhaustion after the equilibrium time, as shown in Figure 3.3. This shows that dye molecules can adsorb to a greater degree at a lower temperature because the dyeing reaction is exothermic.



Desorption of dye molecules from fibres to dye bath takes place at higher dyeing temperatures because of more heat in the dyeing process. Thus, the equilibrium position of this process is shifted to the left hand side.

There are several different intermolecular and intramolecular interactions that are essential for understanding the chemistry of textile dyeing. The four main types of interactions are covalent forces, ionic forces, Van der Waal's forces, hydrogen bonds and electrostatic forces (Christie, 2000; Zollinger, 2003) and will be described below:

Covalent forces

Covalent forces result from the sharing of a pair of electrons by two atoms. An especially important use of covalent bonding in colour application technology is the application of reactive dyes to cellulosic and protein textile fibres (Christie, 2000). After dyeing fibres with reactive dyes, the dyes interact chemically with the fibres to form a covalent bond.

Ionic forces

An ionic bond is formed by electron transfer from one atom to another atom or atoms. The atom that loses electrons becomes a positive-charged species or cation.

The atom that gains the electrons becomes a negative-charged species or anion. Ionic bonds are the resulting electrostatic attraction between these oppositely charged ions. In the dyeing of wool, silk and polyamides with anionic dyes, these fibres contain amino and carboxyl groups. Depending on the pH value in dyeing process, under lower pH these fibres have an overall positive charge (NH_3^+) because the carboxyl groups in the side chains are hardly ionized under acid condition. Therefore, anionic dyes are attracted towards the positively charged amino acid by ionic forces (Chairat *et al.*, 2005).

Van der Waal's forces

Van der Waal's forces or dispersion forces are the forces of attraction involved between non-polar molecules (Christie, 2000). The distances between molecules have an important effect on the strength of van der Waals forces. They are the weakest intermolecular forces. Although in a non-polar molecule there is no overall charge distribution, the electrons are in constant motion so that at any instant, small dipoles will be present. These instantaneous dipoles in turn induce oppositely-oriented dipoles in neighbouring molecules and a weak attraction between the molecules results. Van der Waals forces are therefore only effective for sorption of dyes to fibre molecules if the distance between the dye and the fibre molecules is small. The influence of Van der Waal's forces particularly important in dyeing of cellulosic fibres.

Hydrogen bonding

Hydrogen bonding is an especially strong type of dipole-dipole interactions. This interaction occurs between molecules containing a hydrogen atom which can interact with a nitrogen, oxygen, or fluorine atom (Christie, 2000). A partially positive hydrogen atom of one molecule is attracted to the unshared pair of electrons of the

electronegative atom of another molecule. Intermolecular and intramolecular hydrogen bonding between function groups on dye molecules and fibre molecules play important role in many interaction dye-fibre systems.

Dipolar forces

Dipole-dipole interactions may make a contribution to the forces of attraction between dye and fibre molecules (Christie, 2000). Dipolar intermolecular forces involve the attraction of the positive centers in one polar molecule for the negative centers in another. As a result of these forces, polar molecules are generally attracted to each other more strongly than are non-polar molecules of comparable molecular size. Non-polar molecules are attracted to each other by weak dipole-dipole interactions called London forces. London forces arise from dipoles induced in one molecule by another so a weak attraction between the molecules results. However, as the charges are only partial, dipolar-dipole interactions are weaker than ionic forces.

3.2.2 Kinetic models of adsorption

In order to investigate the controlling mechanism adsorption processes such as mass transfer, diffusion control and chemical reaction, several methods have been used to test the experimental data. A simple kinetic analysis of adsorption is the Lagergren equation. The Lagergren equation, a pseudo first order equation, describes the kinetics of the adsorption process as follows (Ho, 1998; Wu, 2001; Chiou, 2002; Chiou, 2003; Doğan, 2003; Chairat, 2005; Uzun, 2006):

$$\frac{dq_t}{dt} = k_1(q_e - q_t) \quad (3.1)$$

where k_1 is the rate constant of pseudo first-order adsorption (s^{-1}), and q_e and q_t are the amount of dye adsorbed per gram silk (mg/g silk) at equilibrium and time t . After definite integration by applying the initial conditions $q_t = 0$ at $t = 0$ and $q = q_t$ at $t = t$, equation (3.1) becomes

$$\ln (q_e - q_t) = \ln q_e - k_1 t \quad (3.2)$$

A straight line of $\ln(q_e - q_t)$ versus t suggests the applicability of this kinetic model to fit the experimental data. The first-order rate constant k_1 and equilibrium adsorption density q_e were calculated from the slope and intercept of this line.

In addition, the pseudo second order kinetic model (Ho and McKay, 1998; Ho and McKay, 1999; Wu, Tseng and Juang, 2001; Chairat *et al.*, 2006) is based on adsorption equilibrium capacity and can be expressed as:

$$\frac{dq_t}{dt} = k_2 (q_e - q_t)^2 \quad (3.3)$$

where k_2 (g silk/mg min) is the rate constant for pseudo second-order adsorption. Integrating equation (3.3) and applying the initial conditions gives:

$$\frac{1}{(q_e - q_t)} = \frac{1}{q_t} + k_2 t \quad (3.4)$$

or equivalently,

$$\frac{t}{q_t} = \frac{1}{k_2 q_e^2} + \frac{1}{q_e} t \quad (3.5)$$

and

$$h_i = k_2 q_e^2 \quad (3.6)$$

where h_i (Chiou and Li, 2003; Chairat *et al.*, 2005; Chairat *et al.*, 2006) is the initial dye adsorption rate (mg/g silk min). If the pseudo second order kinetics are applicable, the plot of t/q_t versus t show a linear relationship. The slope and intercept of (t/q_t) versus t were used to calculate the pseudo second-order rate constant k_2 and q_e . It is likely that the behaviour over the whole range of adsorption is in agreement with the chemisorption mechanism being the rate-controlling step (Chiou and Li, 2002).

In general, the rates of chemical reactions increase with an increase in the temperature. In the rate law, temperature dependence appears in the rate constant. The dependence of rate constants on temperature over a limited range can usually be represented by an empirical equation proposed by van't Hoff and Arrhenius in 1884 (Laidler *et al.*, 2003):

$$k = A e^{-E_a/RT} \quad (3.7)$$

where A is the pre-exponential factor, E_a is the activation energy and R is the gas constant, equal to $8.3145 \text{ J K}^{-1} \text{ mol}^{-1}$. The pre-exponential factor A has the same units as the rate constant. An alternative form is obtained by taking the logarithm of each side.

$$\ln k = \ln A - \frac{E_a}{RT} \quad (3.8)$$

A straight line is obtained by plotting of the logarithm of the rate constant against with the reciprocal of the absolute temperature. Such a graph is often referred to as an Arrhenius plot. The magnitude of activation energy may give an idea about the type of adsorption. There are two main types of adsorption: physical and chemical are possible. In physical adsorption the reaction is easily reversible, equilibrium is rapidly attained and its energy requirements are small. The activation energy for physical adsorption is usually no more than 4.2 kJ/mol, because the forces involved in physical adsorption are usually weak. So the activation energy is of the same magnitude as the heat of chemical reactions. This type of adsorption is usually referred to as *physisorption*. However, chemical adsorption is specific and involves forces much stronger than in physical adsorption. It is usually referred to as *chemisorption* (Aksu, 2002).

The enthalpy (ΔH^\ddagger), entropy (ΔS^\ddagger) and free energy (ΔG^\ddagger) of activation can be also calculated using the Eyring equation (House, 1997; Laidler *et al.*, 2003) as follows:

$$\ln \left(\frac{k}{T} \right) = \ln \left(\frac{k_b}{h} \right) + \frac{\Delta S^\ddagger}{R} - \frac{\Delta H^\ddagger}{RT} \quad (3.9)$$

where k_b and h refer to the Boltzmann's constant and the Planck's constant respectively. The enthalpy (ΔH^\ddagger) and entropy (ΔS^\ddagger) of activation were calculated from

the slope and intercept of a plot of $\ln(k/T)$ versus $1/T$. Gibbs energy of activation (ΔG^\ddagger) can be written in terms of enthalpy and entropy of activation ((House, 1997; Laidler *et al.*, 2003):

$$\Delta G^\ddagger = \Delta H^\ddagger - T\Delta S^\ddagger \quad (3.10)$$

3.2.3 Adsorption isotherms

The equilibrium adsorption is fundamental in describing the interaction behaviour between solutes and adsorbents, and is important in the design of an adsorption system. Adsorption isotherm data are commonly fitted to the Langmuir isotherm and the Freundlich isotherm as follows:

3.2.3.1 The Langmuir isotherm

A basic assumption of the Langmuir theory is that sorption takes place at specific homogeneous sites within the adsorbent. It is then assumed that once a dye molecule occupies a site, no further adsorption can take place at that site. The Langmuir adsorption isotherm has been successfully applied to many other real sorption processes (Ho and McKay, 1998; Carrillo, Lis and Valleperas, 2002; Kongkachuichay *et al.*, 2002; Chairat *et al.*, 2005; Rattanaphani *et al.*, 2007). Theoretically, therefore, a saturation value is reached beyond which no further sorption can take place. The saturated monolayer curve can be represented by the expression:

$$q_e = \frac{QbC_e}{1+bC_e} \quad (3.11)$$

A linear form of this expression is:

$$\frac{C_e}{q_e} = \frac{1}{Qb} + \left(\frac{1}{Q}\right)C_e \quad (3.12)$$

For lower concentrations, the following form of Langmuir equation is found to be more satisfactory (Bhattacharyya and Sarma, 2003):

$$\frac{1}{q_e} = \frac{1}{Q} + \frac{1}{QbC_e} \quad (3.13)$$

In the above equation, Q is the maximum amount of the dye per unit weight of fibre to form a complete monolayer coverage on the surface bound at high equilibrium dye concentration C_e , q_e is the amount of dye adsorbed per units weight of fibre at equilibrium, and b the Langmuir constant related to the affinity of binding sites. The value of Q represents a practical limiting adsorption capacity when the surface is fully covered with dye molecules and assists in the comparison of adsorption performance. The values of Q and b are calculated from the intercepts and slopes of the straight lines of plot of $1/q_e$ versus $1/C_e$.

The essential characteristics of the Langmuir isotherm can be expressed in terms of the dimensionless constant separation factor for equilibrium parameter, R_L (Kannan and Sundaram, 2001; Wan Ngah *et al.*, 2002; Malik, 2003; Chairat *et al.*, 2005; Wan Ngah *et al.*, 2005), defined as follows:

$$R_L = \frac{1}{1 + bC_0} \quad (3.14)$$

where C_0 is the initial concentration of dye (in ppm or mg/L) and b is the Langmuir constant (L/mg). The values of R_L indicates the type of isotherm to be irreversible ($R_L = 0$), favourable ($0 < R_L < 1$), linear ($R_L = 1$) or unfavourable ($R_L > 1$).

3.2.3.2 The Freundlich isotherm

The Freundlich isotherm (Ho and McKay, 1998; Chiou and Li, 2002) is based on an exponential relationship and is generally applicable to heterogeneous surface energy distribution. The Freundlich equation is shown:

$$q_e = Q_f C_e^{1/n} \quad (3.15)$$

where Q_f is roughly an indicator of the adsorption capacity and $1/n$ of the adsorption intensity. A linear form of the Freundlich expression in the equation (3.15) will yield the constants Q_f and $1/n$.

$$\ln q_e = \ln Q_f + \frac{1}{n} \ln C_e \quad (3.16)$$

Therefore, Q_f and $1/n$ can be determined from the linear plot of $\ln q_e$ versus $\ln C_e$. The magnitude of the exponent $1/n$ gives an indication of the favourability of adsorption. Values of $n > 1$ obtained represent favourable adsorption conditions (Chiou and Li, 2002).

Based on fundamental thermodynamics concept, it is assumed that in an isolated system, energy cannot be gained or lost and entropy change is the only driving force. The Gibbs free energy change, ΔG° , is the fundamental criterion of spontaneity. Reactions occurs spontaneously at a given temperature if ΔG° is a negative quantity. The thermodynamic parameters for the adsorption process, namely Gibbs energy (ΔG°), enthalpy (ΔH°) and entropy (ΔS°) of adsorption are evaluated using the following equations (Chiou and Li, 2003):

$$K_c = \frac{C_{ad,e}}{C_e} \quad (3.17)$$

$$\Delta G^\circ = -RT \ln K_c \quad (3.18)$$

$$\ln K_c = \frac{\Delta S^\circ}{R} - \frac{\Delta H^\circ}{RT} \quad (3.19)$$

In the above equations, K_c is the equilibrium constant, and $C_{ad,e}$ and C_e are the dye concentration adsorbed at equilibrium (mg/L) and the concentration of dye left in the dye bath at equilibrium (mg/L), respectively. T is the solution temperature (K) and R is the gas constant. Enthalpy (ΔH°) and entropy (ΔS°) of the adsorption are calculated from the slope and intercept of van't Hoff plots of $\ln K_c$ versus $1/T$.

3.3 Experimental

3.3.1 Chemicals

- (a) Silk yarn from Pungthungchai, Nakhon Ratchasima
- (b) Morin (FW 204.24) [480-16-0]
- (c) Soap, commercial grade
- (d) Sodium silicate, commercial grade
- (e) Sodium hydroxide, NaOH, Aldrich
- (f) Sodium carbonate, Merck
- (g) Hydrogen peroxide 40% (w/v), commercial grade
- (h) Hydrochloric acid 37% (w/v), HCl, Merck
- (i) Methanol, analytical grade, Merck
- (j) Alum ($KAl(SO_4)_2 \cdot 12H_2O$), Merck

3.3.2 Instruments

- (a) An Agilent 8453 UV-Vis spectrophotometer was employed for absorbance measurements using quartz cells of path length 1 cm.
- (b) A pH meter (Schott) was used to measure the pH values of dye solutions.
- (c) A thermostatted shaker bath (Type SBD-50 cold Heto-Holten A/S, Denmark), operated at 150 strokes/min, was used to study the adsorption kinetic and thermodynamic of dyeing on silk.
- (d) Freeze drier (Heto FD3 model S/N 492497-B, Cat No. 837107, Denmark) was used to dry the crude extract.

3.3.3 Experimental methods

3.3.3.1 Silk yarn preparation (Chairat, 2004)

The silk yarn used was purchased from villagers living in Nakhon Ratchasima, Thailand. To remove the sericin gum, the silk yarn (1 kg) was added to boiling water (5 L) which had been added soap flakes (*ca* 100 g), sodium silicate (10 g), sodium carbonate (50 g) and 40% hydrogen peroxide (100 mL). The mixture was then boiled for 2 hours. The silk was then removed, washed with water, squeezed to remove excess liquor and air dried. Finally, it was treated with 0.5 M HCl (*ca* 3 L) at room temperature for 30 minutes and then removed and washed with deionized water until the rinsed water was neutral. The silk yarn was then dried at room temperature.

3.3.3.2 Stock solutions

Morin stock solution (1.0×10^{-3} M) was prepared in 50% of methanol/H₂O (v/v). Alum, KAl(SO₄)₂·12H₂O, stock solution (1.0×10^{-3} M) was prepared in deionized water. These solutions were diluted with deionized water further as required. Alum-morin stock solution for dyeing on silk yarn were prepared by mixing alum: morin (2:1) from stock solution and diluting to volumetric flask (1000 mL) with deionized water.

3.3.3.3 Pre-, simultaneous and after-mordant for morin dyeing onto silk

Pre-mordanting: Silk yarn was first immersed in alum solutions of 95 mg/L and 190 mg/L, at 30°C, material to liquor ratio (MLR) 1:100. The silks yarn were then dried at the room temperature and then were immersed with morin solution of 30 mg/L at 30°C and MLR of 1:100.

Simultaneous mordanting: Silk yarn was immersed with alum-morin complex solutions of 30 mg/L at 30°C and MLR of 1:100.

After-mordanting: Silk yarn was first immersed in morin solutions of 30 mg/L, at 30°C and MLR of 1:100. The silk yarn was then dried at the room temperature and then were immersed with alum solution of 95 mg/L at 30°C and MLR of 1:100.

3.3.3.4 Effect of pH

Morin and alum-morin (2:1) solutions were prepared by dissolving in deionized water at desired concentration. The pH of the aqueous solutions was adjusted by using 0.1 M NaOH or 0.1 M HCl. Adsorption experiments were carried out by agitating silk with dye solutions of desired concentrations at 30°C in thermostatted shaker water bath. After 30 minutes, the silk yarn (0.5 g), which had been pre-warmed in the thermostatted bath for 30 minutes, was immersed in the dye solution. The silk yarn sample was then rapidly withdrawn at 60 minutes. Dye concentrations were determined at time zero and at 60 minutes using calibration curve based on absorbance at $\lambda_{\max} = 390$ nm (morin) and $\lambda_{\max} = 415$ nm (alum-morin) by an UV-vis spectrophotometer. The amount of dye adsorbed onto silk, q_t (mg/g), was calculated by mass balance relationship (Eq. (3.20))

$$q_t = (C_0 - C_t) \frac{V}{W} \quad (3.20)$$

where C_0 and C_t are the initial and equilibrium concentration of dye, respectively (mg/L), V is the volume of the solution (L), and W is the weight of the silk used (g).

3.3.3.5 Batch kinetic of morin and alum-morin experiments

Alum-morin (2:1) solutions were prepared by dissolving in deionized water at desired concentration. Adsorption experiments were carried out by agitating silk with dye solutions of desired concentrations at 30°C in thermostatted shaker water bath. After 30 minutes, the silk yarn (0.5 g), which had been pre-warmed in the thermostatted bath for 30 minutes, was immersed in the dye solution. The silk yarn sample was then rapidly withdrawn after different immersion times. Dye concentrations were determined at time zero and at subsequent times using calibration curve based on absorbance at $\lambda_{\max} = 390$ nm (morin) and $\lambda_{\max} = 415$ nm (alum-morin) by an UV-vis spectrophotometer. The amount of dye adsorbed onto silk, q_t (mg/g), was calculated by mass balance relationship (Eq. (3.20))

3.3.3.6 Batch equilibrium of alum-morin experiments

Alum-morin complexes were diluted in deionized water to the required concentrations. In experiments of equilibrium adsorption isotherm, 0.5 g silk and 50 mL alum-morin complex solutions were put in a 125 mL flask and were shaken for 60 minutes by using thermostated shaker water bath to control the temperature. The initial and equilibrium alum-morin complex concentrations were estimated by measuring absorbance at maximum wavelength ($\lambda_{\max} = 415$ nm) by an UV-vis spectrophotometer and computing concentration from the calibration curve. The amount of dyed adsorbed onto silk, q_e (mg/g) was calculated by mass balance relationship (Eq. (3.21)).

$$q_e = (C_0 - C_e) \frac{V}{W} \quad (3.21)$$

where C_0 and C_e are the initial and equilibrium concentration of dye, respectively (mg/L), V is the volume of the solution (L), and W is the weight of the silk used (g).

3.3.3.7 Adsorption and desorption studies of morin, alum- morin and alum-extracted dye onto silk

The silk yarn, prepared as noted in previous section, was dyed with an initial dye concentration of 30 mg/L in a thermostatted shaker bath. The adsorption conditions were MLR of 1:100 and 30°C. The absorbance of the dye solutions was monitored until constant absorbance values were obtained. The silk samples were then taken out and dried at room temperature. To study desorption of morin, alum-morin and alum-extracted dye at 30°C, deionized water 50 mL in each conical flask (125 mL) was shaken in a thermostatted shaker bath. After 30 min, the dried silk sample (0.50 g), which had been pre-warmed in the thermostatted bath at 30°C for 30 min, was immersed in deionized water. The silk samples were then rapidly withdrawn after different immersion times. The desorbed dye concentrations (q_{de}) were determined using a calibration curve based on absorbance at λ_{max} 415 nm versus dye concentration in standard solutions. The amount of dye adsorbed on silk after desorption was calculated by subtraction.

3.3.3.8 Extraction of dye

Heartwood of *M. cochinchinensis* was collected from Surin Province, Thailand. The heartwood was chopped into a small piece. A weighed amount of heartwood was extracted with deionized water in a beaker. The ratio of mass of material to the volume of liquid was 1:20; extraction was performed for 60 minutes at

85-95°C. Due to the rather high liquor ratio manual stirring was sufficient to distribute the plant material in the liquid during the extraction period. The extracted dye solution was filtered and the filtrate concentrated under reduced pressure (rotary evaporator) and then dried by using a Freeze dryer to give a crude extracted dye 10% w/w powder which was then used without further purification.

3.3.3.9 Batch kinetic studies of extracted dye onto silk

Extracted dye stock solution (1000 mg/L) was prepared in deionized water. This solution was diluted further as required. Alum-extracted dye complex solutions were prepared by dissolving in deionized water at desired concentration. Sorption experiments were carried out by agitating silk with dye solutions of desired concentrations, and material to liquor ratio at 30°C in thermostatted shaker water bath. After 30 minutes, the silk yarn (0.5 g), which had been pre-warmed in the thermostatted bath for 30 minutes, was immersed in the dye solution. The silk samples were then rapidly withdrawn after different immersion times. Dye concentrations were determined at time zero and at subsequent times using calibration curve based on absorbance at $\lambda_{\text{max}} = 415 \text{ nm}$ by an UV-vis spectrophotometer. The amount of dye adsorbed onto silk, q_t (mg/g), was calculated by mass balance relationship (Eq. (3.20))

3.3.3.10 Batch equilibrium adsorption of alum-extracted dye onto silk

Alum-extracted dye complexes were diluted in deionized water to the required concentrations. In experiments of equilibrium adsorption isotherm, 0.5 g silk and 50 mL alum-extracted dye solutions were put in a 125 mL flask and were shaken for 60 minutes by using thermostated shaker water bath to control the temperature.

The initial and equilibrium alum-extracted dye complex concentrations were estimated by measuring absorbance at maximum wavelength ($\lambda_{\max} = 415$ nm) by an UV-vis spectrophotometer and computing concentration from the calibration curve. The amount of dyed adsorbed onto silk, q_e (mg/g) was calculated by mass balance relationship (Eq. (3.21)).

3.4 Results and discussion

3.4.1 Comparison of pre-, simultaneous and after-mordant for morin dyeing onto silk

Dyeing is a manifold phenomenon, and the precise nature of dye-fibre interactions still remains a matter of debate. The great variety of chemical and physical interactions possible between the dye molecules, fibre, and metal ions in mordant dyeing suggest that a number of different products can be formed in the fibers (Raisanen, Nousiainen and Hynninen, 2001). The mordant is a metal salt or a mixture of tannins used to fix the dye to the fibre, mordants work by forming chemical bonds between the dye molecules and the proteins of the silk fibre. There are three opportunities for immersion mordanting to fibre; pre-mordanting, simultaneous mordanting and after(post)-mordanting. For the effective dyeing of silk with morin, it was considered that mordanting was essential.

Figure 3.4 shows a comparison of morin alone, together with pre-, simultaneous and after-mordanting for morin dyeing onto silk. They were carried out under the conditions of an initial concentration of morin of 30 mg/L, an MLR of 1:100, at pH 4.0, and a temperature of 30°C. It was found that the amount of dye adsorbed per gram of silk (q_t) of morin alone was lower than for alum-morin

(simultaneous mordanting). When pre-mordant with 190 mg/L of alum, the amount of dyes adsorbed of alum-morin is close to using only 95 mg/L of alum in alum-morin dye on silk. The dyeing of silk with alum-morin is chosen throughout this study because the least amount of alum is used.

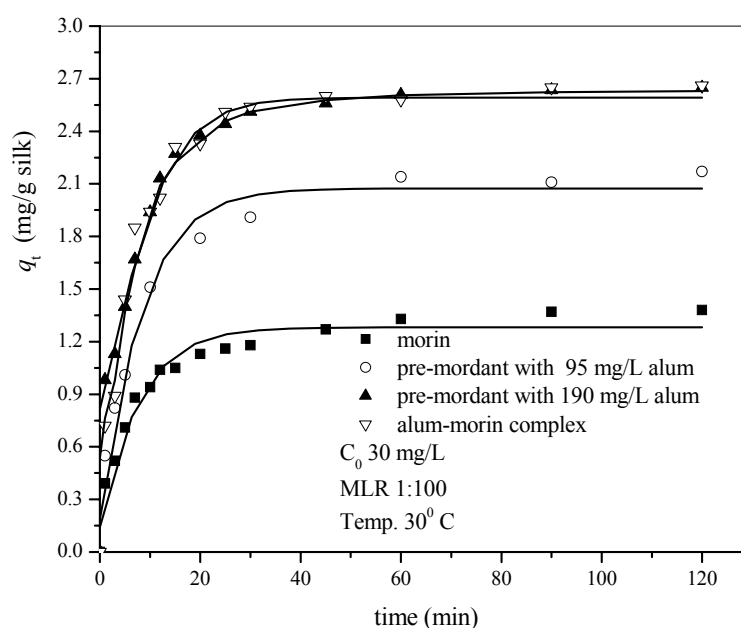


Figure 3.4 Comparison of morin alone, pre- and simultaneous mordanting for morin dyeing onto silk

There are three likely structural possibilities for the Al:morin complexes covering the 1:1, 1:2 and 3:2 complexes as mentioned in chapter II, but only the 1:1 complexes are able to form coordination linkages (Raisanen *et al.*, 2001) between the metal ion and nucleophilic NH and COO⁻ or CO groups in silk. The formation of coordination linkages in silk fibre depends on the nucleophilic properties of the nitrogen and oxygen atoms in the NH and CO backbone groups (Raisanen *et al.*, 2001); however, ligand binding through the serine sidechain hydroxyl group is

another possibility which shouldn't be excluded. The atom with a stronger nucleophilicity forms a coordination linkage with the 1:1 complex as are proposed in the structure in Figures 3.5 (a) and (b). In the case of the 3:2 complex the structures shown in Figures 3.5 (c) and (d) are considered the most likely ones.

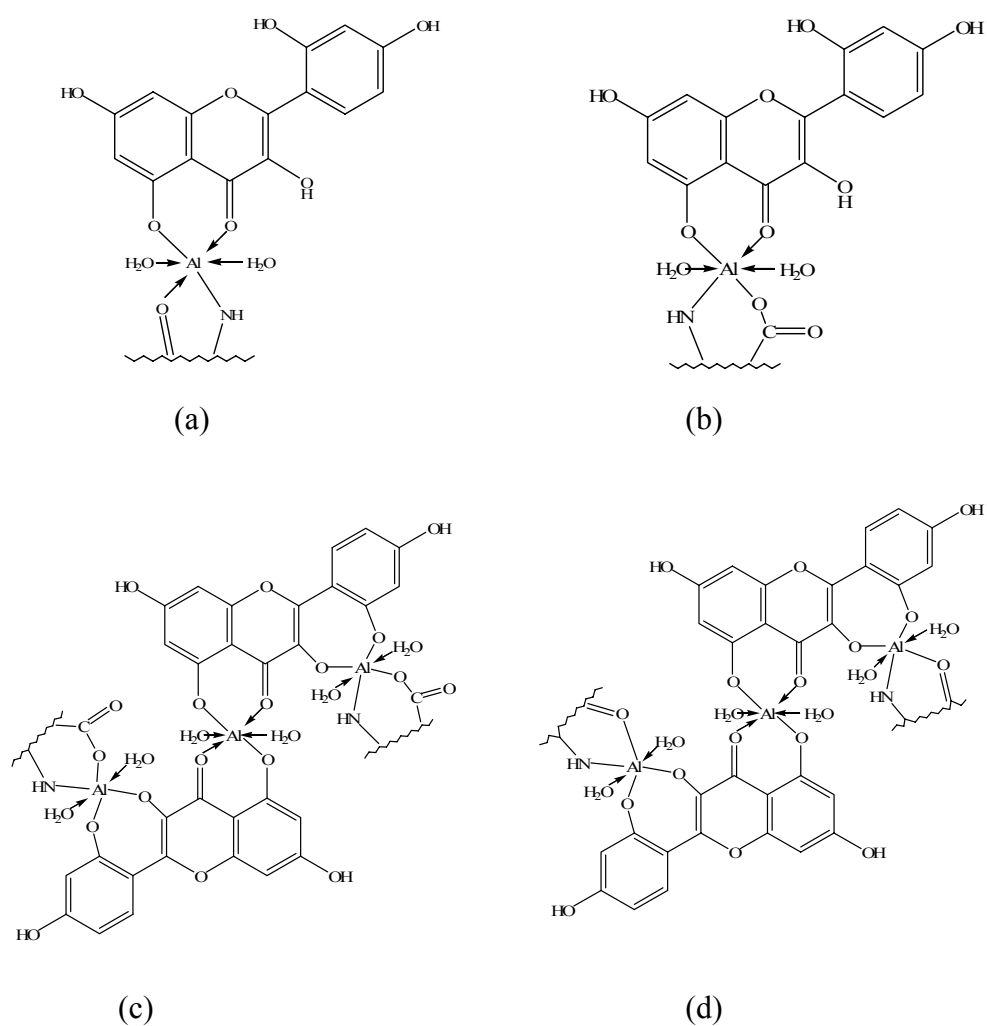


Figure 3.5 Proposed Silk:Al:M coordination linkage structures.

3.4.2 Optimal conditions of silk dyeing with morin and alum-morin

In order to investigate the adsorption of morin and alum-morin on silk, the experiment parameters including pH, material to liquor ratio (MLR), contact time, initial dye concentration and temperature were determined to find the optimal conditions for adsorption. The mechanism of adsorption of alum-morin and alum-extracted dye dyeing onto silk were investigated by using the pseudo first-order and pseudo second-order models. In addition, activation parameters and thermodynamics parameters of adsorption were calculated.

3.4.2.1 The effect of pH on the adsorption of morin and alum-morin onto silk

The pH of the dye solution is one of the most important parameters controlling the adsorption capacity of dye onto silk (Christie *et al.*, 2000; Chairat *et al.*, 2005). To study the influence of pH on the adsorption capacity of morin and alum-morin complex on silk, experiments were performed using different initial solution pH values with no silk present. In these cases, the morin and alum-morin intensities were altered with pH. Therefore, the initial morin intensities were adjusted to the desired values. The obtained results are presented in Figure 3.6. In the case of morin, it was found that the adsorption capacity decreased with increasing pH over the pH range 5.0-9.0. When the pH of the solution was approximately 5.0, the silk would have more positively charged sites, and the area of the morin molecule with high negative potential *i.e.* at the 4-keto-3,5-hydroxy group as shown in Figure 3.7 would thus be attracted by electrostatic forces. This electrostatic attraction plays an important role in enhancing the dye uptake in silk fibres. However, the adsorption capacity was smaller than that observed for the alum-morin complex.

In the case of alum-morin complex, it was found that the adsorption capacity increased with decreasing pH over pH range 3.5-7.0. The maximum adsorption capacity was observed to be at pH of 4.0. Using the alum-morin complex as a model (Figure 2.8), we proposed the possibilities of interaction of alum-morin-silk (Figure 3.5). At pH 3.5-4.5, if the coordination linkages between the silk, alum and morin were the major form of intermolecular interaction, then alum-morin would be expected quite strong bonds with silk fibre (Raisanen *et al.*, 2001). Therefore, alum-morin complex at pH 4.0 was used to study kinetics and thermodynamics of the adsorption process throughout this study.

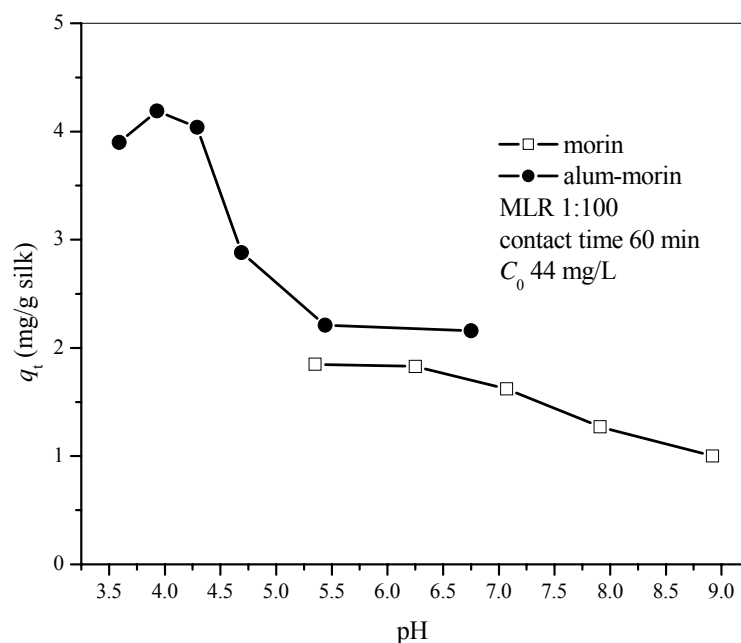


Figure 3.6 Effect of pH on morin and alum-morin dyeing on silk.

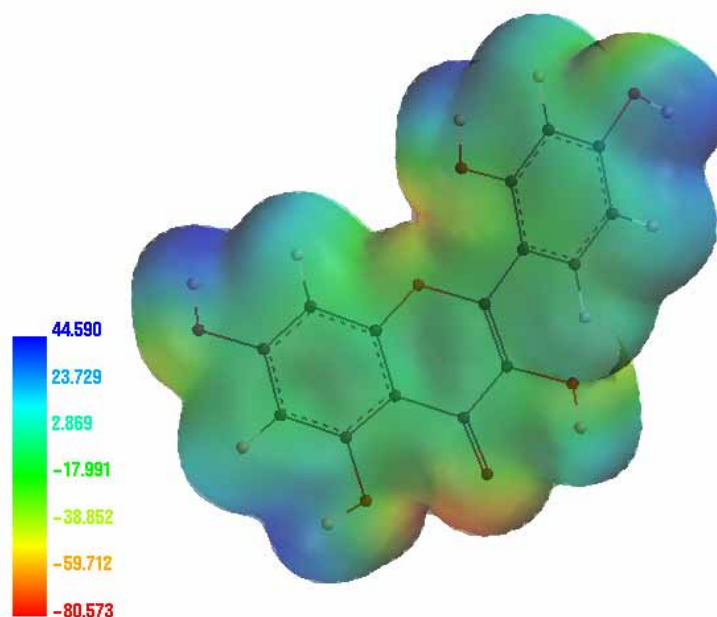


Figure 3.7 Electrostatic potential map of morin (Spartan Program; AM1; Wavefunction Inc.; '02 Linux /Unix).

3.4.2.2 The effect of material to liquor ratio (MLR) on the adsorption of alum-morin onto silk

The results of the material liquor ratio on experiments carried out using initial alum-morin concentration of 44 mg/L morin at pH 4.0 and temperature 30°C are shown in Figure 3.8. It was found that an increase in volume of dye solution resulted in an increase of dye adsorbed onto silk. It indicated that silk yarn is loosely packed in the higher volume of dye solution and the dye solution readily moves past any surface transferring dye molecules to the silk surface in the process. Kinetic parameters from linear plots of pseudo first-order (Figure 3.9) and pseudo second-order (Figure 3.10) models are given in Table 3.1. The data show a good compliance with the pseudo second-order equation and the regression coefficients, R^2 , for the

linear plot were all high (>0.97). The equilibrium sorption capacity, $q_{e,cal}$, for the second-order process is more reasonable than for the first-order process when comparing predicted results with experimental data because of the equilibrium sorption capacities are lower than the experimental results. The overall rate of the alum-morin sorption processes appears to be controlled by the chemical process in this case in accordance with the pseudo second-order reaction mechanism. The amount of dye adsorbed of MLR 1:150 showed highest values when compare with MLR 1:100 and 1:75 (Figure 3.8). However, in order to minimize waste from dyeing process, MLR 1:100 will be used for all the kinetic experiments.

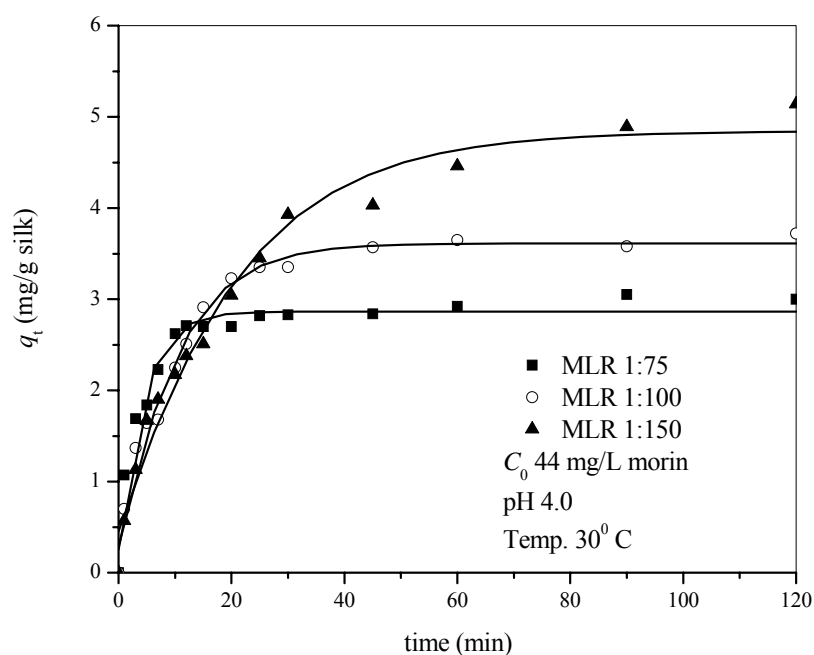


Figure 3.8 The effect of material to liquor ratio on the adsorption of alum-morin onto silk.

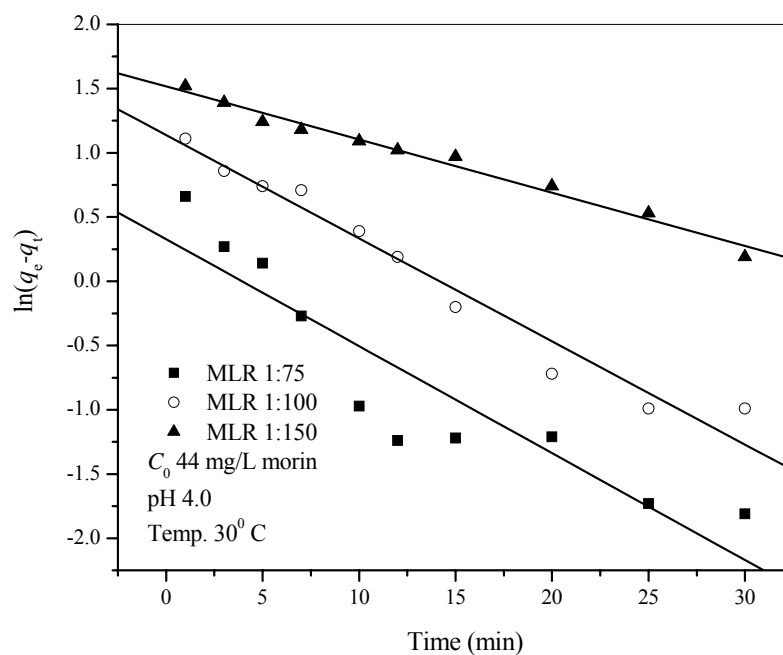


Figure 3.9 Application of the pseudo first-order equation at different material to liquor ratios on the adsorption of alum-morin onto silk.

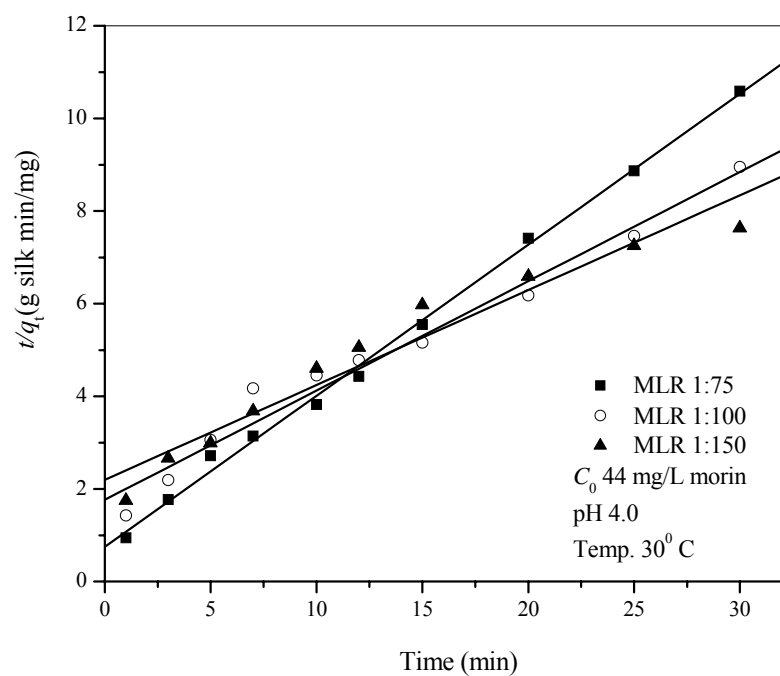


Figure 3.10 Application of the pseudo second-order equation at different material to liquor ratios on the adsorption of the alum-morin onto silk.

3.4.2.3 The effect of contact time and initial dye concentration on the adsorption of alum-morin onto silk

The effect of contact time and initial dye concentration on adsorption of alum-morin complexes dye onto silk is presented in Figure 3.11. The sorption capacities at equilibrium, q_e , increases from 2.66-5.10 mg/g silk with an initial dye concentration from 31-61 mg/L and MLR 1:100 at 30°C and equilibrium was reached after 60 min. The equilibrium time was independent of initial dye concentrations but in the first 30 min, the initial rate of adsorption was greater for higher initial dye concentrations at the same agitation speed. An increase of the dye concentration accelerates the diffusion of dyes from the dye solution onto silk due to the increase in the driving force of the concentration gradient (Chiou and Li, 2002; Chairat *et al.*, 2005).

The characteristic parameters of pseudo-first and pseudo-second order models and correlation coefficients are tabulated in Table 3.1 and in Figure 3.12 and Figure 3.13 are pseudo-first and pseudo-second order plots, respectively, are presented. The correlation coefficients (R^2) of the second-order equation for all concentrations are higher than the first-order model and the calculated equilibrium sorption capacities fit well with the experimental data. These suggest that the pseudo-second order adsorption mechanism is predominant and that the overall of the alum-morin adsorption process appears to be controlled by the chemical process which involving valency forces through sharing or exchange of electrons between sorbent and sorbate (Özacar and Şengil, 2005). A similar phenomenon has also been observed in metal complex dye sorption onto pine sawdust (Özacar and Şengil, 2005). The results in Table 3.1 also show k_2 , h_1 and q_e as a function of initial dye concentration. The

pseudo-second order rate constant (k_2) decreases with an increasing of initial dye concentration, while the initial sorption rate, h_i , increases with an initial dye concentration. An increase in initial dye concentration results in a significant increase in $q_{e,cal}$. The $q_{e,cal}$ for initial dye concentration also increase with an increasing of initial dye concentration.

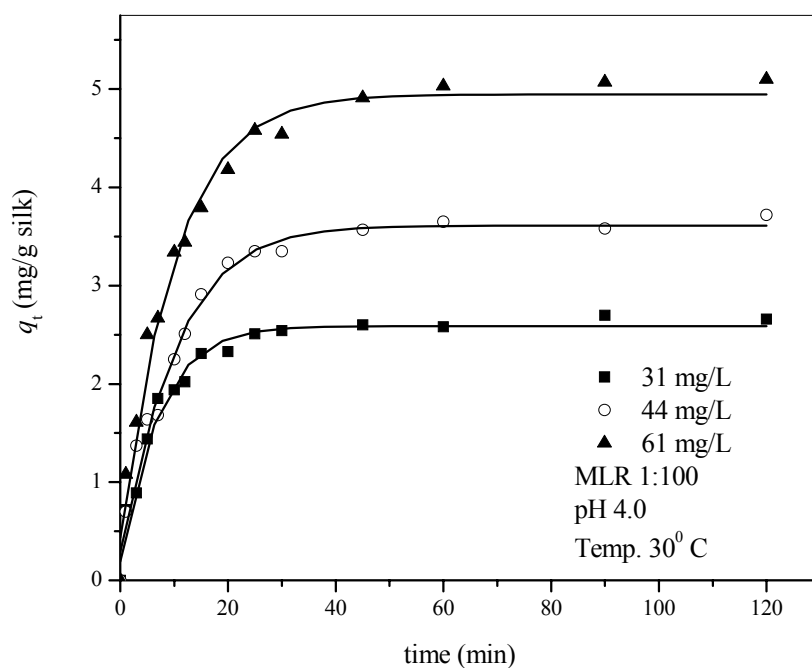


Figure 3.11 The effect of contact time and initial dye concentration and the adsorption of alum-morin onto silk.

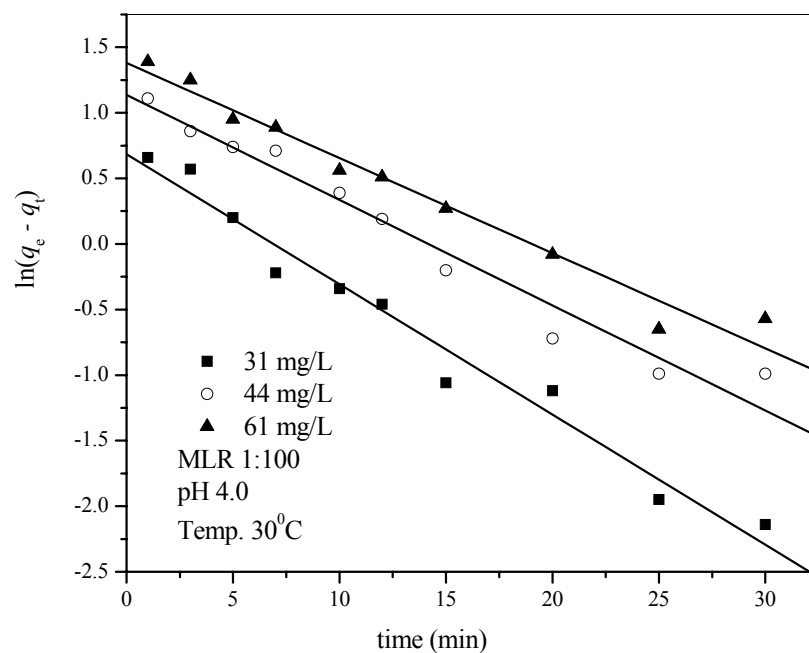


Figure 3.12 The pseudo first-order equation at different initial dye concentrations and the adsorption of alum-morin onto silk.

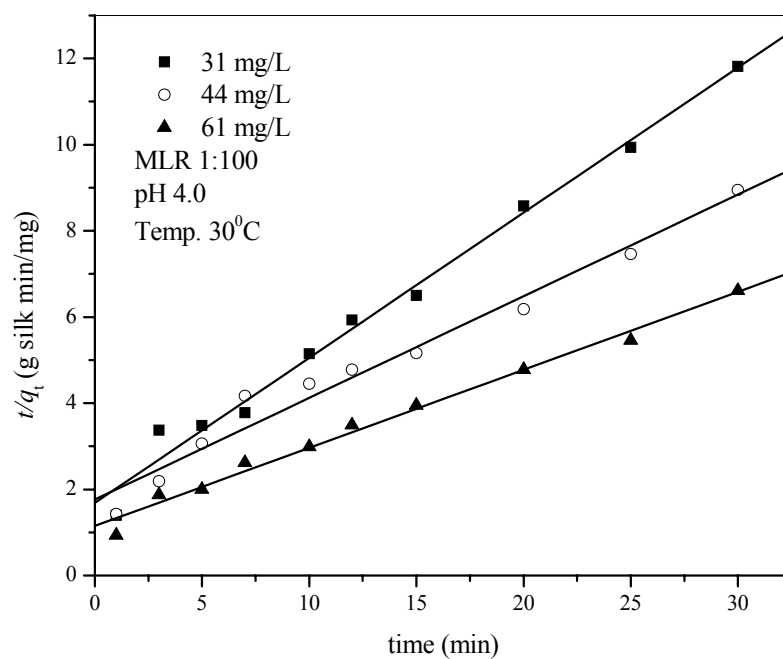


Figure 3.13 The pseudo second-order equation at different initial dye concentrations and the adsorption of alum-morin onto silk.

3.4.2.4 The effect of temperature on the adsorption of alum-morin dye onto silk

Figure 3.14 shows the effect of temperature on adsorption of alum-morin complex onto silk at an initial dye concentration 31 mg/L at pH 4.0 and an MLR of 1:100. A study of the temperature dependence of adsorptions gives valuable information about the enthalpy change during adsorption. The effect of temperature on the adsorption rate was studied by carrying out a series of experiments at 30, 50 and 70°C. An increase in the temperature leads to an increase in initial adsorption rate. Before and after the equilibrium time, the adsorption capacities in Figure 3.14 shows different trend at different temperatures. Before the equilibrium time was established, an increase in the temperature leads to an increase in dye adsorption rate indicative of a kinetically controlled process. After equilibrium, the dye uptake decreases with increasing the temperature suggesting that the adsorption of the alum-morin onto silk is controlled by exothermic process. Similar temperature effect trends on adsorption trend have also been shown in the case of adsorption of lac dye onto silk (Chairat *et al.*, 2005) as well as the adsorption of reactive dye on cross-linked chitosan beads (Chiou and Li, 2003). Our data showed that the time to reach the adsorption equilibrium decreased with increasing temperature, i.e. 60, 30 and 15 min at 30, 50 and 70°C, respectively. This is due to more rapid diffusion to the silk at higher temperatures. However, for consistency the contact time in the equilibrium adsorption experiments was set at 60 min throughout this study.

Table 3.1 lists the results of rate constant and other kinetic parameters studies for different temperatures calculated by the pseudo first-order (Figure 3.15) and pseudo-second order (Figure 3.16) models. The correlation coefficient, R^2 , for the pseudo second-order adsorption model has a higher value suggesting the dye adsorption occurs process is predominantly by the pseudo second-order adsorption mechanism.

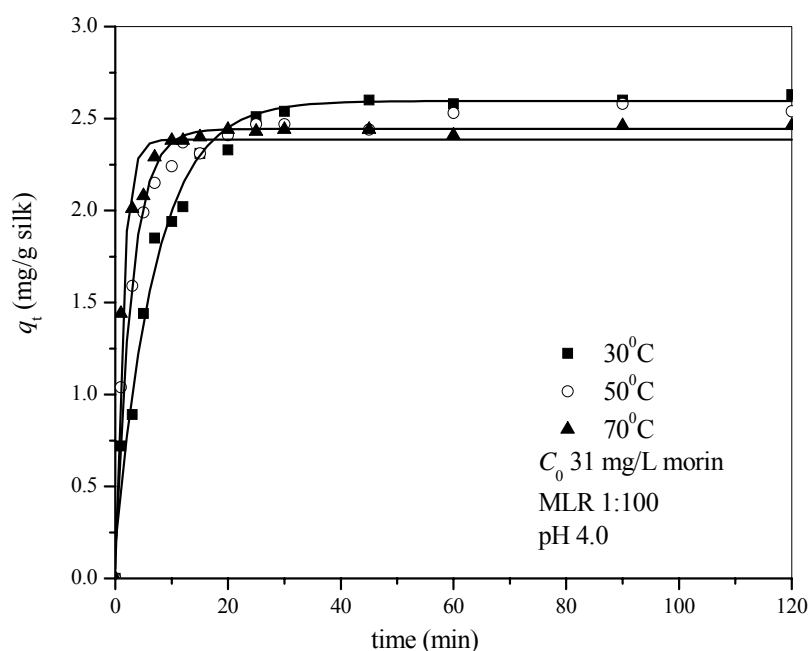


Figure 3.14 The effect of temperature on the adsorption of alum-morin onto silk.

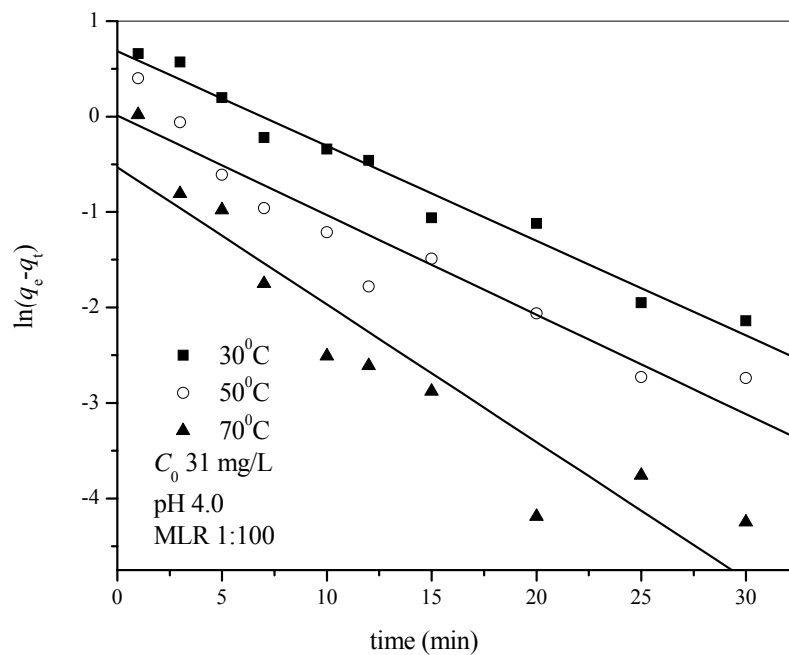


Figure 3.15 The pseudo first-order equation at different temperatures on the adsorption of alum-morin onto silk.

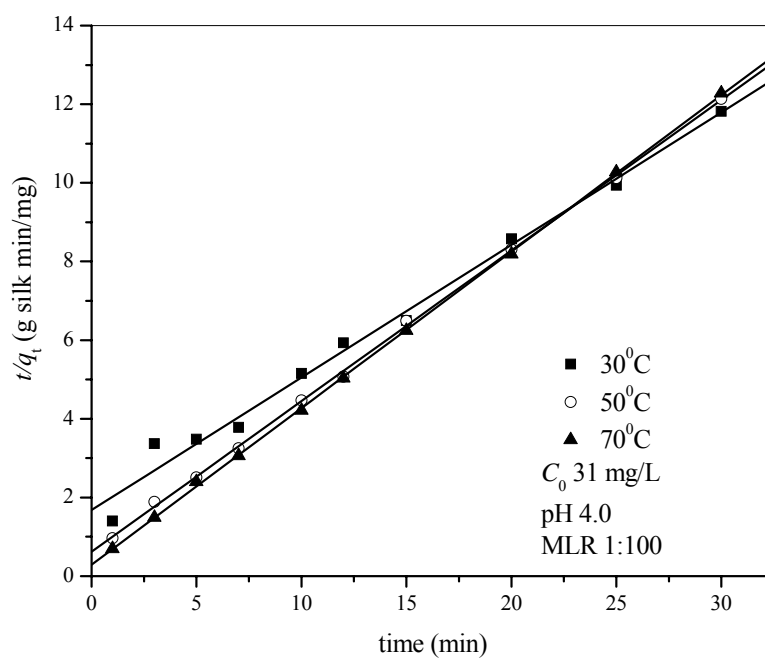


Figure 3.16 The pseudo second-order equation at different temperatures on the adsorption of alum-morin complex onto silk.

Table 3.1 Comparison of the first-order and second order adsorption rate constants, calculated q_e and experimental q_e values for different MLR, initial dye concentrations and temperatures for alum-morin dyeing of silk.

Parameters	$q_{e,exp}$ (mg/g silk)	First-order kinetic model			Second-order kinetic model			
		k_1	$q_{e,cal}$ (mg/g silk)	R^2	k_2	h_i	$q_{e,cal}$ (mg/g silk)	R^2
<i>MLR: initial dye concentration (C_0) 31 mg/L, pH 4.0, temp. 30°C</i>								
1:75	3.00	0.0832	1.39	0.9212	0.1419	1.33	3.07	0.9985
1:100	3.72	0.0802	3.12	0.9819	0.0316	0.57	4.24	0.9865
1:150	5.14	0.0413	4.56	0.9907	0.0191	0.46	4.88	0.9744
<i>Initial dye concentration; (mg/L) : MLR 1:100, pH 4.0, temp. 30°C</i>								
31	2.66	0.0993	1.98	0.9863	0.0675	0.59	2.97	0.9944
44	3.72	0.0803	3.12	0.9820	0.0316	0.57	4.24	0.9865
61	5.10	0.0726	3.98	0.9860	0.0285	0.87	5.52	0.9943
<i>Temperature (°C): initial dye concentration (C_0) 31 mg/L, MLR 1:100, pH 4.0</i>								
30	2.66	0.0992	1.98	0.9863	0.0675	0.59	2.97	0.9944
50	2.54	0.1043	1.01	0.9561	0.2369	1.62	2.61	0.9997
70	2.46	0.1439	0.59	0.9427	0.5439	3.43	2.51	0.9999

3.4.2.5 Activation parameters for the adsorption of alum-morin on silk

The rate constants k_2 for pseudo-second-order reaction at different temperatures listed in Table 3.1 were used to estimate the activation energy of the adsorption of alum-morin onto silk by the Arrhenius equation. The slope of the plot of $\ln k_2$ versus $1/T$ (Figure 3.17) was used to evaluate E_a as listed in Table 3.2.

Table 3.2 Activation parameters for the adsorption of morin and alum-morin onto silk at initial morin concentration 31 mg/L.

Temp (°C)	k_2 (g silk/mg second)	E_a (kJ/mol)	R^2	$\Delta H^\#$ (kJ/mol)	$\Delta S^\#$ (J/mol K)	$\Delta G^\#$ (kJ/mol)	R^2
30	0.0011					91.26	
50	0.0039	45.26	0.9967	42.51	-160.8	94.47	0.9962
70	0.0091					97.69	

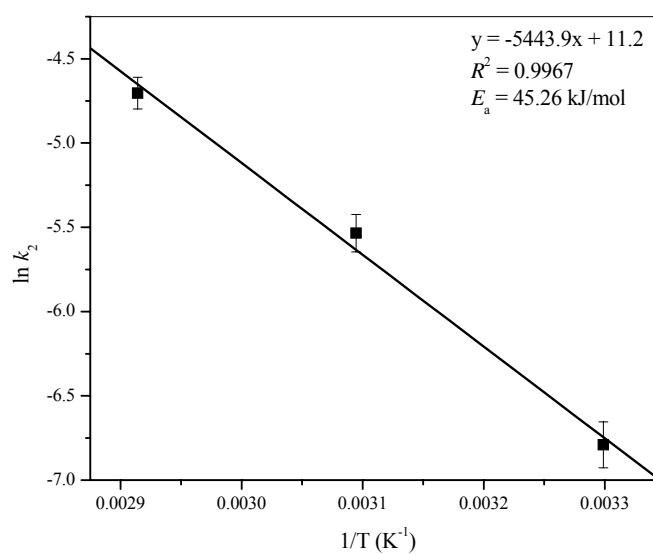


Figure 3.17 Arrhenius plot for the adsorption of alum-morin onto silk.

The observed activation energy (E_a) and enthalpy of activation (ΔH^\ddagger) for alum-morin onto silk yarn is shown in Table 3.2. Physisorption processes usually have low activation energies (5-40 kJ/mol), while higher activation energies (40-800 kJ/mol) suggest chemisorption (Nollet, Roels, Lutgen, Meeren and Verstraete, 2003). For the E_a of 45.26 kJ/mol observed we can infer that the adsorption of alum-morin onto silk yarn is the most likely by a chemisorption process. Some other adsorption process that have been found to be chemisorption-controlled includes: sorption of methylene blue onto palm kernel fibre with E_a 39.57 kJ/mol (Ofomaja, 2007) and methylene blue onto modified diatomite with E_a 99.80 kJ/mol (Al-Ghouti, Khraisheh, Allen and Ahmad, 2005).

From the Eyring equation, the enthalpy (ΔH^\ddagger) and entropy (ΔS^\ddagger) of activation were calculated from the slope and intercept of a plot of $\ln(k/T)$ versus $1/T$ (Figure 3.18) as listed in Table 3.3. The value of ΔG^\ddagger was calculated at 303, 313 and 333 K by using equation (3.10) and these values are listed in Table 3.2, while the negative entropy value (ΔS^\ddagger) reflects more aggregation and the interaction between alum-morin dye and the silk yarn.

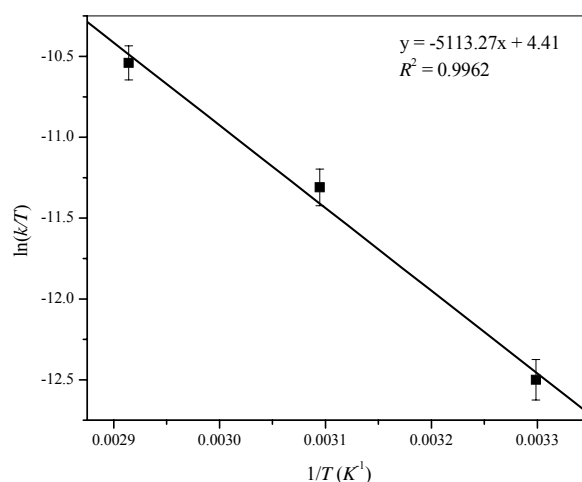


Figure 3.18 Plot of $\ln(k/T)$ against $1/T$ for the adsorption of alum-morin onto silk.

3.4.2.6 Thermodynamic parameters for the adsorption of alum-morin on silk

As mentioned earlier, the alum-morin adsorption onto silk is an exothermic reaction process. In order to confirm this the exothermic behaviour quantitatively the thermodynamic parameters ΔG° , ΔH° and ΔS° of alum-morin adsorption after reaching equilibrium were calculated using the equations (3.16)-(3.18). The results are listed in Table 3.3. The negative values of ΔG° indicate that the adsorption of alum-morin on silk is spontaneous. The negative value of ΔH° confirms that the adsorption process is an exothermic one. Furthermore, the entropy change (ΔS°) in dyeing represents the entropy difference of the dye molecules within the fibre (Kim, 2005). The negative value of ΔS° indicates that adsorbed alum-morin dye become more restrained within the silk fibre molecules than in the dyeing solution.

Table 3.3 Thermodynamic parameters for the adsorption of alum-morin dyeing at an initial morin concentration 31 mg/L.

Temperature (°C)	$\ln K_c$	ΔG° (kJ/mol)	ΔH° (kJ/mol)	ΔS° (J/mol K)	R^2
30	7.04	-17.73			
50	6.15	-16.51	-31.29	-45.7	0.9923
70	5.57	-15.90			

3.4.2.7 Adsorption isotherm for the adsorption of alum-morin on silk

The isothermal equilibrium of alum-morin dye on silk under the conditions of an MLR of 1:100 in the dye concentration range 39-276 mg/L at 30, 50 and 70°C were described employing the Langmuir isotherm equation as shown in Figure 3.19. It was found that the dye uptake decreased with increasing temperature, thereby indicating the process is exothermic.

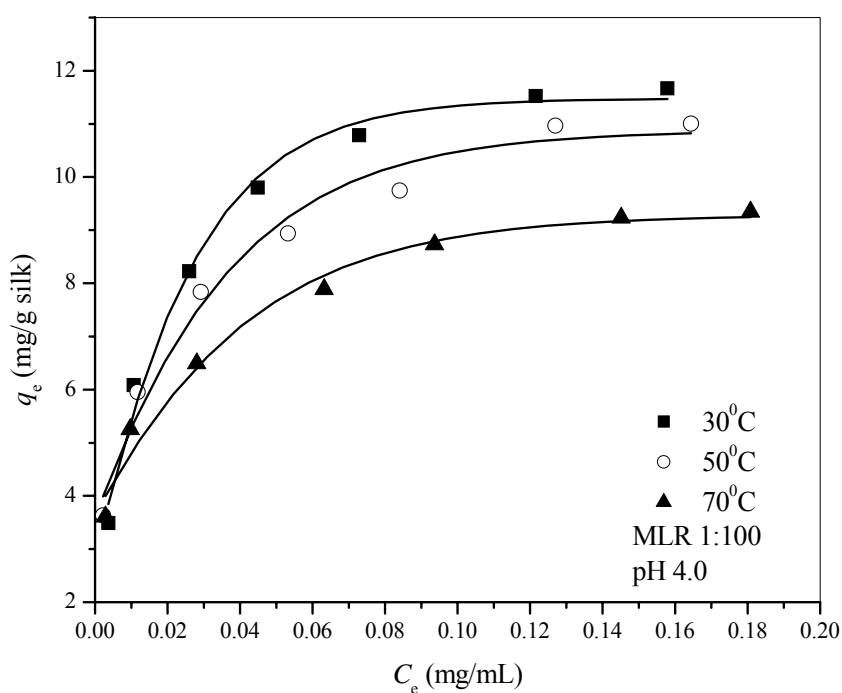


Figure 3.19 Langmuir adsorption isotherms of alum-morin onto silk at 30, 50 and 70°C.

When C_e/q_e is plotted against C_e according to the Eq. (3.12), the Langmuir model fitted the experimental data very well with high correlation coefficients ($R^2 > 0.99$) (Figure 3.20). The values of the Langmuir constants Q and b were calculated from the slopes and intercepts of different straight lines respectively at different temperatures. The calculated results are reported in Table 3.5. It can be seen from the Table 3.5 that Q values decreased with increasing temperature. Similar observations were reported for the adsorption of silk dyeing with lac dye (Kongkachuichay *et al.*, 2002; Chairat *et al.*, 2005). The b values indicated that the the silk yarn has a maximum affinity for alum-morin dye at lower temperature (Chairat *et al.*, 2005).

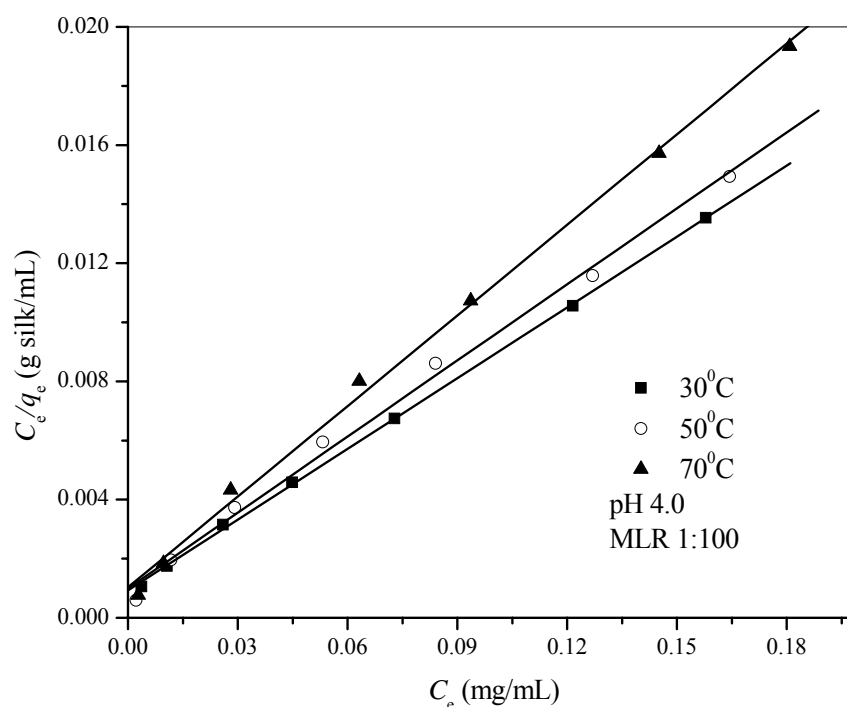


Figure 3.20 A Langmuir plot of C_e/q_e against C_e for the adsorption of alum-morin onto silk at the initial dye concentration range 30-276 mg/L.

Table 3.4 Langmuir and Freundlich isotherm constants for the adsorption of alum-morin onto silk at different temperatures.

Temp (°C)	Langmuir			Freundlich		
	Q (mg/g silk)	b (mL/mg)	R^2	Q_f (mg/g silk)	n	R^2
30	12.5	86.69	0.9997	23.66	3.16	0.9713
50	11.6	86.55	0.9974	18.69	3.83	0.9955
70	9.8	99.22	0.9985	14.54	4.37	0.9946

The equilibrium parameter values, R_L , for the adsorption of alum-morin dyeing on silk were calculated by using Eq. (3.14). It was found that the values of R_L (Table 3.5) were observed to be in the range of 0-1, indicating a favourable that the adsorption of alum-morin was favourable for this study. Similar observations were reported for the lac dyeing of silk (Chairat *et al.*, 2005) and the sorption of methylene blue onto rice husk (Vadivelan and Kumar, 2005)

The Freundlich equation (Eq. (3.16)) was also applied to the results of the adsorption of alum-morin on silk. The values of Q_f and $1/n$ can be determined from the linear plot of $\ln q_e$ versus $\ln C_e$. The magnitude of the exponent $1/n$ gives an indication of the favourability of adsorption. Values of $n > 1$ obtained represent favourable adsorption conditions (Chiou and Li, 2002; Chairat *et al.*, 2005). The Q_f values decreased with increasing temperature which again supported and exothermic process.

Table 3.5 R_L values at different temperatures relating to the initial dye concentrations for alum-morin dyeing of silk.

Temperature (°C)	b (L/mg)	Initial dye concentration C_0 (mg/L)	R_L
30	0.0867	38.99	0.2283
		71.70	0.1386
		108.56	0.0960
		143.20	0.0745
		181.89	0.0596
		237.98	0.0462
		275.80	0.0401
50	0.0865	38.99	0.2286
		71.70	0.1388
		108.56	0.0962
		143.20	0.0747
		181.89	0.0597
		237.98	0.0463
		275.80	0.0402
70	0.0992	38.99	0.2054
		71.70	0.1232
		108.56	0.0849
		143.20	0.0657
		181.89	0.0525
		237.98	0.2283
		275.80	0.1386

3.4.2.8 Adsorption-desorption of morin and alum-morin dye on silk

After the adsorption of morin and alum-morin dye on silk was equilibrated desorption was then carried out in deionized water. From this analysis, the alum-morin showed a higher dye uptake than morin itself on silk (Figure 3.21). Adsorption study showed that dyeing of alum-morin enhanced dye uptake compare with morin alone. After 120 minutes, dye bath was replaced with deionized water and desorption of morin and alum-morin were observed. The amount of morin and alum-morin which desorbed from the silk were shown in Figure 3.21. At 300 minutes, the amount of morin and alum-morin adsorbed on silk was 0.8 and 2.6 mg/g silk, respectively. It was found that morin alone can desorbed easier than alum-morin from the silk fibre. This data supported the proposed model of alum-morin-silk interaction as mentioned in sections 3.4.1 and 3.4.2.1.

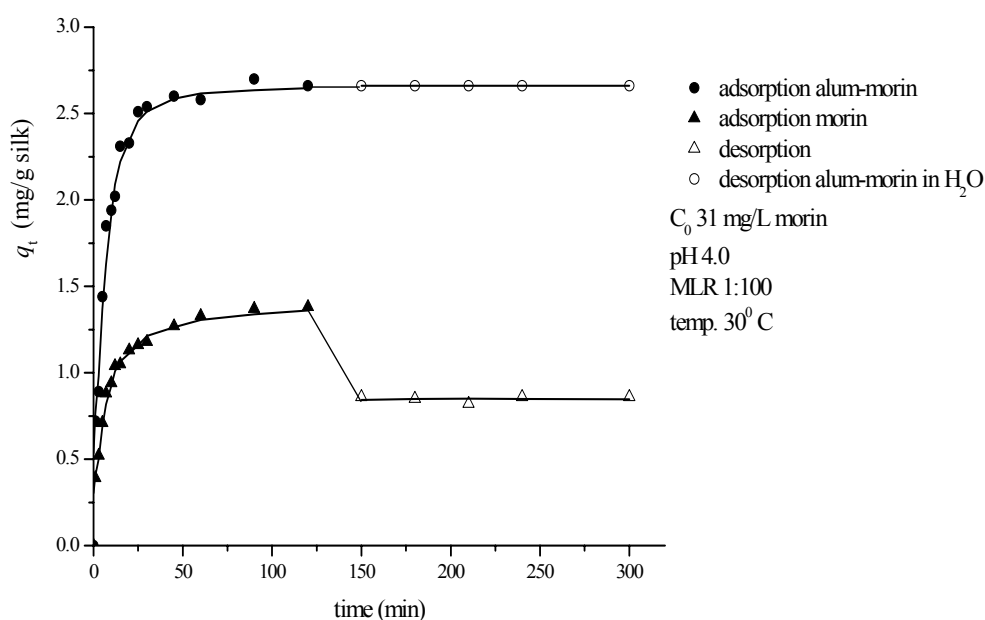


Figure 3.21 Adsorption-desorption analysis of morin and alum-morin dye onto and off silk.

3.4.3 Optimal conditions of silk dyeing with alum-extracted dye

M. cochinchinensis is the plant which is contained mainly morin dye and the amount of morin in the crude extracted dye was estimated in Chapter II section 2.4.4. In order to investigate the adsorption of alum-extracted dye on silk, the experimental parameters including, material to liquor ratio (MLR), contact time, initial dye concentration and temperature were determined to find the optimal conditions for adsorption. The mechanism of adsorption of alum-morin and alum-extracted dye dyeing onto silk were investigated by using the pseudo first-order and pseudo second-order models. In addition, activation parameters and thermodynamics parameters of adsorption have been investigated in this section.

3.4.3.1 The effect of material to liquor ratio (MLR) on the adsorption of alum-extracted dye onto silk

The material to liquor ratio (MLR) is an important parameter which influences the adsorption of dye. The results of the material liquor ratio on experiments carried out using an initial alum-extracted dye concentration of 200 mg/L (contained ~ 34 mg/L morin) extracted dye at pH 4.0 and 30°C are shown in Figure 3.22. It was found that an increase in volume of dye solution resulted in an increase in the amount of dye adsorbed onto silk. Again it indicated that silk yarn is loosely packed in the higher volume of dye solution and the dye solution readily moves past any surface transferring dye molecules to the silk surface in the process (Chairat *et al.*, 2005). Kinetic parameters from linear plots of pseudo first-order (Figure 3.23) and pseudo second-order (Figure 3.24) models are given in Table 3.6. The data show a good compliance with the pseudo second-order equation and the regression coefficients, R^2 , for the linear plot were all high (>0.98). The calculated equilibrium

sorption capacity values, $q_{e,cal}$, for the second-order model are more reasonable than the first-order model when comparing predicted results with experimental data ($q_{e,exp}$), with the calculated equilibrium sorption capacities being lower than the experimental values in the latter model. The overall rate of alum-extracted dye sorption processes appear to be controlled by the chemical-mediated process in this case in accordance with the pseudo second-order reaction mechanism, as observed with the alum-morin sorption onto silk. Also the amount of dye adsorbed of MLR 1:150 showed highest values when compare with MLR 1:100 and 1:75 (Figure 3.22). However, in order to minimize waste from dyeing process, MLR 1:100 will be used for all the kinetic experiments.

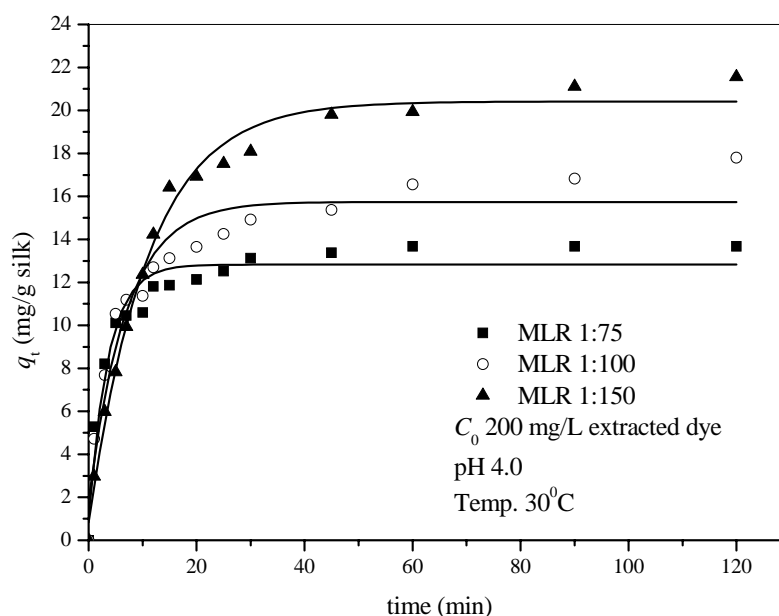


Figure 3.22 The effect of material to liquor ratios (MLR) on the adsorption of alum-extracted dye onto silk.

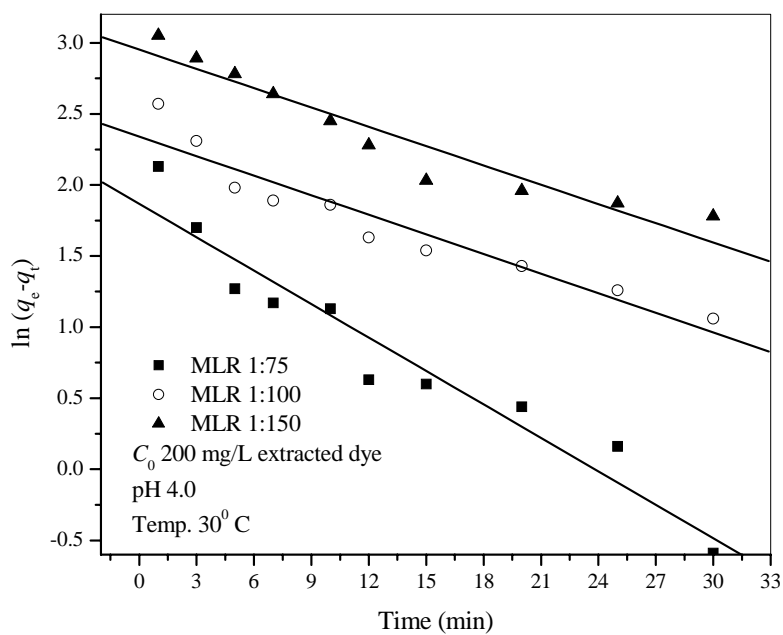


Figure 3.23 A plot of $\ln(q_e - q_t)$ versus time (pseudo first-order equation) at different MLR on the adsorption of alum-extracted dye onto silk.

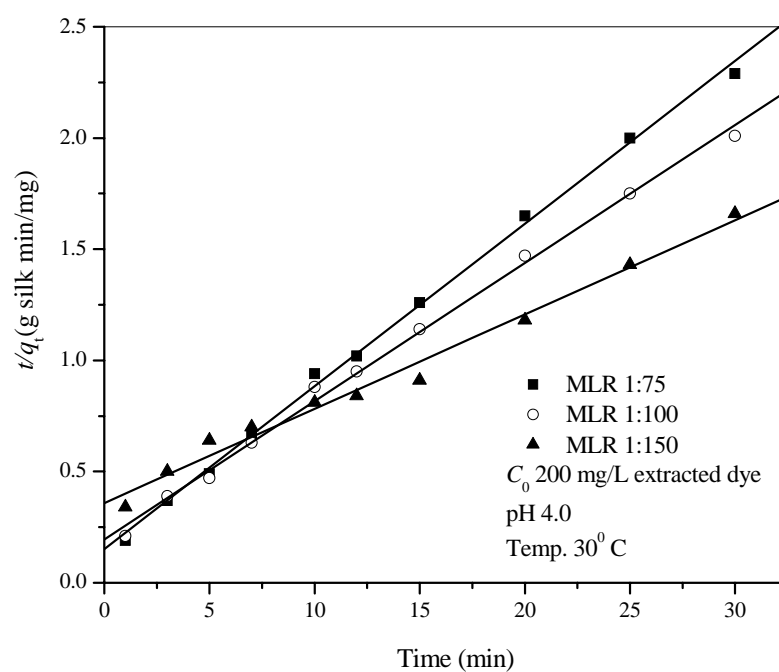


Figure 3.24 A plot of t/q_t versus time (pseudo second-order equation) at different MLR on the adsorption of alum-extracted dye onto silk.

3.4.3.2 The effect of contact time and initial dye concentration on the adsorption of alum-extracted dye onto silk

The effect of contact time and initial dye concentration on adsorption of alum-extracted dye onto silk are presented in Figure 3.25. The sorption capacities at equilibrium, $q_{e,exp}$, increases from 17.8-38.2 mg/g silk with an increase in initial dye concentration from 200-450 mg/L (contained ~ 34-76 mg/L morin) with an MLR of 1:100 at pH 4.0, and 30°C with equilibrium reached after 60 min. The equilibrium time is independent of initial dye concentrations. But in the first 30 min, the initial rate of adsorption was greater for higher initial dye concentrations. Because the diffusion of dye molecules through the solution to the surface of the adsorbents is affected by this concentration (at a constant agitation speed). An increase of the dye concentration accelerates the diffusion of dyes from the dye solution onto adsorbents due to the increase in the driving force of the concentration gradient which similar to the results of alum-morin adsorbed onto silk.

The characteristic parameters of the pseudo-first and pseudo-second order models and correlation coefficients are tabulated in Table 3.6. Figure 3.26 and Figure 3.27 are based on pseudo-first and pseudo-second order plots, respectively. The correlation coefficients (R^2) for the second-order model equation for all concentrations are higher than for the first-order model and the calculated equilibrium sorption capacities fit well with the experimental data in the former model. These suggest that the pseudo-second order adsorption mechanism is predominant and that the overall of the alum-extracted dye which similar to the results of alum-morin adsorbed onto silk as described in section 3.4.2.3. The results in Table 3.6 also show k_2 , h_i and q_e as a function of initial dye concentration. For the pseudo second-order

model, the rate constant decreases with an increasing of initial dye concentration, while the initial sorption rate, h_i , increases with an initial dye concentration. An increase in initial dye concentration results in a significant increase in $q_{e,cal}$.

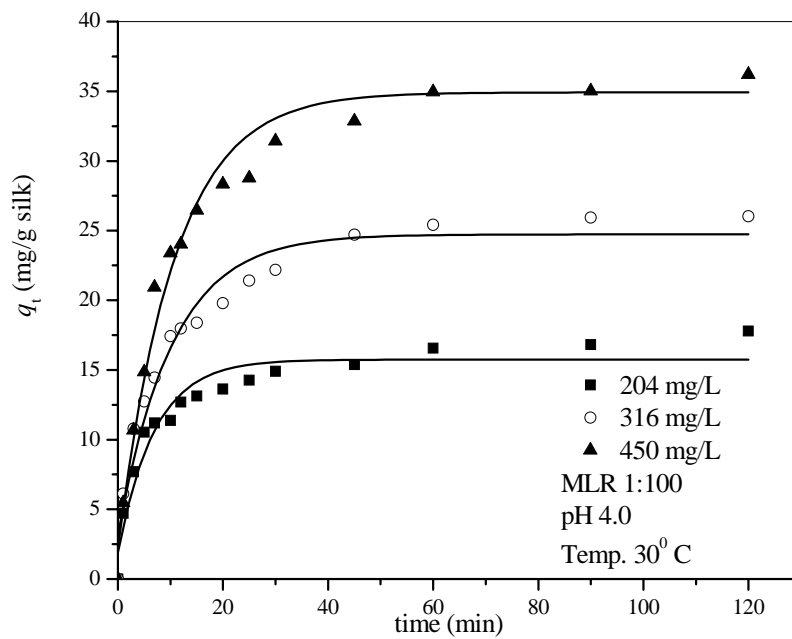


Figure 3.25 The effect of contact time and initial dye concentrations on the adsorption of alum-extracted dye onto silk.

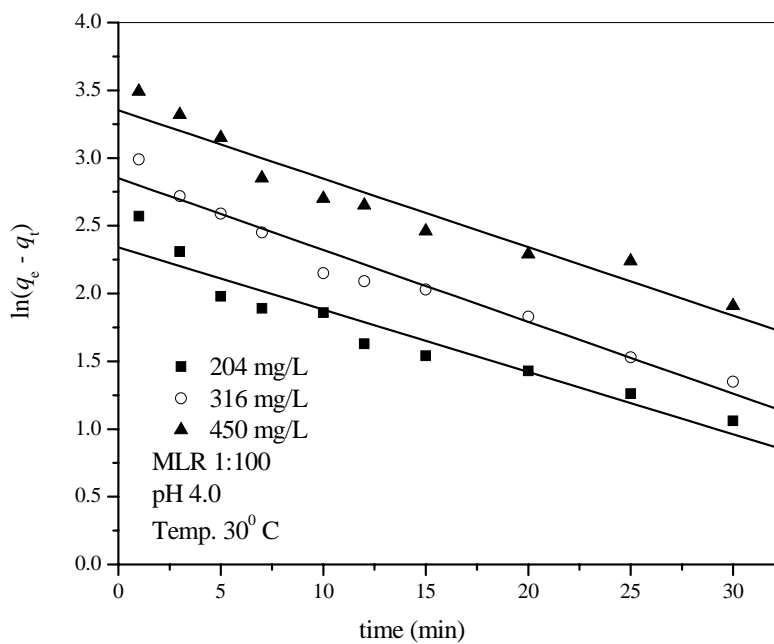


Figure 3.26 A plot of $\ln(q_e - q_t)$ versus time (pseudo first-order equation) at different initial dye concentrations on the adsorption of alum-extracted dye onto silk.

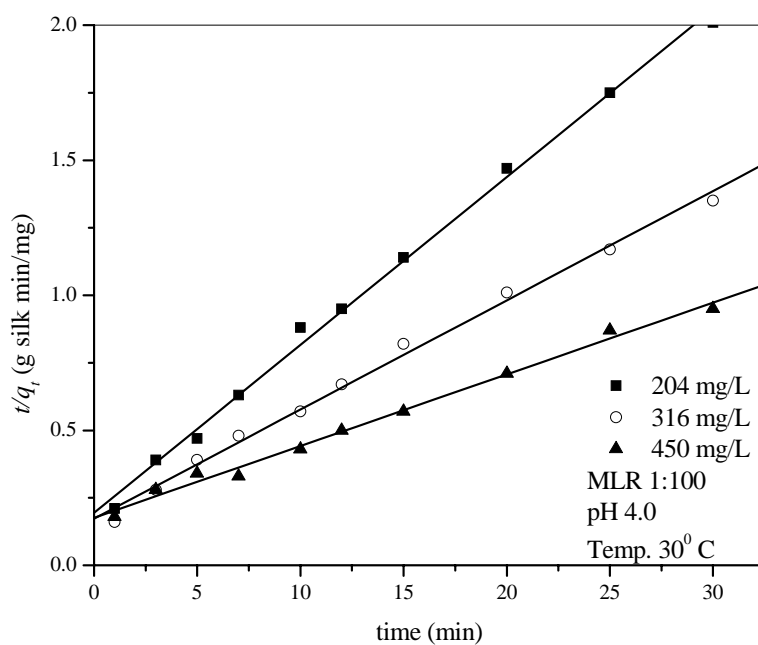


Figure 3.27 A plot of t/q_t versus time (pseudo second-order equation) at different initial dye concentrations on the adsorption of alum-extracted dye onto silk.

3.4.3.3 The effect of temperature on the adsorption of alum-extracted dye onto silk

The effect of temperature on adsorption of alum-extracted dye onto silk has been investigated at an initial dye concentration 200 mg/L (contained ~ 34 mg/L morin) at pH 4.0 and an MLR of 1:100. A study of the temperature dependence of adsorptions gives valuable information about the enthalpy change during adsorption. The effect of temperature on the adsorption rate was studied by carrying out a series of experiments at 30, 50 and 70°C. An increase in the temperature leads to an increase in initial adsorption rate. Before and after the equilibrium time, the adsorption capacities show a different trend at different temperatures (Figure 3.28). Before the equilibrium was reached, an increase in the temperature lead to an increase in dye adsorption rate which indicates a kinetically controlled process. After equilibrium, the uptake decreased with increasing the temperature indicating that the adsorption of alum-extracted dye onto silk is controlled by and exothermic process. A similar temperature effect on adsorption trend has also been shown in the case of adsorption of lac dye onto silk (Chairat *et al.*, 2005) and the adsorption of reactive dye on cross-linked chitosan beads (Chiou and Li, 2003). Our data showed that the time to reach the adsorption equilibrium decreased with increasing temperature, i.e. 60, 30 and 15 min at 30, 50 and 70°C, respectively. This is due to more rapid diffusion to the silk with higher temperatures.

The results of rate constant studies for different temperatures calculated by the pseudo first-order and pseudo-second order models are listed in Table 3.6. The correlation coefficient, R^2 , for the pseudo second-order adsorption model (Figure 3.30) has a higher value suggesting the dye adsorption process is predominantly by a pseudo second-order adsorption mechanism.

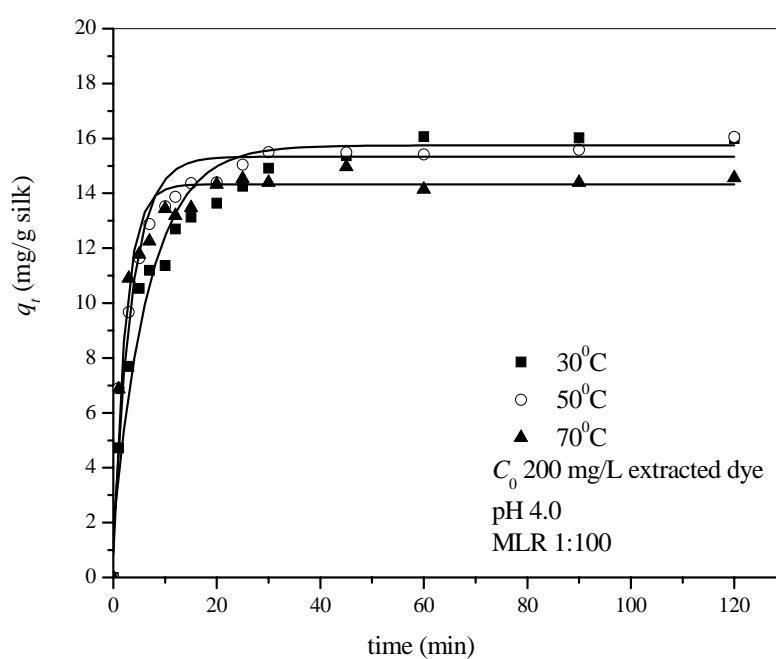


Figure 3.28 The effect of temperature on the adsorption of alum-extracted dye onto silk.

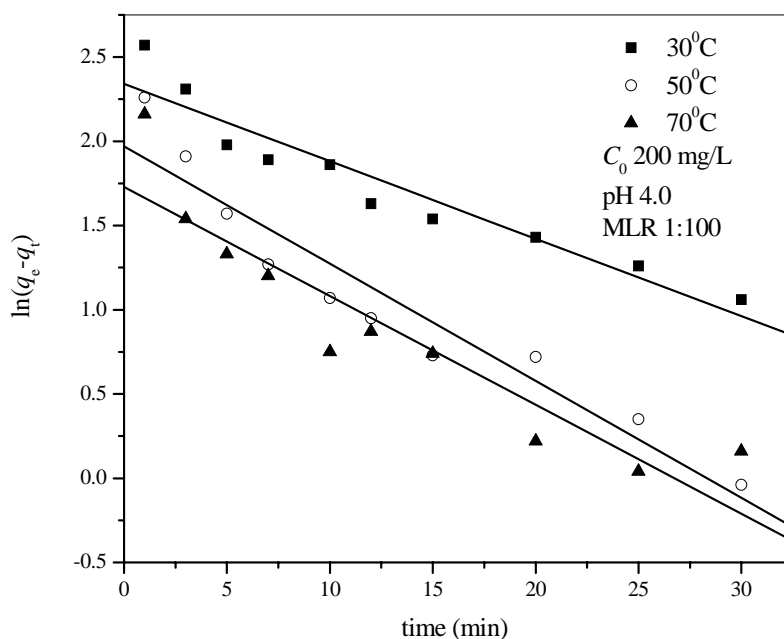


Figure 3.29 A plot of $\ln(q_e - q_t)$ versus time (pseudo first-order equation) at different temperatures on the adsorption of alum-extracted dye onto silk.

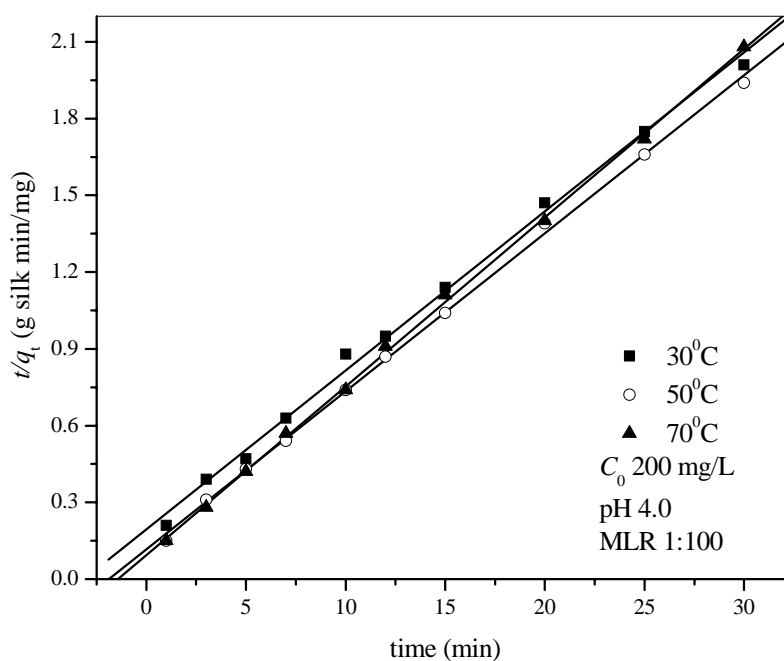


Figure 3.30 A plot of t/q_t versus time (pseudo second-order equation) at different temperatures on the adsorption of alum-extracted dye onto silk.

Table 3.6 Comparison of the first-order and second order adsorption rate constants, calculated q_e and experimental q_e values for different MLR, initial extracted dye concentrations and temperatures for adsorption of extracted dye on silk.

Parameter rs	$q_{e,exp}$ (mg/g silk)	First-order kinetic model			Second-order kinetic model			
		k_1	$q_{e,cal}$ (mg/g silk)	R^2	k_2	h_i	$q_{e,cal}$ (mg/g silk)	R^2
<i>MLR: initial dye concentration (C_0) 200 mg/L; pH 4.0; temp. 30°C</i>								
1:75	13.68	0.0784	6.46	0.9320	0.0351	6.56	13.68	0.9975
1:100	17.80	0.0460	10.41	0.9103	0.0199	5.14	16.08	0.9968
1:150	24.00	0.0454	19.17	0.9185	0.0050	2.78	23.58	0.9862
<i>Initial dye concentration (mg/L): MLR 1:100; pH 4.0; temp. 30°C</i>								
200	17.80	0.0460	10.41	0.9103	0.0199	5.14	16.08	0.9968
316	26.02	0.0531	17.32	0.9616	0.0094	5.76	24.75	0.9946
450	38.20	0.0484	37.75	0.9744	0.0040	5.67	37.74	0.9932
<i>Temperature (°C): initial dye concentration (C_0) 200 mg/L ; pH 4.0; MLR 1:100</i>								
30	17.80	0.0460	10.41	0.9103	0.0199	5.14	16.08	0.9968
50	16.45	0.0697	7.18	0.9205	0.0330	8.65	16.18	0.9988
70	15.56	0.0648	5.64	0.8616	0.0472	10.81	15.13	0.9991

3.4.3.4 Activation parameters of the adsorption of alum-extracted dye on silk

The activation energy of the diffusion can be calculated using Eq. (3.10) that is known as the Arrhenius equation. This parameter describes the dependence of the diffusion coefficient on the dyeing temperature and also represents the energy barrier that the dye molecule should overcome to diffuse into the fibre molecules (Kim, 2005). The activation energy of the diffusion can be obtained from the slope in the linear relationship between $\ln k$ and $1/T$ shown in Figure 3.31. The calculated activation energy is presented in Table 3.7.

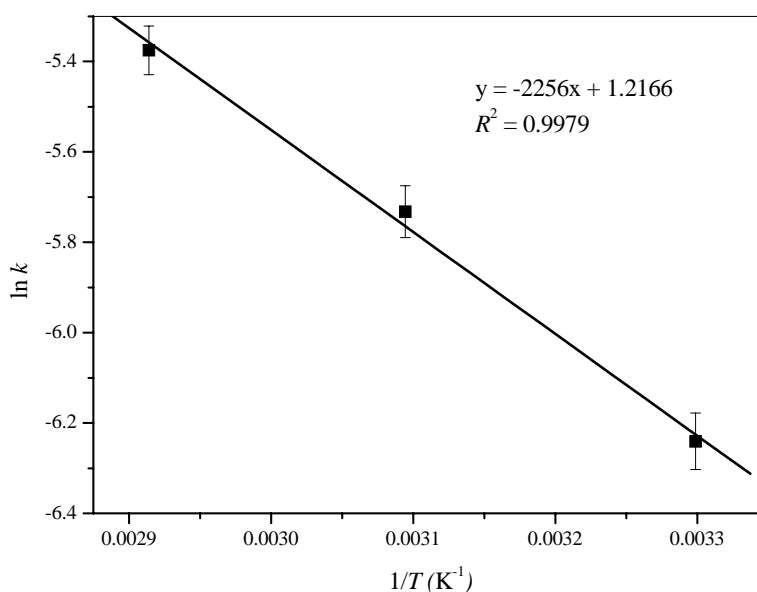


Figure 3.31 Relationship between $\ln k$ and $1/T$ on activation energy of alum-extracted dye onto silk.

From the Eyring equation, the enthalpy (ΔH^\ddagger) and entropy (ΔS^\ddagger) of activation were calculated from the slope and intercept of a plot of $\ln(k/T)$ versus $1/T$ (Figure

3.18) as listed in Table 3.7. The value of ΔG^\ddagger was calculated at 303, 313 and 333 K by using equation (3.10) and these values are listed in Table 3.7, while the negative entropy value (ΔS^\ddagger) reflects more aggregation and the interaction between alum-extracted dye and silk yarn.

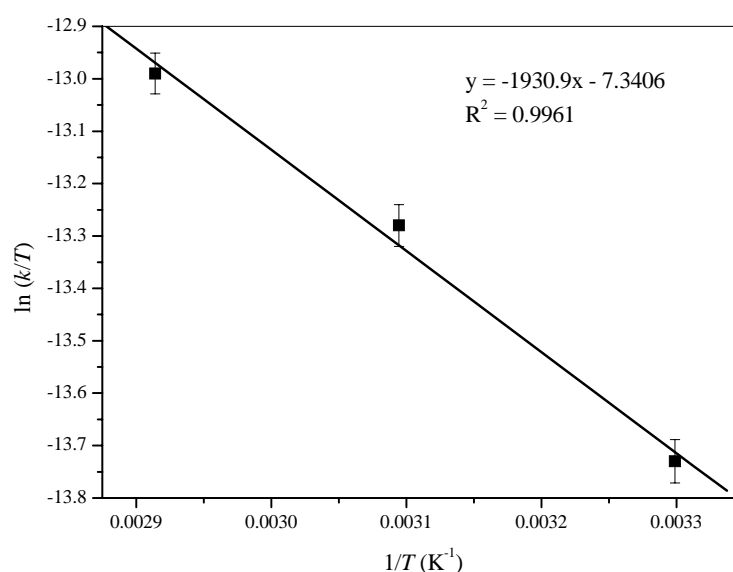


Figure 3.32 Plot of $\ln(k/T)$ against $1/T$ for the adsorption of alum-extracted dye onto silk.

Table 3.7 Activation parameters for the adsorption of alum-extracted dye onto silk.

Temp (°C)	k_2 (g silk/mg second)	E_a (kJ/mol)	R^2	ΔH^\ddagger (kJ/mol)	ΔS^\ddagger (J/mol K)	ΔG^\ddagger (kJ/mol)	R^2
30	0.0199					94.27	
50	0.0330	18.73	0.9959	16.05	-258.6	99.43	0.9940
70	0.0472					104.59	

The value of E_a of adsorption of alum-extracted dye onto silk is 18.73 kJ/mol (Table 3.7). The E_a obtained is low but the adsorption of alum-extracted dye showed similar trend to alum-morin it may be crude extracted dye contained other components which can act as a catalyst of alum-extracted dye on silk.

3.4.3.5 Thermodynamic parameters of the adsorption of alum-extracted dye on silk

In order to provide supporting evidence for the exothermic behaviour of alum-extracted dye onto silk, after reaching equilibrium, the thermodynamic parameters ΔG° , ΔH° and ΔS° of alum-extracted dye adsorption were calculated by using the Eqs. (3.16)-(3.18). The results are listed in Table 3.8. The negative of ΔH° suggests that the adsorption of alum-extracted dye onto silk is an exothermic process. The negative values of ΔG° indicate that the adsorption of process is spontaneous. Meanwhile, the entropy change (ΔS°) on dyeing represents the entropy difference of the dye molecules within the fibre (Kim, 2005). The negative value of ΔS° indicates that adsorbed alum-extracted dye become more restrained within silk fibre molecules than in the dyeing solution.

Table 3.8 Thermodynamic parameters for the adsorption of alum-extracted dye onto silk.

Temp. (°C)	$\ln k_c$	ΔG° (kJ/mol)	ΔH° (kJ/mol)	ΔS° (J/mol K)	R^2
30	8.87	-22.35			
50	8.50	-22.84	-14.16	-30.75	0.9995
70	8.21	-23.15			

3.4.3.6 Adsorption isotherm of alum-extracted dye onto silk

The adsorption equilibrium data were analyzed using the Langmuir and Freundlich expression. The adsorption constants of alum-extracted dye onto silk are shown in Table 3.9. The experimental data were found to fit well to the Langmuir isotherm, with the former being slightly better as indicated by the higher R^2 values compared with that from the Freundlich expression. The applicability of the Langmuir isotherm suggests monolayer coverage of the dye on the surface of the silk.

The effect of isotherm shape can be used to predict whether a sorption system is “favourable” or “unfavourable”. The essential features of the Langmuir isotherm of alum-extracted dye on silk can be expressed in terms of a dimensionless constant separation factor or equilibrium parameter R_L , which is defined by the Eq. (3.14). The R_L values at 30°C relating to the initial dye concentrations are found in the range of 0.4429-0.2191 (Table 3.10) showing favourable adsorption.

Table 3.9 Langmuir and Freundlich isotherm constants for the adsorption of alum-extracted dye onto silk at 30°C.

Q (mg/g silk)	Langmuir		R^2	Q_f (mg/g silk)	Freundlich	
	b (mL/mg)				n	R^2
33.3	30.0	0.9130	165.03	1.47	0.8826	

The Freundlich equation describes heterogeneous systems and reversible adsorption; and is not limited to the formation of a complete monolayer. It can be seen from Table 3.9 that the correlation coefficients for the Freundlich isotherms are only

slightly less than those obtained for the Langmuir expression. Thus, Freundlich isotherm cannot be totally rejected in these equilibrium studies. Also the values of n more than 1 (Table 3.10) indicate favourable adsorption.

Table 3.10 R_L values at 30°C relating to the initial extracted dye concentrations.

Initial extracted dye concentration, C_0 (mg/L)	R_L
41.93	0.4429
58.63	0.3625
71.41	0.3182
86.56	0.2780
100.23	0.2496
118.77	0.2191

3.4.3.7 Adsorption-desorption of alum-extracted dye on silk

After the adsorption of alum-extracted dye on silk were equilibrated desorption was carried out in deionized water. It was found that an adsorption capacity of alum-extracted dye at 120 minutes is 16.8 mg/g silk (Figure 3.33). The amount of alum-extracted dye which desorbed from the silk was also shown in Figure 3.33. It was found that at 300 minutes, the amount of alum-extracted dye adsorbed on silk was still very close to the adsorption.

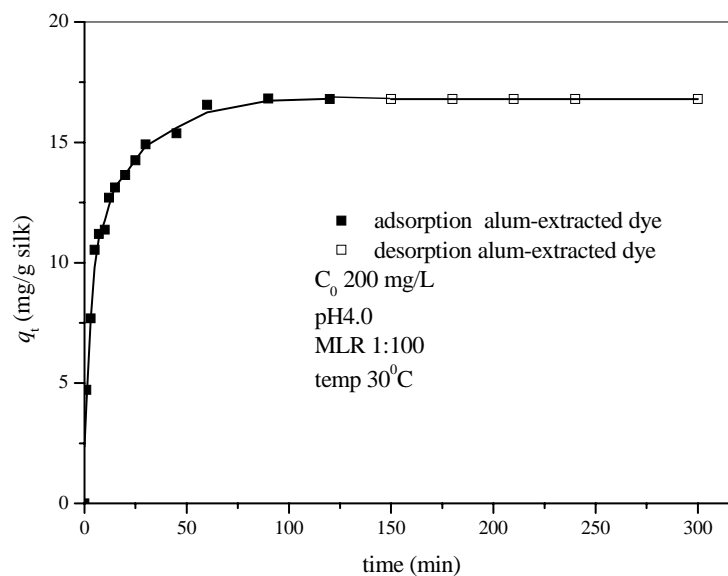


Figure 3.33 Adsorption-desorption of alum-extracted dye onto silk.

3.4.4 Comparison of activation and thermodynamic parameter and desorption between alum-morin and alum-extracted dyeing on silk

Crude extracted dye (hot water) from *M. cochinchinensis* is composed mainly of morin dye (17%). For the dyeing with extracted dye by villagers in the northeast of Thailand, the dye is usually used without purification. Kinetics and thermodynamics parameters for alum-morin and alum-extracted dye dyeing onto silk are given in Tables 3.11 and 3.12, respectively.

3.4.4.1 Comparison of activation parameters between alum-morin and alum-extracted dye dyeing on silk

The activation parameters of alum-morin and alum-extracted dye are shown in Table 3.11. It was found that the activation energy for extracted dye was smaller than for alum-morin dye indicating that the former may contain other substances that could help binding of the extracted dye dyeing onto silk. The entropic

values obtained in this investigation of alum-morin and alum-extracted complexes are both negative, indicating an increase in the order of the system in each case.

A value of the activation energy for alum-morin dyeing onto silk was > 40 kJ/mol (45.26 kJ/mol), and it is thus concluded that the adsorption kinetic of alum-morin onto silk involved a chemical reaction in the adsorption process while the activation energy of alum-extracted dye was lower than that of alum-morin dye onto silk. It is possible that crude extracted dye contained other components which can act as a catalyst for alum-extracted dye adsorbed on silk as mentioned previously.

Table 3.11 Activation parameters for the adsorption of alum-morin and alum-extracted dye dyeing on silk

	Temp (°C)	k_2 (g silk/mg second)	E_a (kJ/mol)	R^2	$\Delta H^\#$ (kJ/mol)	$\Delta S^\#$ (J/mol K)	$\Delta G^\#$ (kJ/mol)	R^2
alum-	30	0.0011					91.26	
morin	50	0.0039	45.26	0.9967	42.51	-160.8	94.47	0.9962
	70	0.0091					97.69	
alum-	30	0.0199					94.27	
ext.	50	0.0330	18.73	0.9959	16.05	-258.6	99.43	0.9940
dye	70	0.0472					104.59	

3.4.4.2 Comparison of thermodynamics parameters between alum-morin and alum-extracted dyeing on silk

The Gibbs energy of alum-morin and alum-extracted dyeing onto silk are favorable for the formation of these complexes with silk. The results are shown in Table 3.12. These values are exothermic with -17.73 and -22.35 kJ/mol for the alum-morin mixture and the alum-extracted dye mixture, respectively. The negative of ΔH° in both cases confirm that the adsorption of alum-morin and alum-extracted dye onto silk are exothermic processes, which is supported by the decreasing adsorption with the increasing in temperature. The negative value of ΔS° indicates that the adsorbed alum-morin and alum-extracted dyes become more restrained within the silk fibre molecules than in the respective dyeing solutions.

Table 3.12 Thermodynamic parameters for the adsorption of alum-morin and alum-extracted dye dyeing on silk.

	Temp (°C)	lnK _c	ΔG° (kJ/mol)	ΔH° (kJ/mol)	ΔS° (J/mol K)	R ²
alum-morin	30	7.04	-17.73			
	50	6.15	-16.51	-31.29	-45.7	0.9923
	70	5.57	-15.90			
alum-extracted dye	30	8.87	-22.35			
	50	8.50	-22.84	-14.16	-30.75	0.9995
	70	8.21	-23.15			

3.4.4.3 Comparison of adsorption-desorption of morin, alum-morin and alum-extracted dye onto silk.

The adsorption-desorption of morin, alum-morin and alum-extracted dye onto silk were shown in Figure 3.34. It was found that at 300 minutes, the amount of alum-morin, alum-morin from extracted dye (about 34 mg/L of morin from extracted dye) and alum-extracted dye adsorbed on silk was higher than using morin without mordant. The reason was discussed previously on sections 3.4.1 and 3.4.2.1.

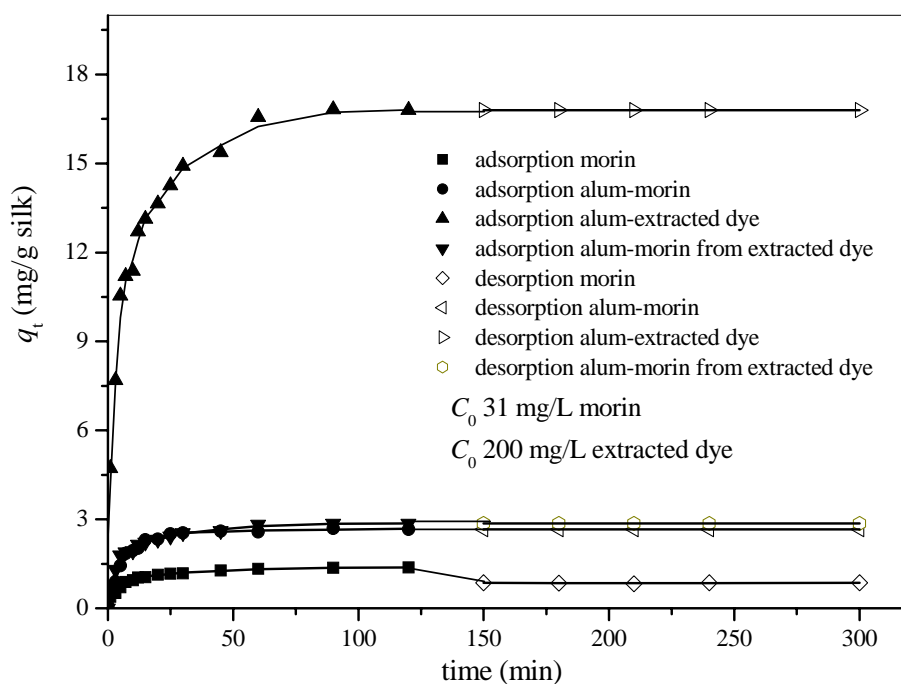


Figure 3.34 Adsorption-desorption of morin, alum-morin and alum-extracted dye onto silk.

3.5 Conclusion

Mordanting to fibre techniques such as pre-mordant, simultaneous mordant and post-mordant were tested to find the best condition for dyeing. It was found that the highest amount of dye adsorbed onto silk was the simultaneous mordanting technique. The adsorption kinetics and isotherm of alum-morin dye dyeing onto silk were studied in this work. The most important parameters include pH, the material to liquor ratio (MLR), the initial dye concentration, and temperature, which all influence the dyeing process and hence were investigated. It was found that the adsorption capacity was dependent on the pH of the dye solution and optimal uptake on silk occurred at pH 4.0. The initial dye adsorption rate of alum-morin dye on silk yarn was very fast with an increase in adsorption rate observed with an increase in temperature. Before equilibrium was reached, an increase in temperature led to an increase in the initial dye adsorption rate which indicated a kinetically controlled process. A pseudo second-order kinetic model indicated with an activation energy of 45.26 kJ/mol. This suggested that the overall rate of alum-morin dye adsorption is likely to be controlled by the chemical process. The values of the enthalpy (ΔH^\ddagger) and entropy of activation (ΔS^\ddagger) were 42.51 kJ/mol and -160.8 J/mol K respectively. The free energy of activation (ΔG^\ddagger) at 30°C was 91.26 kJ/mol. The free energy (ΔG°), enthalpy (ΔH°) and entropy (ΔS°) terms for alum-morin dyeing were also determined, and the negative values of ΔG° and ΔH° obtained indicated that the alum-morin dye adsorption process is a spontaneous and an exothermic one. The experimental data fitted well to the Langmuir and Freundlich isotherms with a high correlation coefficient (R^2).

The adsorption kinetics and isotherm of alum-extracted dye dyeing onto silk were also studied. The adsorption capacities are significantly affected by the material to liquor ratio (MLR), the initial dye concentration, and temperature. It was found that the results showed similar trend with alum-morin dyeing onto silk. The dye uptake increased at higher initial dye concentration of alum-extracted dye and was influenced by the material to liquor ratio (MLR). In addition, the initial dye adsorption rates (h_i) onto silk before equilibrium time increased at higher dyeing temperatures. The adsorption kinetics of alum-extracted dye on silk was also found to follow the pseudo second-order kinetic model. The activation energy for the adsorption of alum-extracted dye on silk was evaluated using the pseudo second-order rate constants. The free energy (ΔG°), enthalpy (ΔH°) and entropy (ΔS°) terms for alum-extracted dyeing were also showed similar results with alum-morin dye adsorption process.

3.6 References

- Aksu, Z., (2002). Determination of the equilibrium, kinetic and thermodynamic parameters of the batch biosorption of nickel(II) ions onto *Chlorella vulgaris*. **Process Biochemistry** 38: 89-99.
- Al-Ghouti, M. A., Khraisheh, M. A. M., Allen, S. J. and Ahmad, M. N. (2005). Thermodynamic behaviour and the effect of temperature on the removal of dye from aqueous solution using modified diatomite: a kinetic study. **Colloid and Interface Science** 287: 6-13.
- Bhattacharyya, K. G. and Sarma, A. (2003). Adsorption characteristics of the dye, Brilliant Green, on Neem leaf powder. **Dyes and Pigments** 57: 211-222.

- Brisbane rainforest action & information network. (2007). Available:
http://www.brisrain.webcentral.com.au/01_cms/details_pop.asp?ID=70
- Bruce, R. L. and Broadwood, N. V. (2000). Kinetics of wool dyeing with acid dyes. **Textile Research Journal** 70: 525-531.
- Carr, C. M. (1995). **Chemistry of the textiles industry**. Glasgow: Blackie Academic & Professional.
- Carrillo, F., Lis, M. J. and Valdeperas, J. (2002). Sorption isotherms and behaviour of direct dyes on lyocell fibres. **Dyes and Pigments** 53: 129-136.
- Chairat, M. (2004). **Extraction and characterization of lac dye from Thai stick lac and development of lac dyeing on silk and cotton**. Ph.D. Thesis, Suranaree University of Technology.
- Chairat, M., Rattanaphani, S., Bremner, J. B. and Rattanaphani, V. (2006). Adsorption kinetic study of lac dyeing on cotton. **Dyes and Pigments**: Article in press doi:10.1016/j.dyepig.2006.09.008.
- Chairat, M., Rattanaphani, S., Bremner, J. B. and Rattanaphani, V. (2005). An adsorption and kinetic study of lac dyeing on silk. **Dyes and Pigments** 64: 231-241.
- Chiou, M. S. and Li, H. Y. (2002). Equilibrium and kinetic modeling of adsorption of reactive dye on cross-linked chitosan beads. **Journal of Hazardous Materials** 93: 233-248.
- Chiou, M. S. and Li, H. Y. (2003). Adsorption behavior of reactive dye in aqueous solution on chemical cross-linked chitosan bead. **Chemosphere** 50: 1095-1105.

- Christie, R. M., Mather, M. M. and Wardman, R. H. (2000). **The Chemistry of Colour Application**. Oxford: Blackwell Science.
- Dechsree, S. (1998). **Isolation of active components against herpes simplex virus from *Maclura cochinchinensis* (Lour.) Corner heartwood**. M.Sc. Thesis, Mahidol University.
- Ding, P., Huang, K. L., Li, G. Y., Liu, Y. F. and Zeng, W. W. (2006). Kinetics of adsorption of Zn(II) ion on chitosan derivatives. **International Journal of Biological Macromolecules** 39: 222-227.
- Doğan, M. and Alkan, M. (2003). Adsorption kinetics of methyl violet onto perlite. **Chemosphere** 50: 517-528.
- Ho, Y. S. and McKay, G. (1999). Pseudo-second order model for sorption processes. **Process Biochemistry** 34: 451-465.
- Ho, Y. S. and McKay, G. (1998). Sorption of dye from aqueous solution by peat. **Chemical Engineering Journal** 70: 115-124.
- House, J. E. (1997). **Principles of chemical kinetics**. Dubuque, IA: Wm. C. Brown Publishers.
- Kannan, N. and Sundaram, M. M. (2001). Kinetics and mechanism of removal of methylene blue by adsorption on various carbons-a comparative study. **Dyes and Pigments** 51: 25-40.
- Kaplan, D., Adam, W. W., Farmer, B. and Viney, C. (1994). **Silk polymers: Materials science and Biotechnology**. Washington: American Chemical Society.
- Kim, T. K., Son, Y. A. and Lim, Y. J. (2005). Thermodynamic parameters of disperse dyeing on several polyester fibers having different molecular structure. **Dyes and Pigments** 67: 229-234.

- Kongkachuichay, P., Shitangkoon, A. and Chinwongamorn, N. (2002). Thermodynamics of adsorption of laccic acid on silk. **Dyes and Pigments** 53: 179-185.
- Laidler, K. J., Meiser, J. H. and Sanctuary, B. C. (2003). **Physical Chemistry**. Boston: Houghton Mifflin.
- Lin, J. X., Zhan, S. L., Fang, M. H. Qian, X. Q. and Yang, H. (2007). Adsorption of basic dye from aqueous solution onto fly ash. **Journal of Environmental Management** Article in press doi:10.1016/j.jenvman.2007.01.001.
- Malik, P. K. (2003). Use of activated carbons prepared from sawdust and rick-husk for adsorption of acid dyes: a case study of Acid Yellow 36. **Dyes and Pigments** 56: 239-249.
- Moeyes, M. (1993). **Natural Dyeing in Thailand**. Bangkok: White Lotus.
- Nollet, H., Roels, M., Lutgen, P., Meeren, P. V. and Verstraete, W. (2003). Removal of PCBs from wastewater using fly ash. **Chemosphere** 53: 655-665.
- Ofomaja, A. E. (2007). Sorption dynamics and isotherm studies of methylene blue uptake on to palm kernel fibre. **Chemical Engineering Journal** doi:10.1016/j.cej.2006.08.022.
- Özacar, M. and Şengil, İ. A. (2005). A kinetic study of metal complex dye sorption onto pine sawdust. **Process Biochemistry** 40: 565-572.
- Perkins, W. S. (1996). **Textile coloration and finishing**. North Carolina: Carolina Academic Press.
- Raisanen, R., Nousiainen, P. and Hynninen, P. H. (2001). Emodin and dermocybin natural anthraquinones as mordant dyes for wool and polyamide. **Textile Research Journal** 71: 1016-1022.

- Rattanaphani, S., Chairat, M., Bremner, J. B. and Rattanaphani, V. (2007). An adsorption and thermodynamic study of lac dyeing on cotton pretreated with chitosan. **Dyes and Pigments** 72: 88-96.
- Tsatsaroni, E., Liakopoulou-Kyriakides, M. and Elefthriadis, I. (1998). Comparative study of dyeing properties of two yellow natural pigments-effect of enzymes and proteins. **Dyes and Pigments** 37: 307-315.
- Uzun, I. (2006). Kinetics of the adsorption of reactive dyes by chitosan. **Dyes and Pigments** 70: 76-83.
- Vadivelan, V. and Kumar, K. V. (2005). Equilibrium, kinetics, mechanism, and process design for the sorption of methylene blue onto rice husk. **Journal of Colloid and Interface Science** 286: 90-100.
- Wan Ngah, W. S., Ab Ghani, S. and Kamari, A. (2005). Adsorption behaviour of Fe(II) and Fe(III) ions in aqueous solution on chitosan and cross-linked chitosan beads. **Bioresource Technology** 96: 443-450.
- Wan Ngah, W. S., Endud, C. S. and Mayanar, R. (2002). Removal of copper(II) ions from aqueous solution onto chitosan and cross-linked chitosan beads. **Reactive and Functional Polymers** 50: 181-190.
- Wu, F.-C., Tseng, R.-L. and Juang, R.-S. (2001). Kinetic modeling of liquid-phase adsorption of reactive dyes and metal ions on chitosan. **Water Research** 35: 613-618.
- Yu, Y., Zhuang, Y. Y. and Wang, Z. H. (2001). Adsorption of water-soluble dye onto functionalized resin. **Journal of Colloid and Interface Science** 242: 288-293.
- Zollinger, H. (2003). **Colour Chemistry**. Weinheim: Wiley-VCH.

CHAPTER IV

AN ADSORPTION STUDY OF Al(III) IONS ONTO CHITOSAN

4.1 Abstract

The adsorption of Al(III) from aqueous solutions onto chitosan was studied in a batch system. The isotherms and the kinetics of adsorption with respect to the initial Al(III) concentration and temperature were investigated. Langmuir and Freundlich adsorption models were applied to describe the experimental isotherms. Equilibrium data fitted very well to the Langmuir model in the entire concentration range (5-40 mg/L). The negative values of free energy (ΔG°) and enthalpy (ΔH°) for the adsorption of Al(III) onto chitosan indicated that the adsorption process is a spontaneous and exothermic one. Two simplified kinetic models, based on pseudo first-order and pseudo second-order equations, were tested to describe the adsorption mechanism. The pseudo second-order kinetic model resulted in an activation energy of 56.4 kJ/mol. It is suggested that the overall rate of Al(III) ion adsorption is likely to be controlled by the chemical process. The values of the enthalpy (ΔH^\ddagger) and entropy (ΔS^\ddagger) of activation were 53.7 kJ/mol and -164.4 J/mol K, respectively. The free energy of activation (ΔG^\ddagger) at 30°C was 103.5 kJ/mol.

4.2 Introduction

As part of a comprehensive study of dyeing silk and cotton with natural dyes (Chairat, Rattanaphani, Bremner, Rattanaphani and Perkins, 2004; Chairat, Rattanaphani, Bremner and Rattanaphani, 2005; Rattanaphani, Chairat, Bremner and Rattanaphani, 2007) we have investigated the aqueous stream from the dyeing process.

Alum, potassium aluminium sulphate, is widely used as a mordant-fixative for natural fibres with natural dyes (Moeyes, 1993). It is released into ground or river without treatment especially from domestic dyeing. Aluminium exists only as a trivalent cation and is too reactive to be found in its elemental state in nature (Yokel, 2002). In aqueous solutions aluminum solubility is highly pH dependent (Suwalsky, Kiss and Zatta, 2002). Under acidic or alkaline conditions, or in the presence of appropriate ligands, soluble species are formed, but in the range of physiological pH values (between 6 and 8) Al(III) is generally insoluble. At low pH values ($\text{pH} < 5$), the main species is $\text{Al}[(\text{H}_2\text{O})_6]^{3+}$. However, as the pH increases, $\text{Al}(\text{OH})^{2+}$ and $\text{Al}(\text{OH})_2^+$ are gradually formed and at neutral pH amorphous $\text{Al}(\text{OH})_3$ precipitates; at basic pH this precipitate dissolves to form $\text{Al}(\text{OH})_4^-$.

Since aluminium is a potential concern with respect to Alzheimer's disease in humans (Gauthier, Fortier, Courchesne, Pepin, Mortimer and Gauvreau, 2000; Becaria, Lahiri, Bondy, Chen, Hamadeh, Li, Taylor and Campbell, 2006; Walton, 2006), the removal of aluminium from process or waste effluents becomes environmentally important, and in this context the use of activated carbon has been investigated (Ghazy, Samra, Mahdy and E-Morsy, 2006).

There are various other natural adsorbents such as chitin, chitosan, natural zeolites, perlite, and agricultural wastes for metal ion removal from contaminated

water. Chitosan has received considerable attention for metal ion removal due to its excellent metal binding capacities (Majeti and Kumar, 2000) and its ready availability. It is a partially deacetylated polymer of acetylglucosamine (2-acetamido-2-deoxy-D-glucose-(*N*-acetylglucan)) which is found in the shells of crabs and shrimps. The chemical structure of chitosan is shown in Figure 4.1. Various studies of metal ion adsorption by chitosan have been undertaken in recent years, such as the removal of Cu(II) ions from aqueous solution onto chitosan and cross-linked chitosan beads (Wan Ngah, Endud and Mayanar, 2002). The equilibrium sorption studies of Cu(II) ions onto chitosan were found to follow the Langmuir model (Ng, Cheung and McKay, 2002). In addition, chitosan can be used to achieve adsorption of chromium (Sağ and Aktay, 2002), cadmium (Evans, Davids, MacRae and Amirbahman, 2002), iron (Wan Ngah, Ab Ghani and Kamari, 2005), and nikel (Pradhan, Shukla and Dorris, 2005) ions from aqueous solution.

The aim of the present work was to determine the thermodynamic values related to the interaction of Al(III) ions with chitosan in aqueous solution and the results are reported in this paper. The adsorption rates were determined quantitatively with respect to initial Al(III) concentration and temperature. These results can be useful for understanding the mechanism of interaction and also for further applications in Al(III) removal from wastewater from dyeing processes.

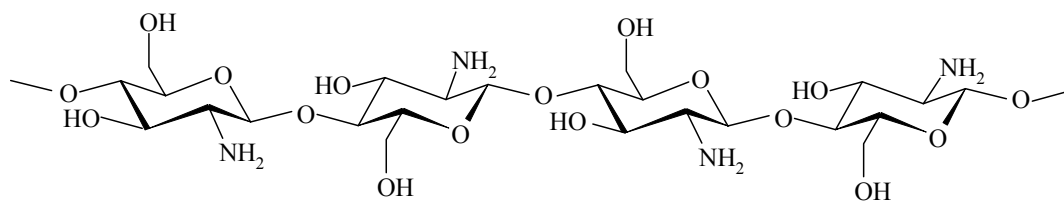


Figure 4.1 The chemical structure of chitosan.

4.3 Experimental

4.3.1 Materials

The chitosan (medium molecular weight, viscosity 200,000 cps, CAS 9012-76-4, FW of repeating unit, 161) used in the present investigation was obtained from the Aldrich Chemical Company. The BET surface area of chitosan ($1.49 \text{ m}^2/\text{g}$) was measured from N_2 adsorption isotherms with a Micrometrics ASAP 2010. Stock solution (1000 mg/L) of Al(III) ions were prepared by using alum, $\text{KAl}(\text{SO}_4)_2 \cdot 12\text{H}_2\text{O}$ (Merck) in deionized water.

4.3.2 Instruments

An atomic absorption spectrophotometer (AAS) (Varian SpectrAA 250 Plus) was used for quantitative determination of the concentration of Al(III) ions. The AAS was equipped with an Al hollow cathode lamp at a wavelength of 396.2 nm and nitrous oxide-acetylene flame. A calibration curve was obtained from a stock solution (1000 mg/L) of $\text{KAl}(\text{SO}_4)_2 \cdot 12\text{H}_2\text{O}$ in 0.1 M HNO_3 .

A pH meter (Laboratory pH Meter CG 842, SCHOTT) was used to measure the pH values of the Al(III) solutions.

A thermostatted shaker bath (Type SBD-50, HetoHolten A/S, Denmark), operated at 150 strokes/min, was used to study the adsorption of Al(III) ions onto chitosan.

4.3.3 Batch adsorption experiments

4.3.3.1 Batch pH studies

Batch pH studies were conducted by shaking 50 mL of an aqueous Al(III) solution with 0.01 g of chitosan for 24 h by using a thermostatted shaker bath operated at 30°C, over a range of initial pH values from 3.0 to 6.5. The pH of the aqueous solutions was adjusted by using 0.1 M NaOH or 0.1 M HNO₃. The solution was filtered after pH adjustment. After equilibrium, the aqueous samples were filtered through 0.45 µm filters (RC-membrane, Minisart) and the concentrations of Al(III) in the filtrate were analyzed using an AAS. After adsorption, the suspensions were acidified with HNO₃ to decrease pH below 3 in order to avoid Al precipitation before Al measurement. The pH values were measured before and after equilibrium. Each experiment was carried out three times under identical conditions. The amount of adsorption at equilibrium q_e (mg/g chitosan) was obtained as follows:

$$q_e = (C_0 - C_e) \frac{V}{W} \quad (4.1)$$

where C_0 (mg/L) and C_e (mg/L) are the concentrations in the solution at time $t = 0$ and at equilibrium time t , respectively, V is the volume of the solution (L), and W is the weight of chitosan (g) used.

4.3.3.2 Batch kinetic studies

The batch kinetics experiments were performed in a similar manner to the batch pH studies. The effect of initial concentration was studied in the range of 5-20 mg/L at pH_a 4.0 and 30°C. The effect of temperature was investigated at an initial concentration of 20 mg/L (pH_a 4.0). At pre-set time intervals the amount of adsorption at time t , q_t (mg/g chitosan) was obtained as follows:

$$q_t = (C_0 - C_t) \frac{V}{W} \quad (4.2)$$

where C_0 (mg/L) and C_t (mg/L) are the concentration in the solution at time $t = 0$ and at time t , respectively, V is the volume of the solution (L), and W is the weight of chitosan (g) used.

4.3.3.3 Batch isotherm studies

The batch adsorption isotherm studies were conducted in a similar manner to the batch pH studies by varying the Al(III) concentration 5-40 mg/L (pH_a 4.0) at 30, 45 and 60°C. The initial and equilibrium Al(III) concentrations were analyzed by using an AAS. The amount adsorbed at equilibrium (q_e) was calculated by using Eq. (4.1).

4.4 Results and discussion

4.4.1 Effect of pH

The pH of a solution strongly affects the adsorption capacity of the chitosan (Wan Ngah *et al.*, 2005). It was noted that the pH values of the equilibrated solution of Al(III) with chitosan were considerably different from the pH values before chitosan addition. The Al(III) ion is a Lewis acid (electron pair acceptor; electrophile) (Yokel, 2002), and the pH values of waste from the dyeing process which contained aluminium were varied from 3 to 6 which depending on the amount of alum used. The results of the pH measurements are summarized in Table 4.1. The adjusted pH of the aqueous Al(III) solution is pH_a . The measured pH after equilibration with chitosan is pH_e , and the equilibrium Al(III) concentration is C_e . The results (Figure 4.2) showed that the adsorption of Al(III) increased with increasing pH_a of the solution from 3.0 to 4.0 and decreased after pH 4.0. At low pH, more protons will be available to protonate the amine groups in chitosan (Wan Ngah *et al.*, 2005), thus reducing the number of binding sites for the adsorption of Al(III). On the other hand at pH values higher than 4.0, aluminium hydroxide precipitation took place thus decreasing the adsorption with increasing pH_a . The initial pH of 4.0 was used throughout this study.

Table 4.1 pH values of Al(III) solutions (V , 50 mL; W , 0.01 g; temp, 30°C; contact time 24 h); pH_a was adjusted by using 0.1 M NaOH or 0.1 M HNO₃ and pH_e is the pH value of the aqueous solution after equilibration at concentration C_e .

C_0 (mg/L)	pH_a	C_e (mg/L)	pH_e
21.03	3.09	19.89	4.24
21.38	3.43	14.94	4.30
21.19	4.00	8.80	4.36
21.22	4.41	5.16	4.44
21.90	4.83	0.00	5.79
21.80	5.50	0.00	5.98
21.90	6.52	0.00	6.58

4.4.2 Kinetics of adsorption

4.4.2.1 Effect of initial Al(III) concentration

Figure 4.3 shows a plot of the amount of Al(III) adsorbed per gram of chitosan (q_t) (mg/g chitosan) at various times versus contact time (t) for different initial Al(III) concentrations of 5, 10 and 20 mg/L at pH_a 4.0 and 30°C. It was found that the adsorption capacity varied with the initial concentration of Al(III). An increase in the initial concentration led to an increase in the amount of Al(III) adsorbed onto chitosan. This may be a result of an increase in the driving force of the concentration gradient with the increase in the initial concentration (Chiou and Li, 2002). This indicated that the initial concentration plays an important role in the adsorption capacity of Al(III) on chitosan. In all subsequent experiments an initial Al(III) concentration of 20 mg/L was used.

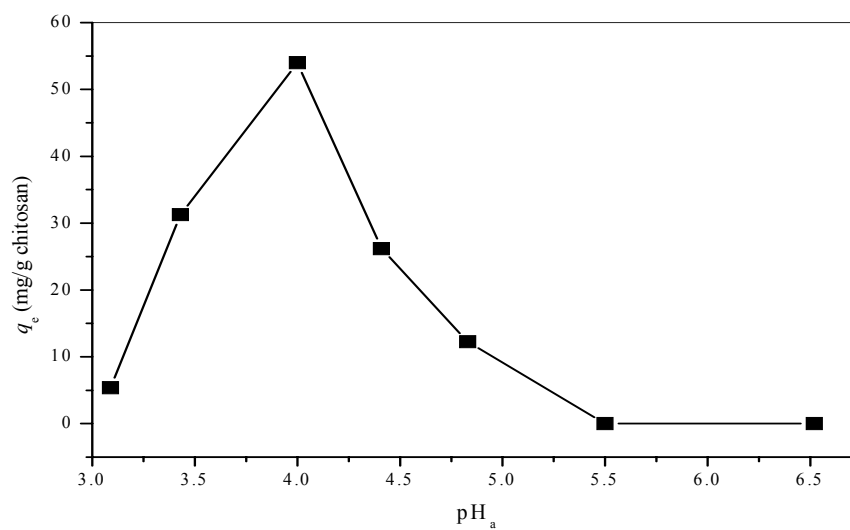


Figure 4.2 Effect of initial pH (C_0 , 21 mg/L; W , 0.01 g; V , 50 mL; temp, 30°C; contact time 24 h) for Al(III) adsorption on chitosan.

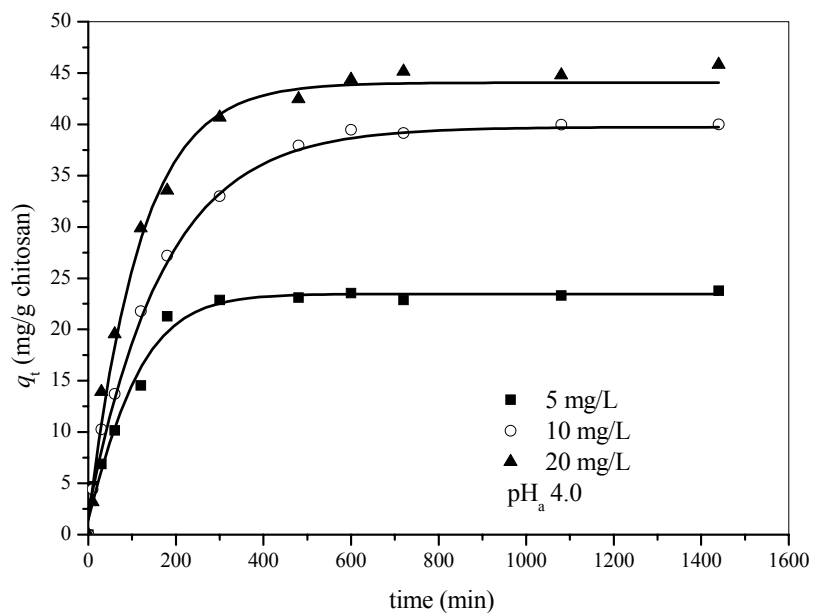


Figure 4.3 Adsorption kinetics for Al(III) onto chitosan at different initial Al(III) concentrations (W , 0.01 g; V , 50 mL; temperature 30°C; pH_a 4.0).

4.4.2.2 Effect of temperature

The effect of temperature on adsorption of Al(III) onto chitosan at an initial Al(III) concentration of 20 mg/L at pH_a 4.0 is shown in Figure 4.4. Before equilibrium was reached, an increase in the temperature led to an increase in the Al(III) adsorption rate, which indicated a kinetically controlled process. After the equilibrium was attained, the adsorption of Al(III) decreased with increased temperatures consistent with the adsorption being controlled by an exothermic process.

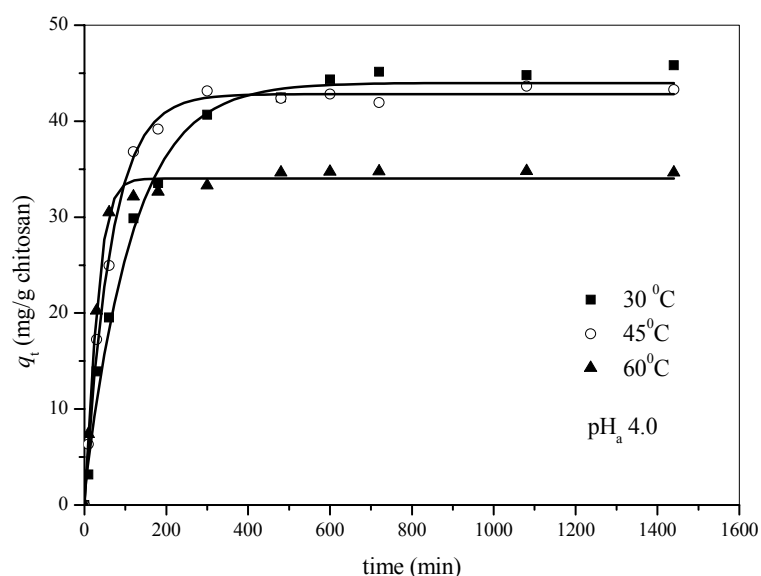


Figure 4.4 Adsorption kinetics for Al(III) onto chitosan at different temperatures (C_0 , 20 mg/L; V , 50 mL; M , 0.01 g; pH_a 4.0).

4.4.3 Rate constant studies

In order to investigate the controlling mechanism of the adsorption processes, pseudo-first order and pseudo-second order kinetic analyses were undertaken. The pseudo-first order equation (Eq. (4.3)) has been used extensively to describe the

adsorption kinetics (Wu, Tseng and Juang, 2001; Chiou and Li, 2002; Sağ and Aktay, 2002; Chairat *et al.*, 2005) (Eq. (4.3)).

$$\ln(q_e - q_t) = \ln q_e - k_1 t \quad (4.3)$$

where k_1 is the rate constant of pseudo first-order adsorption (min^{-1}), q_e and q_t are the amount of Al(III) adsorbed per gram of chitosan (mg/g chitosan) at equilibrium and time t , respectively. A straight line for the plot of $\ln(q_e - q_t)$ versus t would then suggest the applicability of this kinetic model to fit the experimental data. The first-order rate constant k_1 and equilibrium adsorption density (q_e) can be calculated from the slope and intercept of this line.

The pseudo-second order kinetic model for a sorption process (Ho and McKay, 1999) is expressed as:

$$\frac{t}{q_t} = \frac{1}{k_2 q_e^2} + \frac{1}{q_e} t \quad (4.4)$$

where k_2 (g chitosan/mg min) is the rate constant for a pseudo second-order adsorption.

And

$$h_i = k_2 q_e^2 \quad (4.5)$$

where h_i is the initial Al(III) adsorption rate (mg/g chitosan min). If pseudo second-order kinetics are applicable, the plot of t/q_t versus t would show a linear relationship. The slope and intercept can then be used to calculate the pseudo second-order rate constant k_2 and q_e .

Table 4.2 Comparison of the pseudo first- and second-order adsorption rate constants and the calculated and experimental q_e values for different initial Al(III) concentrations and temperatures.

Parameters	$q_{e,exp}$ (mg/g chitosan)	Pseudo first-order model			Pseudo second-order model			
		k_1 (min ⁻¹)	$q_{e,cal}$ (mg/g chitosan)	R^2	k_2 (g chitosan/mg min)	$q_{e,cal}$ (mg/g chitosan)	h_i (mg/g chitosan min)	R^2
<i>Initial Al(III) concentration; C_0 (mg/L): temp 30 °C; V 50 mL; pH_a 4.0; chitosan 0.01 g</i>								
5	23.8	7.96×10^{-3}	18.5	0.9524	7.26×10^{-4}	24.8	0.45	0.9988
10	40.0	5.89×10^{-3}	37.2	0.9986	2.20×10^{-4}	43.6	0.44	0.9985
20	45.8	5.05×10^{-3}	36.1	0.9776	2.27×10^{-4}	49.0	0.58	0.9988
<i>Temperature (°C): initial Al(III) concentration (C_0) 20.49 mg/L; V 50 mL; pH_a 4.0; chitosan 0.01 g</i>								
30	45.8	5.05×10^{-3}	36.1	0.9776	2.40×10^{-4}	49.0	0.58	0.9987
45	43.3	9.85×10^{-3}	25.4	0.8338	6.12×10^{-4}	44.8	1.23	0.9995
60	34.7	1.44×10^{-2}	22.3	0.9479	1.68×10^{-3}	35.3	2.09	0.9998

Table 4.2 lists the results of rate constant studies for different initial concentrations and temperatures calculated from the pseudo first-order and pseudo second-order models. The correlation coefficient R^2 for the pseudo second-order model had the highest value (>0.99) and its calculated equilibrium adsorption capacities $q_{e,cal}$ fit well with the experimental data, suggesting the Al(III) adsorption process is mediated predominantly via the pseudo second-order adsorption mechanism.

The pseudo second-order kinetic model is based on the assumption that the rate-limiting step may be chemisorption involving valency forces through sharing or exchange of electrons between the $-NH_2$ groups in chitosan and Al(III) (Sağ and Aktay, 2002; Wan Ngah *et al.*, 2005).

4.4.4 Activation parameters

The values of the rate constant k_2 at different temperatures listed in Table 4.2 were applied to estimate the activation energy of the adsorption of Al(III) onto chitosan by the Arrhenius equation (House, 1997) as follows:

$$\ln k = \ln A - \frac{E_a}{RT} \quad (4.6)$$

where A is the pre-exponential factor and E_a is the activation energy. The pre-exponential factor A has the same units as the rate constant. A straight line is obtained by plotting of the logarithm of the rate constant against the reciprocal of the absolute temperature and the results are listed in Table 4.3.

Table 4.3 Activation parameters for the adsorption of Al(III) onto chitosan.

Temp (°C)	k_2 (g chitosan/mg second)	E_a (kJ/mol)	R^2	ΔH^\ddagger (kJ/mol)	ΔS^\ddagger (J/mol K)	ΔG^\ddagger (kJ/mol)	R^2
30	3.72×10^{-6}					103.5	
45	1.02×10^{-5}	56.4	0.9996	53.7	-164.4	106.0	0.9996
60	2.79×10^{-5}					108.5	

The enthalpy (ΔH^\ddagger), entropy (ΔS^\ddagger) and free energy (ΔG^\ddagger) of activation can be also calculated using the Eyring equation (House, 1997) as follows:

$$\ln\left(\frac{k}{T}\right) = \ln\left(\frac{k_b}{h}\right) + \frac{\Delta S^\ddagger}{R} - \frac{\Delta H^\ddagger}{RT} \quad (4.7)$$

where k_b and h refer to the Boltzmann's constant and the Planck's constant respectively. The enthalpy (ΔH^\ddagger) and entropy (ΔS^\ddagger) of activation were calculated from the slope and intercept of a plot of $\ln(k/T)$ versus $1/T$. The Gibbs free energy of activation (ΔG^\ddagger) can be written in terms of enthalpy and entropy of activation:

$$\Delta G^\ddagger = \Delta H^\ddagger - T\Delta S^\ddagger \quad (4.8)$$

The observed activation energy (E_a) and enthalpy of activation (ΔH^\ddagger) for Al(III) onto chitosan shown in Table 4.3 agreed well with those calculated from the

activated complex theory of reaction in solution ($E_a = \Delta H^\ddagger + RT$). The observed activation energy ($E_a > 42$ kJ/mol) indicated a chemically controlled process (Yu, Saha, Kozak and Huang, 2006) for the adsorption of Al(III) onto chitosan.

The value of ΔG^\ddagger was calculated at 303, 318 and 333 K for an initial Al(III) concentration of 20 mg/L by using Eq. (4.8) and these values are listed in Table 4.3, while the negative ΔS^\ddagger reflects the expected structural interaction in the activated state between Al(III) and chitosan. A similar ΔS^\ddagger value was obtained from the adsorption kinetics of methyl violet onto perlite (Doğan and Alkan, 2003).

4.4.5 Adsorption isotherm

The Langmuir and Freundlich models are used to describe equilibrium adsorption isotherms. The most widely used Langmuir equation, which is valid for monolayer adsorption onto a surface with a finite number of identical sites, is expressed as (Langmuir, 1918):

$$q_e = \frac{QbC_e}{1 + bC_e} \quad (4.9)$$

where Q (mg/g chitosan) is the maximum amount of the Al(III) per unit weight of chitosan to form a complete monolayer coverage on the surface bound at high equilibrium Al(III) concentration C_e , q_e is the amount of Al(III) adsorbed per unit weight of chitosan at equilibrium and b is the Langmuir constant related to the affinity of binding sites. Figure 4.5 shows the experimental equilibrium isotherms for adsorption of Al(III) onto chitosan at different temperatures.

$$\frac{C_e}{q_e} = \frac{1}{Qb} + \left(\frac{1}{Q}\right)C_e \quad (4.10)$$

From the Eq. (4.10) a linearized plot of (C_e/q_e) versus C_e is obtained as shown in Figure 4.6, and Q and b are computed from the slopes and intercepts of Eq. (4.10). Table 4.4 lists the calculated values of the parameters Q and b . It was found that the adsorption capacity (Q) values decreased with increasing temperature. The result indicated that the adsorption of Al(III) onto chitosan is an exothermic process.

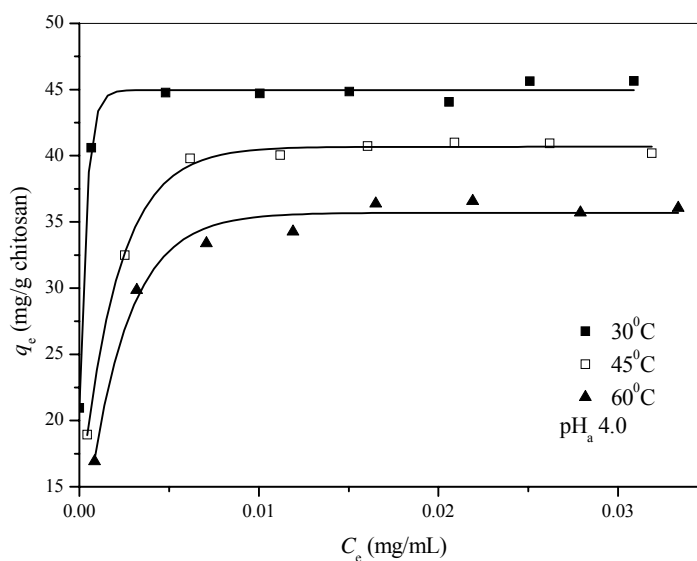


Figure 4.5 Langmuir adsorption isotherms for the adsorption of Al(III) onto chitosan

(W , 0.01 g; V , 50 mL; C_0 , 5-40 mg/L; pH_a 4.0, contact time 24 h).

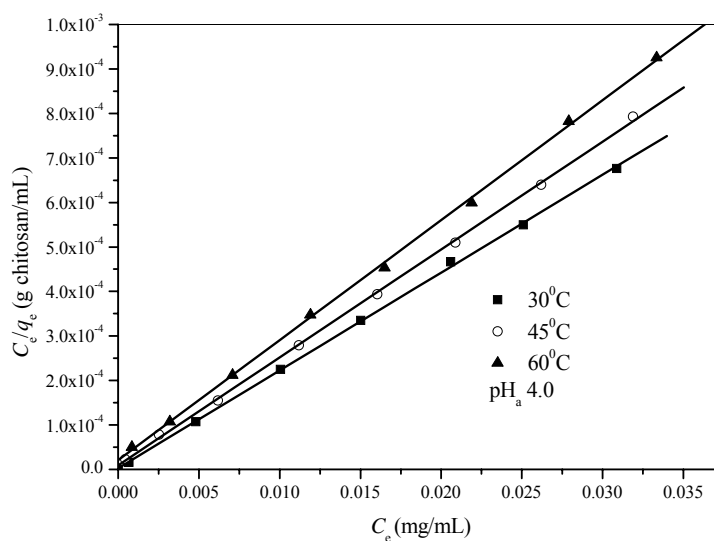


Figure 4.6 The linearized Langmuir adsorption isotherms for the adsorption of Al(III) onto chitosan (W , 0.01 g; V , 50 mL; C_0 , 5-40 mg/L; pH_a 4.0, contact time 24 h).

The Langmuir constant b is related to the energy of adsorption ($b \propto (\exp(-\Delta H^\circ/RT))$). Therefore, the thermodynamic parameters including the free energy change (ΔG°), enthalpy change (ΔH°) and entropy change (ΔS°) were also evaluated using the following equations (Panday, Prasad and Singh, 1985):

$$\Delta G^\circ = -RT \ln b \quad (4.11)$$

$$\ln(b) = \frac{\Delta S^\circ}{R} - \frac{\Delta H^\circ}{RT} \quad (4.12)$$

$$\Delta G^\circ = \Delta H^\circ - T\Delta S^\circ \quad (4.13)$$

The free energy (ΔG°) change was evaluated using Eq. (4.11), while enthalpy (ΔH°) and entropy changes of adsorption were calculated (Eq. (4.12)) from the slope of the straight line of a graph of $\ln(b)$ versus $1/T$. The values of ΔH° and ΔG° were then used together with Eq. (4.13). The results are listed in Table 4.5. The negative values of ΔG° and ΔH° indicate that the adsorption of Al(III) on chitosan is spontaneous and exothermic. The negative value of entropy change (ΔS°) of the process also indicates that the randomness decreases at the solid-solution interface during the adsorption of Al(III) onto chitosan. The obtained thermodynamic parameters reconfirmed values reported in our previous study (Septum, Rattanaphani, Bremner and Rattanaphani, 2006).

Table 4.4 Langmuir and Freundlich isotherm constants for the adsorption of Al(III) onto chitosan at different temperatures.

Temperature (°C)	Langmuir			Freundlich		
	Q (mg/g chitosan)	b (mL/mg)	R^2	Q_f (mg/g chitosan)	n	R^2
30	45.45	7829	0.9995	50.27	36.76	0.8139
45	41.32	2545	0.9995	55.14	12.84	0.6953
60	37.17	1269	0.9994	48.87	12.35	0.8607

Table 4.5 Thermodynamic parameters for the adsorption of Al(III) onto chitosan at different temperatures.

Temp (°C)	<i>b</i> (mL/mg)	ΔG° (kJ/mol)	ΔH° (kJ/mol)	ΔS° (J/mol K)	R^2
30	7829	-5.52		-150.19	
45	2545	-5.44	-51.03	-150.46	0.9884
60	1269	-5.44		-150.46	

The essential characteristics of the Langmuir isotherm can be expressed in terms of the dimensionless constant separation factor for equilibrium parameter, R_L

$$R_L = \frac{1}{1 + bC_0} \quad (4.14)$$

where C_0 is the initial concentration of Al(III) (in mg/L), and b is the Langmuir constant (L/mg). The values of R_L indicate whether the type of isotherm is irreversible ($R_L = 0$), favourable ($0 < R_L < 1$), linear ($R_L = 1$) or unfavourable ($R_L > 1$).

In the present study, the values of R_L (Table 4.6) were observed to be in the range of 0-1, indicating that the adsorption of Al(III) onto chitosan was favourable for this study.

Table 4.6 Langmuir isotherm data for adsorption of Al(III) on chitosan at different temperatures.

Temp (°C)	<i>b</i> (L/mg)	Initial Al(III) concentration <i>C</i> ₀ (mg/L)	<i>R</i> _L
30	7.829	4.57	0.0272
		9.35	0.0135
		14.29	0.0089
		19.44	0.0065
		24.36	0.0052
		29.58	0.0043
		35.04	0.0036
		40.56	0.0031
45	2.545	4.57	0.0792
		9.35	0.0403
		14.29	0.0268
		19.44	0.0198
		24.36	0.0159
		29.58	0.0131
		35.04	0.0111
		40.56	0.0096
60	1.269	4.57	0.1471
		9.35	0.0777
		14.29	0.0523
		19.44	0.0390
		24.36	0.0313
		29.58	0.0259
		35.04	0.0220
		40.56	0.0191

The other widely used empirical equation, the Freundlich equation, is based on adsorption on a heterogeneous surface and is given by:

$$q_e = Q_f C_e^{1/n} \quad (4.15)$$

where Q_f is roughly an indicator of the adsorption capacity and $1/n$ of the adsorption intensity. A linear form of the Freundlich expression (Eq.(4.16)) will yield the constants Q_f and $1/n$.

$$\ln q_e = \ln Q_f + \frac{1}{n} \ln C_e \quad (4.16)$$

Therefore, Q_f and $1/n$ can be determined from the linear plot of $\ln q_e$ versus $\ln C_e$. The magnitude of the exponent $1/n$ gives an indication of the favourability of adsorption. Values of $n > 1$ obtained represent favourable adsorption conditions. Table 4.4 lists the calculated results. The exponent n is larger than 10 for the adsorption of Al(III) onto chitosan. However, the low correlation coefficients ($R^2 < 0.86$) indicate poor agreement of the Freundlich isotherm data with the experimental data.

4.5 Conclusion

The adsorption isotherm and kinetics for the adsorption of Al(III) onto chitosan have been investigated. The following results were obtained:

1. The batch pH studies indicated that the Al(III) adsorption capacity was dependent on the pH of the Al(III) solution.
2. Before equilibrium was reached, an increase in temperature lead to an increase in adsorption rate which indicated a kinetically controlled process, while the adsorption of Al(III) on chitosan was controlled by an exothermic process.
3. A pseudo second-order kinetic model agreed well with the behaviour for the adsorption of Al(III) on chitosan, and supported chemical adsorption being the rate-limiting step.
4. The Langmuir equation agrees very well with the experimental data at a high correlation coefficient ($R^2 > 0.99$).
5. The negative values of free energy (ΔG°) and enthalpy (ΔH°) terms for the adsorption of Al(III) onto chitosan indicated that the adsorption process is a spontaneous and exothermic one.

4.6 References

- Becaria, A., Lahiri, D. K., Bondy, S. C., Chen, D., Hamadeh, A., Li, H. and Taylor, R., Campbell, A. (2006). Aluminum and copper in drinking water enhance inflammatory or oxidative events specifically in the brain. **Journal of Neuroimmunology** 176: 16-23.

- Chairat, M., Rattanaphani, S., Bremner, J. B. and Rattanaphani, V. (2005). An adsorption and kinetic study of lac dyeing on silk. **Dyes and Pigments** 64: 231-241.
- Chairat, M., Rattanaphani, V., Bremner, J. B., Rattanaphani, S. and Perkins, D. F. (2004). An absorption spectroscopic investigation of the interaction of lac dyes with metal ions. **Dyes and Pigments** 63: 141-150.
- Chiou, M. S. and Li, H. Y. (2002). Equilibrium and kinetic modeling of adsorption of reactive dye on cross-linked chitosan beads. **Journal of Hazardous Materials** 93: 233.
- Doğan, M. and Alkan, M. (2003). Adsorption kinetics of methyl violet onto perlite. **Chemosphere** 50: 517-528.
- Evans, J. R., Davids, W. G., MacRae, J. D. and Amirbahman, A. (2002). Kinetics of cadmium uptake by chitosan-based crab shells. **Water Research** 36: 3219-3226.
- Gauthier, E., Fortier, I., Courchesne, F., Pepin, P., Mortimer, J. and Gauvreau, D. (2000). Aluminum forms in drinking water and risk of Alzheimer's disease. **Environmental Research Section A** 84: 234-246.
- El-Sayed Ghazy, S., El-Sayed Samra, S., Mahdy, A. E. F. M. and El-Morsy, S. M. (2006). Removal of aluminium from some water samples by sorptive-flotation using powdered modified activated carbon as a sorbent and oleic acid as a surfactant. **Analytical Sciences** 22: 377-382.
- Ho, Y. S. and McKay, G. (1999). Pseudo-second order model for sorption processes. **Process Biochemistry** 34: 451.

- House, J. E. (1997). **Principles of chemical kinetics**. Dubuque, IA: Wm. C. Brown Publishers.
- Langmuir, I. (1918). Adsorption of gases on plain surfaces of glass mica platinum. **Journal of the American Chemical Society** 40: 1361-1403.
- Majeti, N. V. and Kumar, R. (2000). A review of chitin and chitosan applications. **Reactive and Functional Polymers** 46: 1-27.
- Moeyes, M. (1993). **Natural Dyeing in Thailand**. Bangkok, White Lotus.
- Ng, J. C. Y., Cheung, W. H. and McKay, G. (2002). Equilibrium studies of the sorption of Cu(II) ions onto chitosan. **Journal of Colloid and Interface Science** 255(1): 64.
- Panday, K. K., Prasad, G. and Singh, V. N. (1985). Copper(II) removal from aqueous solutions by fly ash. **Water Research** 19: 869-873.
- Pradhan, S., Shukla, S. S. and Dorris, K. L. (2005). Removal of nickel from aqueous solutions using crab shells. **Journal of Hazardous Materials** (B125): 201-204.
- Rattanaphani, S., Chairat, M., Bremner, J. B. and Rattanaphani, V. (2007). An adsorption and thermodynamic study of lac dyeing on cotton pretreated with chitosan. **Dyes and Pigments** 72: 88-96.
- Sağ, Y. and Aktay, Y. (2002). Kinetic studies on sorption of Cr(VI) and Cu(II) ions by chitin, chitosan and *Rhizopus arrhizus*. **Biochemical Engineering Journal** 12: 143-153.

- Septum, C., Rattanaphani, S., Bremner, J. B. and Rattanaphani, V. (2006). Kinetics of the adsorption of Al(III) ions onto chitosan. **International Conference on Applied Science**, Vientiane, Laos.
- Suwalsky, M. N., B., Kiss, T. and Zatta, P. (2002). Effects of Al(III) speciation on cell membranes and molecular models. **Coordination Chemistry Reviews** 228: 285-295.
- Walton, J. R. (2006). Aluminum in hippocampal neurons from humans with Alzheimer's disease. **NeuroToxicology** 27: 385-394.
- Wan Ngah, W. S., Ab Ghani, S. and Kamari, A. (2005). Adsorption behaviour of Fe(II) and Fe(III) ions in aqueous solution on chitosan and cross-linked chitosan beads. **Bioresource Technology** 96: 443-450.
- Wan Ngah, W. S., Endud, C. S. and Mayanar, R. (2002). Removal of copper(II) ions from aqueous solution onto chitosan and cross-linked chitosan beads. **Reactive and Functional Polymers** 50(2): 181.
- Wu, F. C., Tseng, R. L. and Juang, R. S. (2001). Kinetic modeling of liquid-phase adsorption of reactive dyes and metal ions on chitosan. **Water Research** 35(3): 613.
- Yokel, R. A. (2002). Aluminum chelation principles and recent advances. **Coordination Chemistry Reviews** 228: 97-113.
- Yu, G., Saha, U. K., Kozak, L. M. and Huang, P. M. (2006). Kinetics of cadmium adsorption on aluminum precipitation products formed under the influence of tannate. **Geochimica et Cosmochimica Acta** 70: 5134-5145.

CHAPTER V

CONCLUSION

The interaction of morin and quercetin with aluminium ions and the kinetics and thermodynamics of the adsorption of morin and aqueous extracted dye (from the heartwood of *M. cochinchinensis*) onto silk were carried out in this research. Applying the molar ratio method, it was determined that stoichiometric compositions of complexes formed are Al_3M_2 , AlM and AlQ in aqueous solution. Alum caused a bathochromic shift of the visible absorption bands in morin and quercetin. The bathochromic shifts observed are consistent with the lone pair electrons in the donor atoms (O in the dyes) participating in metal ion coordination and stabilizing the excited state relative to the ground state.

Electrospray mass spectra (positive ion) of $Al:M$, $Ga:M$, $Al:Q$ and $Ga:Q$ complexes showed the stoichiometry of the major complex formed on ionisation in each case to be 1:2. Calculated heats of formation of were reasonable for these complexes and indicated possible structures. The stoichiometries of the $Ser:Al:M$, $Ser:Ga:M$, $Ser:Al:Q$ and $Ser:Ga:Q$ complexes observed mass spectrometrically were 1:1:1 and 1:1:2. These water excluded structures may have some relevance to those formed on interaction with silk.

Mordanting to fibre techniques such as pre-mordanting, simultaneous mordanting and post-mordanting were tested to find the best conditions for dyeing. It was found that the highest amount of dye adsorbed onto silk was achieved with

simultaneous mordanting technique. The adsorption kinetics and isotherms for alum-morin dye dyeing onto silk were studied in this work. The most important parameters included pH, the material to liquor ratio (MLR), the initial dye concentration, and temperature, which all influence the dyeing process. It was found that the adsorption capacity was dependent on the pH of the dye solution and optimal uptake on silk occurred at pH 4.0. The initial dye adsorption rate of alum-morin dye on silk yarn was very fast with an increase in adsorption rate being observed with an increase in temperature. Before equilibrium was reached, an increase in temperature lead to an increase in the initial dye adsorption rate which indicated a kinetically controlled process. A pseudo second-order kinetic model was indicated for this process with an activation energy of 45.26 kJ/mol. This suggested that the overall rate of alum-morin dye adsorption is likely to be controlled by the chemical process. The values of the enthalpy (ΔH^\ddagger) and entropy of activation (ΔS^\ddagger) were 42.51 kJ/mol and -160.8 J/mol K respectively. The free energy of activation (ΔG^\ddagger) at 30°C was 91.26 kJ/mol. The free energy (ΔG°), enthalpy (ΔH°) and entropy (ΔS°) terms for alum-morin dyeing were also determined, and the negative values of ΔG° and ΔH° obtained indicated that the alum-morin dye adsorption process is a spontaneous and an exothermic one. The experimental data fitted well to the Langmuir and Freundlich isotherms with a high correlation coefficient (R^2).

The adsorption kinetics and isotherm of alum-extracted dye dyeing onto silk were also studied. The adsorption capacities were significantly affected by the material to liquor ratio (MLR), the initial dye concentration, and temperature. It was found that the results showed similar trends with alum-morin dyeing onto silk. The dye uptake increased at higher initial dye concentration of alum-extracted dye and

was influenced by the material to liquor ratio (MLR). In addition, the initial dye adsorption rates (h_i) onto silk before equilibrium was established increased at higher dyeing temperatures. The adsorption kinetics of alum-extracted dye on silk was also found to follow the pseudo second-order kinetic model. The activation energy for the adsorption of alum-extracted dye on silk was evaluated using the pseudo second-order rate constants. The free energy (ΔG°), enthalpy (ΔH°) and entropy (ΔS°) terms for alum-extract dye dyeing were similar to those for the alum-morin dye adsorption process.

In addition, the adsorption isotherm and kinetics for the adsorption of Al(III) onto chitosan were investigated. The batch pH studies indicated that the Al(III) adsorption capacity on chitosan was dependent on the pH of the Al(III) solution. Before equilibrium was reached, an increase in temperature led to an increase in adsorption rate which indicated a kinetically controlled, exothermic process. A pseudo second-order kinetic model agreed well with the behaviour for the adsorption of Al(III) on chitosan, and supported chemical adsorption being the rate-limiting step. The Langmuir equation agreed very well with the experimental data with a high correlation coefficient ($R^2 > 0.99$). The negative values of the free energy (ΔG°) and enthalpy (ΔH°) terms for the adsorption of Al(III) onto chitosan indicated that the adsorption process is a spontaneous and exothermic one.

APPENDIX

APPENDIX

Calibration of morin dye solution

In order to determine the calibration curve of morin dye solution, the various concentrations of morin dye solution were prepared in aqueous solution. The absorbances of dye solution were measured using UV-VIS spectrophotometer at 390 nm. Then the relationship between morin dye concentration and its absorbance are plotted as shown in Figure A.1.

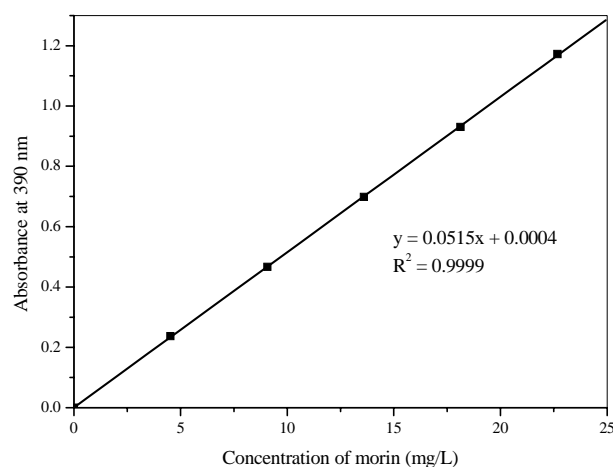


Figure A.1 Calibration curve of morin dye solution.

Calculation of dye concentration from calibration curve

Equation of calibration curve: $y = 0.0515x + 0.0004$

When y = absorbance and x = morin dye concentration (mg/L)

$$\text{Diluted dye concentration} = \frac{\text{Absorbance} - 0.0004}{0.0515}$$

Calibration of alum-morin complex solution

Morin solution was complexed with alum (alum-morin 2-1 mole ratio) in aqueous solution. The absorbance of alum-morin complex was quantified using UV-VIS spectrophotometer at 415 nm. The obtained calibration was found to be a straight line as shown in Figure A.2.

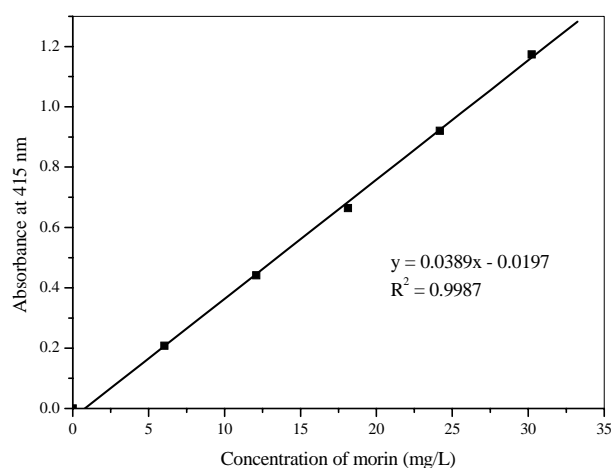


Figure A.2 Calibration curve of alum-morin dye solution.

Calculation of dye concentration from calibration curve

Equation of calibration curve: $y = 0.0389x - 0.0197$

When y = absorbance and x = morin dye concentration (mg/L)

$$\text{Diluted dye concentration} = \frac{\text{Absorbance} + 0.0197}{0.0389}$$

Calibration of alum-extracted dye complex solution

Extracted dye solution was complexed with alum in aqueous solution. The absorbance of alum-extracted dye complex was quantified using UV-VIS spectrophotometer at 415 nm. The obtained calibration was found to be a straight line as shown in Figure A.3.

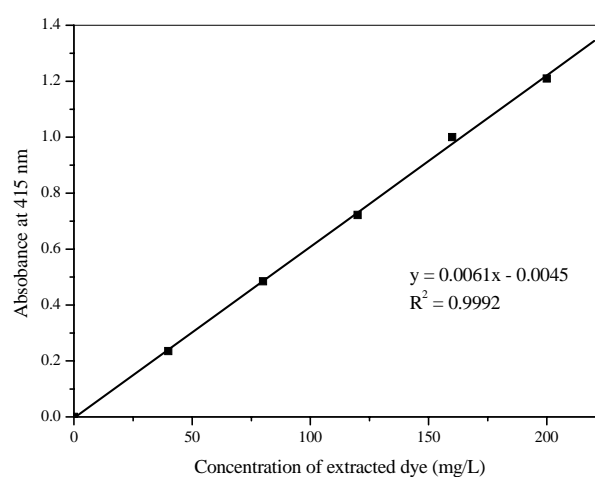


Figure A.3 Calibration curve of alum-extracted dye solution.

Calculation of dye concentration from calibration curve

Equation of calibration curve: $y = 0.0061x + 0.0045$

When y = absorbance and x = extracted dye concentration (mg/L)

$$\text{Diluted dye concentration} = \frac{\text{Absorbance} + 0.0045}{0.0061}$$

CURRICULUM VITAE

CHUTIMA SEPTHUM

E-mail: csepthum@yahoo.com

Born: 12 April, 1974 in Nakhon Si Thammarat, Thailand

Nationality: Thai

Education:

1992-1996 B.Sc. (Chemistry), Prince of Songkla University, Songkhla, Thailand

1996-2000 M.Sc. (Applied Chemistry), King Mongkut' s Institute of
Technology Ladkrabang, Bangkok, Thailand

Experiences:

2000-present Lecturer, Suratthani Rajabhat University, Suratthani, Thailand

2005 Ph.D. research at University of Wollongong, Australia

Publications:

1. Septhum, C., Rattanaphani, S., Bremner, J. B. and Rattanaphani, V. (2006). Kinetics of the adsorption of Al(III) ions onto chitosan. **Laos J. Appl. Sci.** 1: 318-324.
2. Septhum, C., Rattanaphani, V. and Rattanaphani, S. (2007). UV-Vis spectroscopic study of natural dyes with alum as a mordant. **Suranaree J. Sci. Tech.** 14: 91-97.
3. Septhum, C., Rattanaphani, S., Bremner, J. B. and Rattanaphani, V. (2007). An adsorption study of Al(III) ions onto chitosan. **J. Hazard. Mater.** Doi:10.1016/j.jhazmat.2007.02.024